Oneida Basin, Glacial Lake Iroquois, and Archaeologic Contexts

Northeast Friends of the Pleistocene

79th Annual Field Excursion, June 3-5 2016

In honor of:

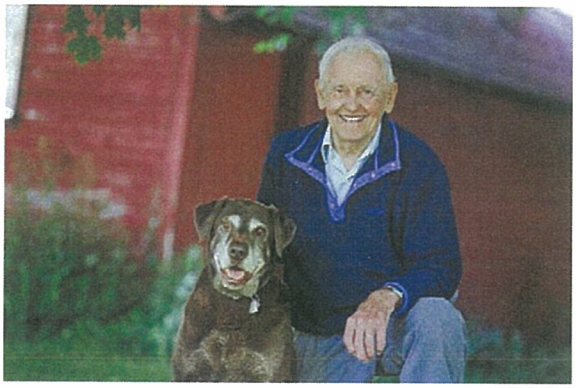

Donald Potter, Hamilton College

livesLived Lives Lived is a space to share your memories of a Queen's community member who recently died. Email your submissions to *andrew.carroll@queensu.ca*

Loss of an extraordinary geographer and friend

Dr. Robert Gilbert, a Professor Emeritus in the Department of Geography, born in 1945, passed away April 27.

BY PAUL TREITZ

Robert Gilbert passed away on April 27 after a brave battle with cancer. We have lost an extraordinary geographer and friend.

Professor Gilbert was a highly productive, dedicated and creative scientist. He joined the Geography Department at Queen's University in 1975 from the University of Alberta where he was a Postdoctoral Fellow.

Robert Gilbert

He received his BA, MA and PhD degrees from the University of British Columbia in 1968, 1970 and 1972 respectively.

At Queen's, his research focused on the processes that occur in lakes and the sea, especially on how sediments are delivered to, distributed through, and deposited in water bodies in the Great Lakes region, western Canada, the Canadian Arctic, Greenland, Antarctica, Nepal and the southern United States. In 2004, he and a team of international researchers discovered an active underwater volcano off the coast of Antarctica that towered 700 metres above the ocean floor. Professor Gilbert led by example through his passion for research and a deep commitment to teaching at all levels.

Professor Gilbert taught undergraduate courses in Earth System Science, physical limnology and arctic and periglacial environments. At the graduate level he taught and supervised students in lacustrine and marine systems. Throughout his distinguished career, he has been a champion for the discipline.

Dr. Gilbert established the Robert Gilbert Postdoctoral Fellowship in the Department of Geography in 2007. The purpose of this award is to support young scholars in the field of Physical Geography/Earth System Science for a two-year postdoctoral experience.

These postdoctoral fellows work closely on research projects affiliated with a faculty member in the Department of Geography at Queen's. At the time the Fellowship was established Bob said, "it seemed like a useful thing to do in this department to enhance the research. There's limited funding for post-docs in any field. There are always more people wanting to take up a post-doc than there are funds to support them."

To date, the department has welcomed three Robert Gilbert Postdoctoral Fellows, with the fourth to start in July 2015.

Paul Treitz is Professor and Head of the Department of Geography

Robert Gilbert, Queen's University

Oneida Basin, Glacial Lake Iroquois, and Archaeologic Contexts

Northeast Friends of the Pleistocene

79th Annual Field Excursion, June 3-5 2016

By

Eugene W. Domack, University South Florida and Colgate University

Jonathan C. Lothrop, New York State Museum

Michael Beardsley, Beauchamp chapter, NYSAA

Mark Clymer, Beauchamp chapter, NYSAA

Susan Winchell-Sweeney, New York State Museum

Meredith H. Younge, New York State Museum

Scott Ingmire, Madison County Planning Office

Brad Rosenheim, University of South Florida

Amy Leventer, Colgate University

Carol Griggs, Cornell University

all editorial errors due to E. Domack

but thanks to Katie Smith and Theresa King

supported by

Colgate University

University of South Florida

Special thanks to all landowners whose permission was granted to visit their properties.

Timing of late Quaternary landscape development across the eastern end of Oneida Lake, New York State, defined by LiDAR topography, and luminescence and radiocarbon dating

Madhav Krishna Murari[a*], Eugene W. Domack[b,c], Lewis A. Owen[a]

[a] *Department of Geology, University of Cincinnati, Cincinnati, OH 45221-0013*, USA

[b] *Department of Geoscience, Hamilton College, Clinton, NY, 13323*, USA

[c] *now at: College of Marine Science-University of South Florida, 140 7th Avenue South, St. Petersburg, Florida, USA*

Keywords: Laurentide ice sheet; Glacial Lake Iroquois; Holocene; glacial geology and geomorphology; shorelines; deltas; OSL dating; radiocarbon dating

ABSTRACT

Oneida Lake contains abundant aeolian features developed deltas, spits, and paleo-shorelines of Glacial Lake Iroquois. The first radiocarbon and optically stimulated luminescence (OSL) ages were determined on these features to define the timing for aeolian dune formation for two systems: 1) the Rome Sand Plains; and 2) barrier beach dunes. Shallow excavations within a parabolic dune form in the Rome Sand Plains yield OSL ages of 11.8±0.5 to 13.6±0.4 ka. These dunes were developed upon a relict "terrace" feature, of deltaic or ice contact origin, consisting of subaqueously deposited sands and gravelly sands. Excavations within this "terrace" yielded OSL ages from 21 to 29 ka. Relict coastal dunes are present upon littoral sandy gravels, of relict spits and barrier beaches, several kilometers east of the Oneida Lake. One of these dune complexes yielded OSL ages of 10.3±0.9 to 11.6±1.3 ka, underlain by shell bearing gravels with radiocarbon ages of 12.9 to 13.1 ka. The numerical ages and field relationships of the landforms show that lowering of lake levels within the easternmost extent of Glacial Lake Iroquois and its transition to Oneida Lake occurred at about 13.2 ka, consistent with revised models for outflow via the St Lawrence drainage.

*corresponding author: murarimk@ucmail.uc.edu

Introduction

Emergence of the Adirondack Mountains in the Late Glacial from beneath the surface of the Laurentide Ice Sheet facilitated the formation and encircling flow of the Ontario Lobes and Mohawk Lobes; together which drained into the Oneida and upper Mohawk Basins from the northwest and east southeast, respectively (Fig. 1). The drainage divide near Rome, New York (at an elevation of ~ 131 m above sea level [asl]) served as an important spillway for melt waters that would have drained off the Ontario Lobe as the ice receded toward the west northwest. This setting initiated the formation of Glacial Lake Iroquois (GLI), an impoundment that remained in existence and grew in extent as the Ontario Lobe continued to recede into the modern basin of Lake Ontario (the Ontario Lowland; Pair and Rodrigues, 1993). GLI began to drain once other outlets began to open, beginning with breaching of the Covey Hill Ice Dam along the northeastern edge of the Adirondacks (Fig. 1) and finally with the opening of the St. Lawrence drainage. There is a range of ages (13.2 to 13.6 ka*) for the initial and final draining of GLI (Table 1). Sediment cores and landform sediment associations within Lake Ontario suggest a drainage event at 13.5 ka followed by inundation of the Champlain Sea into the St. Lawrence Lowland at 12.9 ka and a period of lake isolation between 8.3-12.3 ka (Anderson and Lewis, 2012). These events are consistent with isobase reconstructions for important shoreline and spillway elevations within the Lake Ontario and Oneida basins (Anderson and Lewis, 2012, their Fig. 4). Rayburn et al. (2011) examined sediment sequences and dated fossils in the vicinity of Lake Champlain and they suggest a two stage-drop in GLI levels. These drainage events corresponded to a stepwise exposure of the Covey Hill Ice Dam with resultant GLI drainage into the Champlain lowland and Glacial Lake Vermont first beginning at 13.2 ka, where a lower Lake Frontenac Level was obtained (Table 1). A larger drop in lake levels took place soon after wherein

* All published radiocarbon ages have been calibrated using CALIB 6.0 routine of Stuiver et al. (2011).

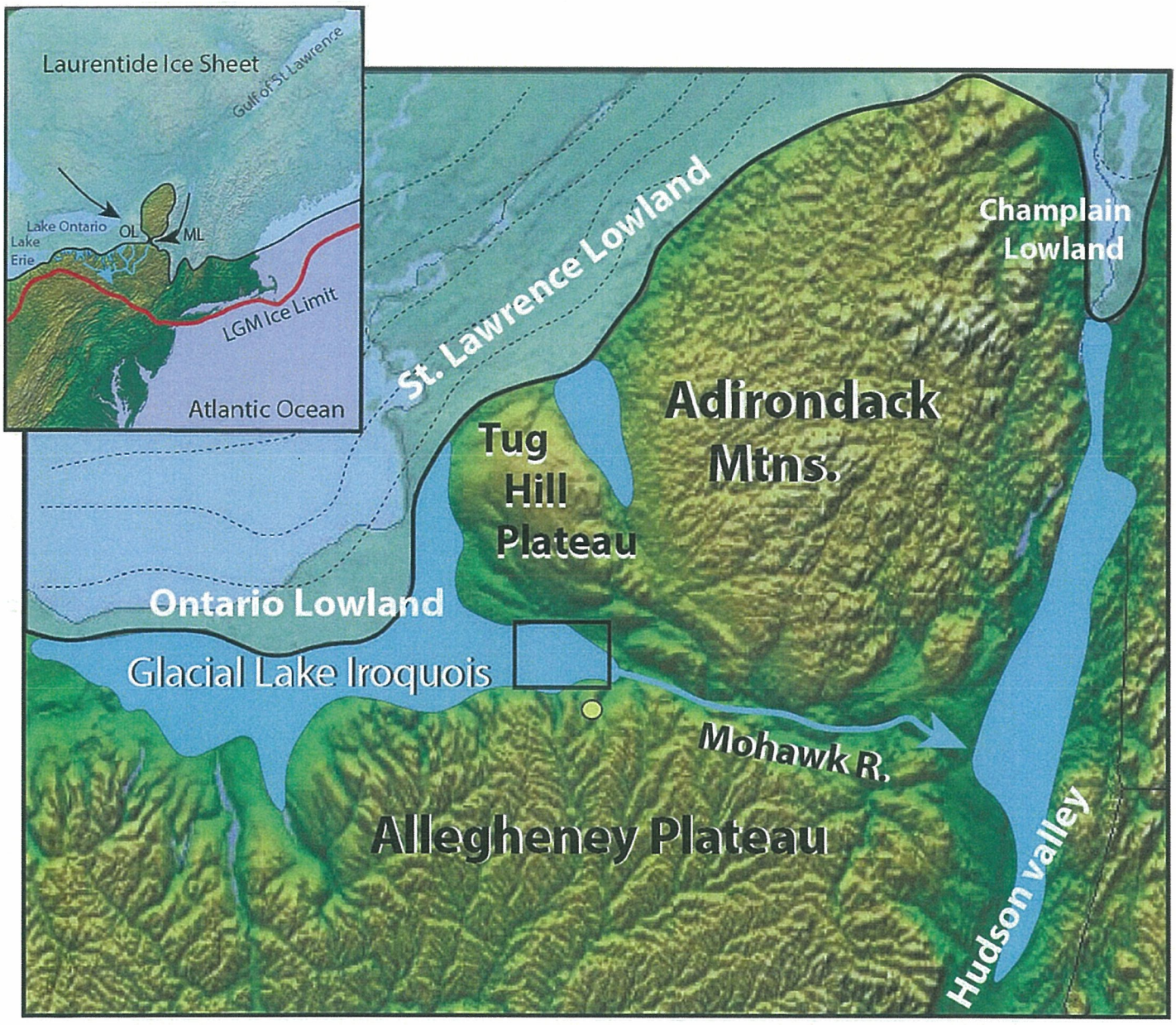

Fig. 1. Physiographic map of northeastern North America showing routing of ice lobes associated with late stage of the Laurentide Ice Sheet (OL = Ontario Lobe, ML = Mohawk Lobe). Also shown is the Covey Hill region ice dam (CH), which routed meltwater of Glacial Lake Iroquois down into the Champlain Lowland. Inset shows the Oneida Lake Lowland (OL), and surrounding physiographic regions mentioned in the text including location (yellow dot) of pre LGM sand exposure near Clinton, N.Y.

Table 1

Inferred timing of events (cal yr) in evolution of GLI and Oneida Lake.

Initiation of GL Iroquios	Drainage of GL Iroquios	Champlain Sea Phase	Great Lakes Lowstand	Reference
14.5 ka	13.5 ka	12.9 ka	12.3-8.3ka	Anderson & Lewis (2012)
	13.2ka, Lake Fontenac Level(~24m), Fort Ann Phase (-50m)			Rayburn et al., (2011)
14.7 ka	~13.6 ka	~13.4-12.9ka		Ridge (2004)
	13.35ka			Donnely, et al., 2005
	At least 4 distinct levels for GLI			Pair and Rodriques, 1993

GLI became confluent with Glacial Lake Vermont via a 50 m drop in elevation resulting in the Fort Ann Phase (Table 1). Earlier studies of varve chronology within the Mohawk and Champlain Valleys, and their correlation to the Connecticut Valley, suggest initiation of GLI at 14.7 ka, its drainage at 13.6 ka, and Champlain Sea inundation at 13.4-12.9 ka (Ridge, 2004). Donnelly et al., (2005) suggest a single drainage event down the Champlain Lowland and Hudson Valley at 13.35 ka. Of additional interest is the observation of at least four distinct GLI shorelines along the SE perimeter of the St Lawrence Lowland (Pair and Rodriguez, 1993). While no direct age control is provided for these shorelines they do recognize a set of higher shorelines (Watertown, Iroquios-Main, and Frontenac) separated by about 90 m from a lower set of stranded shorelines (Belleville and Trenton Phase; Pair and Rodrigues, 1993 their Fig. 4).

Thus the timing of the GLI drainage event is defined to within ~400 years and the various authors have therefore correlated it with the onset of the Younger Dryas cold episode ~ 12.9 to 13.2 ka. The final emptying of GLI may have also facilitated drainage of larger glacial lakes within the Great Lakes Basin including Glacial Lake Agassiz (Hillaire-Marcel and Occhietti, 1977; Parent and Occheitti, 1988; Rayburn et al., 2005, 2006, 2011; Franzi et al., 2007; Cronin et al., 2012).

From these results it is inferred that Oneida Lake must have become isolated in two stages, first at the final emptying of GLI (at around 13.6 ka) and again in a more retracted phase in the early Holocene (between 12.3 and 8.3 ka). This later event is related to climate driven changes in precipitation and evaporation that forced all the Laurentian Great Lakes into restricted basins and brackish water conditions (Anderson and Lewis, 2012).

Oneida Lake and the associated alluvial valleys of Fish, Wood, and Oneida Creek are located within the eastern end of the Ontario Lowland (Figs. 1 and 2). Relict landforms of Late Quaternary age border this modern fluvial landscape and consist of ground moraine, aeolian dune fields, lake sediments, and beach ridges (Wright, 1972; Muller and Cadwell, 1986). These relict Late Quaternary

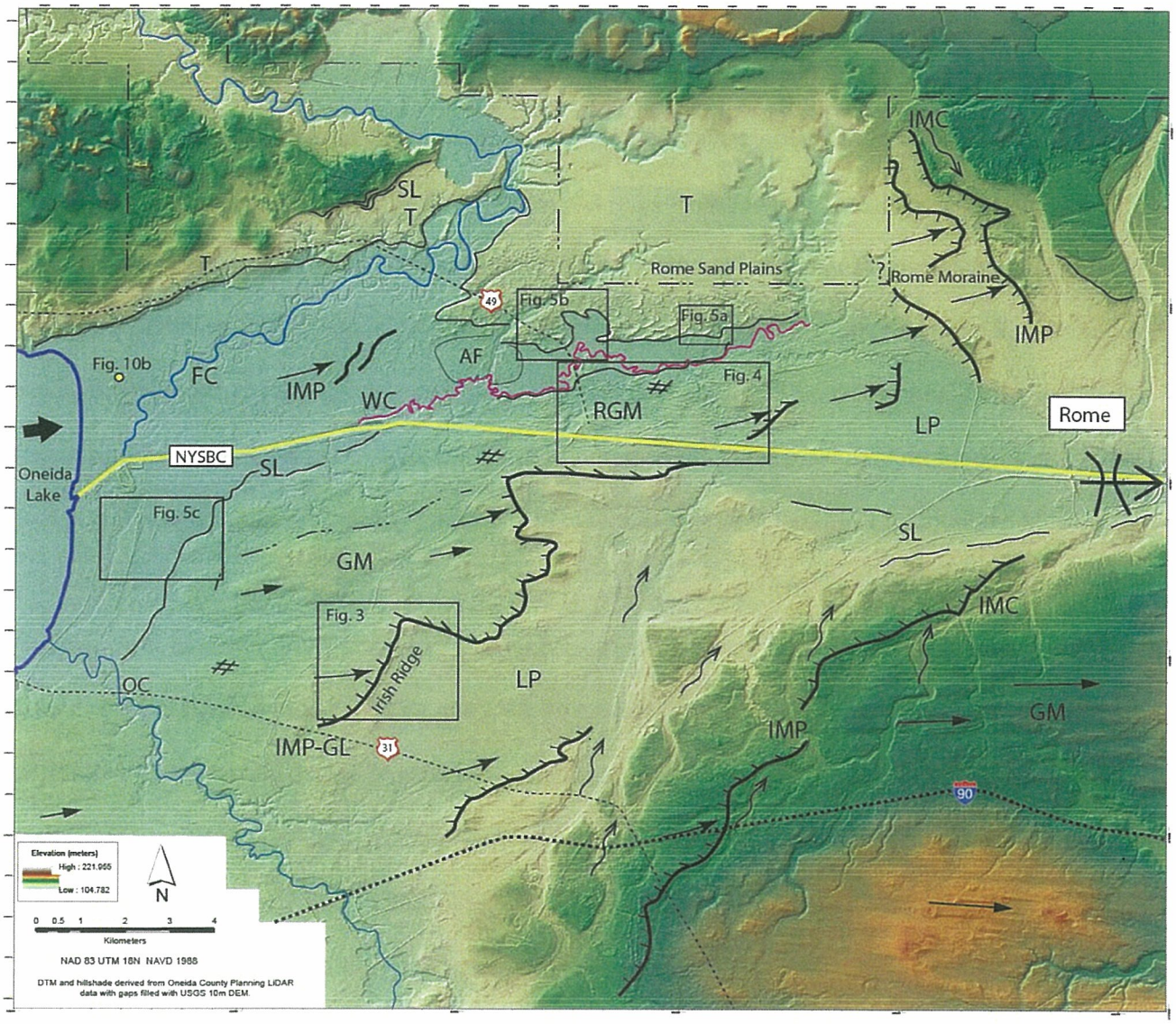

Fig. 2. Topography of the Oneida Lake Lowland (basin) and surrounding uplands of the Allegheny and Tug Hill Plateaus (southeast and north, respectively) showing detailed landforms, locations of key localities or features, and additional figures as follows: city of Rome N.Y., Interstate Route 90, State Routes 31 and 49 (dashed lines), New York State Barge Canal (NYSBC and yellow line), lake plains (LP), ground moraine (GM), ice marginal position (IMP and solid bold line), grounding line (GL), shoreline (SL), ice marginal channels (IMC and wavy arrows), reticulated ground moraine (RGM and cross hatched lines), alluvial fan (AF), terrace (T), Fish Creek (FC, blue line), Oneida Creek (OC, blue line), Wood Creek (WC, purple line), directions of glacial flow (small strait and curved arrows), main axis of Oneida Lake (large bold arrow), and drainage divide south of Rome N.Y. (vertical saddle with arrow). Elevations are provided by Oneida County Lidar data and USGS 10 m DEM as delineated by dashed and dotted boundary line as rendered by D. Tewksbury (Hamilton College).

features hold important information regarding the recession of ice lobes and glacial lakes from Central New York at the close of the last glaciation, since the regional topography divides in three major ways within the area (Fig. 1). The Oneida Lake Lowland is the easternmost extent of the Ontario Lowland and is bordered by the Tugg Hill Plateau to the north and the Onondaga bench (edge of Alleghany Plateau) to the south (Figs. 1 and 2). The drainage divide (col) near Rome N.Y., which has an elevation of ~131 m asl marks the lowland's eastern boundary. Since the eastern end of the Oneida Lake Basin was the first to experience the effects of a newly formed GLI, and continued to be influenced by it during its entire existence, the landforms present within the Oneida Lake Basin contain a valuable record of temporal and limnic changes in the region. Within the central axis of the lowland there is a very low gradient to the landscape with only a minor saddle between the modern Lake Ontario and Oneida Lake shoreline, which means that past changes in lake levels and the effects of changes in outlet far afield would have produced large swings in the position of paleo-shorelines. Landforms related to these shores therefore provide accurate dipsticks by which to define the timing of climatic events and/or help understand ice sheet dynamics across the entire region if they can be numerically dated.

Despite these obvious attributes the detailed morphology and landform associations are poorly defined. Surficial mapping completed by Wright (1972) identified only a few of the more prominent landforms across the area and did not adequately account for complexity of landform superposition, whereby surficial landforms have been superimposed upon underlying Late Quaternary features (Figs. 3-5). The early mapping studies also did not clearly address cross-cutting relationships between adjacent landforms. For instance, discordance amongst several sets of beach ridges east of the modern shoreline of Oneida Lake (Fig. 5c) are included within a single general map unit of lacustrine sediment (Muller and Cadwell, 1986) and units mapped as lacustrine sand are clearly ice marginal, kame deposits or moraines (Fig. 3).

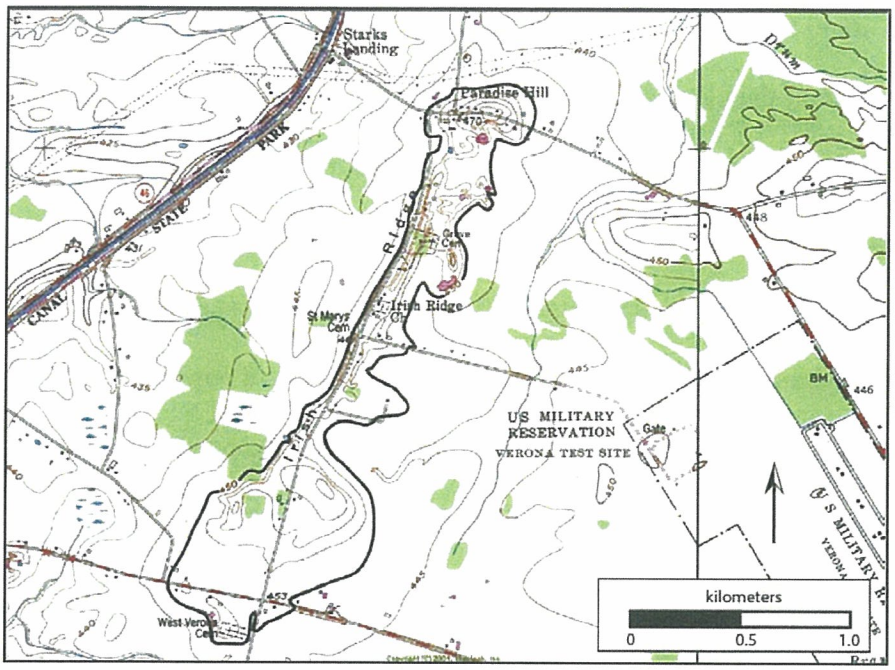

Fig. 3. Topography along portion of Irish Ridge Road with 450' contour in bold, from USGS quadrangle contour interval = 5'.

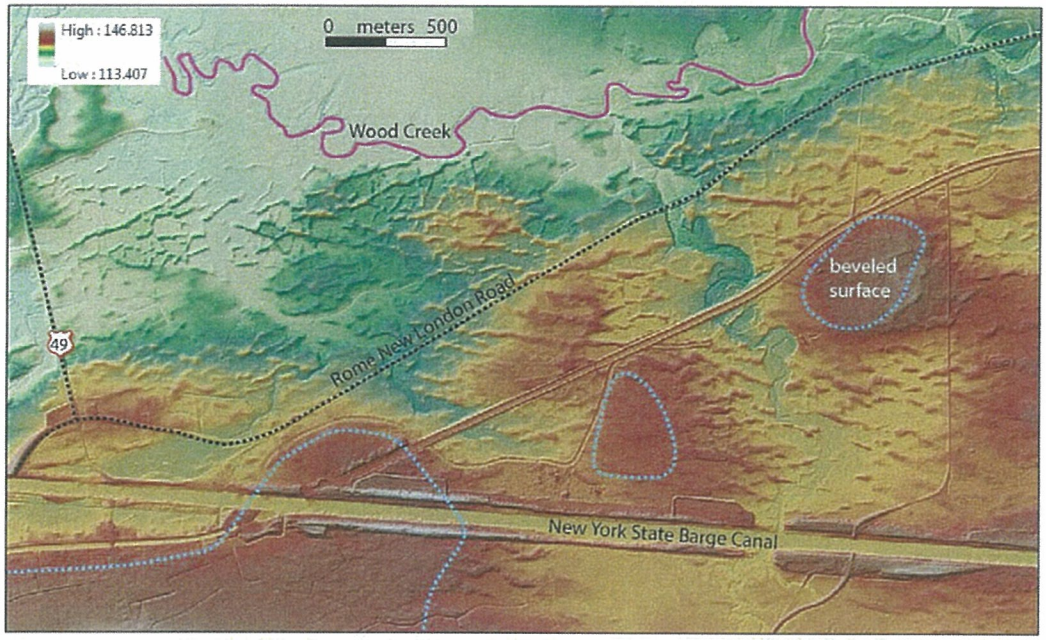

Fig. 4. Lidar topographic image of reticulated ground moraine as seen in eastern end of basin, along the New York State Barge Canal and the Rome to New London Road. Note less relief or limited expression on the higher elevations (beveled surface as outlined by blue dashed line) and erosion of landforms along Wood Creek, to the north.

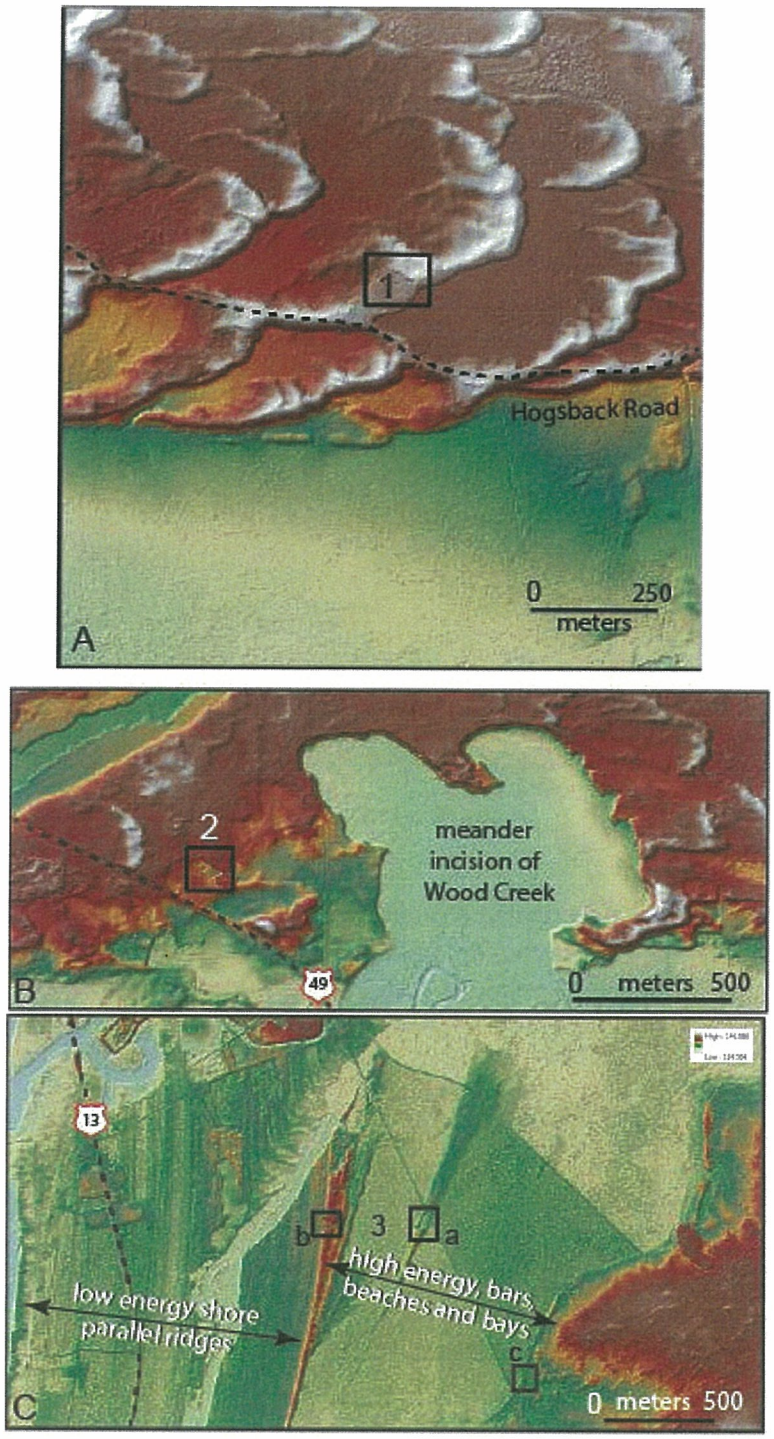

Fig. 5. (A) Lidar topography of Rome Sand Plains with location of dated section 1, (B) sand terrace near State Route 49, with location of subaqueous sand beds 2, and, (C) paleo-shorelines with locations of dated sections 3a, b, and c.

Relationships to the specific positions of GLI (as discussed above) are equally unclear within the Lake Oneida basin. Illustrations of shoreline position (Pair and Rodriques, 1993, their Fig. 5) do not correspond to any specific feature identifiable on either the topographic maps of the basin or the surficial mapping compiled by Muller and Cadwell (1986). Pair and Rodriques (1993) dispute the location of the GLI spillway, variously assumed to be at Rome NY (elevation ~ 131 m asl), but recognized by earlier workers to have been located at about 155 m asl, across the crystalline bedrock sill at Little Falls, NY (Fig. 1). Further, there are no published numerical ages on any of the landform associations within this complicated landscape (Fig. 2).

For these reasons we began a long-term investigation on the Quaternary landforms on the eastern end of the Oneida Lake Basin with the goal of refining surficial mapping, reinterpreting peculiar landforms, and establishing a chronostratigraphy for the Late Quaternary landforms (Arnold, 2004; Hiscott, 2000; Fadem, 2001a,b; Cleary, 2002; Panyushkina, et al., 2012; Domack, 2010; Domack, et al., 2011; Murari, et al., 2011). This effort has been enabled recently by the acquisition of Lidar topographic data, obtained via Oneida County's effort at flood hazard rezoning. This paper deals with the first set of radiocarbon and optically stimulated luminescence (OSL) ages on aeolian landforms in the area and the surfaces upon which they developed.

Methods

Mapping

Landforms were mapped using LiDAR aided by field investigations at critical sites. The landforms and sediments were described using standard methods and nomenclature as outlined in Benn and Evans (2010). We focused our studies in several areas including the Allegheny Escarpment, Rome Sand Plains, "Irish Ridge" System, and Reticulate Ridges along the Rome New London Road (Fig. 2).

Optically stimulated luminescence (OSL) dating

OSL samples were collected by hammering 20-cm-long, 5 cm-diameter steel tubes into cleaned, logged sediment faces. Tubes were kept sealed until opened in the laboratory at the University of Cincinnati. A 3 cm-thick layer of sediment was removed from each end of the tube to obtain sediment from the center of the tube for processing and to reduce the possibility of any analyzed sediment having been exposed to daylight while sampling. The sediment from the end of the tubes was dried to determine the water content of each sample (Table 2). The sediment was then crushed and sent to the U.S. Geological Survey in Denver, Colorado for instrumental neutron activation analysis (INAA) to determine the U, Th and K concentrations for dose rate (D_R) determination (Table 2). The sediment from the center of the tubes was pretreated with 10% HCl and 10% H_2O_2 to remove carbonates and organic matter, respectively. The pretreated samples were rinsed in water, dried and sieved to collect the 90-250 μm particle size fraction. This fraction was etched using 44% HF acid for 80 minutes to remove the outer, alpha irradiated, layer from quartz particles also it dissolves feldspar. Any fluoride precipitates were removed using concentrated HCl. The quartz sample was then rinsed in distilled water and acetate, then dried and sieved to obtain a grain size fraction of 90-150 μm in diameter. A low field controlled Frantz isodynamic magnetic separator (LFC Model-2) was used to separate feldspar and magnetic minerals from quartz in the 90-150 μm particle size fraction (Porat, 2006) with the forward and side slopes were set at 100° and 15°, respectively, in order to get clean quartz, each sample passed through magnetic separator for three times by varying magnetic field intensity.

An automated Risoe OSL reader model TL-DA-20 was used for OSL measurements and irradiation. Aliquots, containing approximately several hundred grains of each sample, were mounted onto ~9.7 mm-stainless steel discs as a small central circle approximately 3 mm in diameter. Feldspar

Table 2

OSL sample locations, radioisotope data, equivalent dose and dose rate data, and ages.

Sample name	Latitude (°N)/ Longitude (°W)	Altitude (m asl)	Depth (cm)	Water content (%)	Uranium (ppm)	Thorium (ppm)	Potassium (%)	Cosmic dose rate (μGy/ka)	Total Dose rate (Gy/ka)	Number of aliquots measured	Weighted mean equivalent dose (Gy)	Mean equivalent dose[#] (Gy)	Weighted mean age[#] (ka)	Mean age (ka)[#‡]
HESS 1	43.18139/75.70298	118	94	8.5±0.9	0.37±0.02	1.10±0.06	0.46±0.02	178±36	0.71±0.05	27(36)	10.7±0.1	10.3±0.5	15.1±1.0	14.5±0.7
HESS 2	43.18139/75.70298	118	109	10.1±1.0	0.59±0.03	1.56±0.08	0.55±0.03	173±35	0.84±0.05	21(36)	9.3±0.1	10.4±0.5	11.1±0.8	12.4±0.7
HESS 3	43.22971/75.56737	126	132	3.7±0.4	0.59±0.03	1.44±0.07	0.54±0.03	167±33	0.87±0.05	24(36)	11.8±0.1	11.9±0.3	13.5±0.9	13.6±0.4
HESS 4	43.22971/75.56737	126	191	3.8±0.4	0.79±0.04	2.49±0.12	0.54±0.03	150±30	0.96±0.05	24(36)	11.0±0.1	11.4±0.3	11.5±0.9	11.8±0.5
HESS 5	43.22971/75.56737	126	295	2.9±0.3	1.05±0.05	3.29±0.16	0.56±0.03	126±25	1.07±0.06	27(36)	12.8±0.2	13.0±0.6	12.0±1.0	12.2±0.8
HESS 6	43.22960/75.60000	87	215	3.0±0.3	0.95±0.05	3.20±0.16	0.73±0.04	143±29	1.21±0.06	27(36)	26.4±0.3	27.3±0.9	21.8±2.0	22.5±1.4
HESS 7	43.22960/75.60000	87	320	3.2±0.3	0.69±0.03	2.43±0.12	0.54±0.03	121±24	0.91±0.05	28(36)	27.3±0.2	28.2±0.7	30.0±2.0	31.0±1.1
HESS 8	43.22960/75.60000	87	420	3.1±0.3	0.80±0.04	2.61±0.13	0.58±0.03	103±21	0.96±0.05	26(36)	26.3±0.3	26.5±0.7	27.2±1.9	27.4±1.0
HESS 9	43.22910/75.72197	59	30	5.5±0.5	0.52±0.05	1.90±0.19	0.48±0.02	198±40	0.87±0.05	18(24)	5.1±0.1	5.4±0.3	5.9±0.5	6.2±0.4
HESS 10	43.22910/75.72197	59	100	14.2±1.4	0.39±0.04	0.91±0.09	0.10±0.01	174±35	0.41±0.04	20((24)	5.7±0.1	5.8±0.2	13.9±0.7	14.0±0.3
DALE 5	43.18743/75.71421	119	125	10.0±5.0[*]	0.36±0.04	1.17±0.12	0.45±0.02	183±18	0.72±0.04	25(28)	6.5±0.4	7.4±0.4	9.0±0.8	10.3±0.9
DALE 6	43.18767/75.70892	119	225	10.0±5.0[*]	0.76±0.08	2.10±0.21	0.71±0.04	163±16	1.07±0.06	22(28)	10.4±0.7	12.4±0.8	9.7±0.9	11.6±1.3
M1-A	43.05094/75.40944	274	350	2.0±0.2	1.52±0.08	4.23±0.21	0.93±0.05	119±24	1.7±0.1	22(24)	72.3±0.5	80.8±3.8	43.5±1.9	48.6±3.1
M1-B	43.05094/75.40944	274	446	2.0±0.2	1.19±0.08	3.67±0.18	0.95±0.05	102±20	1.6±0.1	23(24)	84.6±0.6	91.4±3.2	54.0±2.3	58.3±3.3
M2-A	43.05094/75.40944	274	350	2.0±0.2	1.25±0.08	3.50±0.18	0.82±0.04	119±24	1.4±0.1	23(24)	71.3±0.7	87.2±4.4	49.3±2.1	60.4±4.0
M2-B	43.05094/75.40944	274	446	2.0±0.2	1.10±0.08	3.22±0.18	0.97±0.05	102±20	1.5±0.1	23(24)	65.6±0.4	79.6±4.4	42.7±1.9	51.8±3.7

*Numbers of aliquots used in calculating the age with total number of aliquots measured shown in parentheses.

[#]Uncertainty is expressed as a standard error.

[†]Dose rate is very low and may reflect leaching of K from the sediment.

[‡]Ages were calculated using the software of Grün (1991)

[·]Water content was not measured directly in laboratory and values were estimated

contamination was checked on several aliquots of each sample using infrared stimulated luminescence (IRSL) at room temperature before the main OSL measurements were undertaken (Jain & Singhvi, 2001). If a sample did not pass the IRSL test then further etching in 44% HF for further 30 minutes was undertaken remove any remaining feldspar, followed by 10% HCl treatment and repeat of sieving. Samples that then passed IRSL test after this treatment were then measured.

Aliquots of samples were illuminated using blue LEDs stimulating at a wavelength of 470 nm (blue light stimulated luminescence – BLSL). The detection optics consisted of a Hoya U-340 and Schott BG-39 color glass filters, coupled to an EMI 9235 QA photomultiplier tube. The samples were irradiated using a $^{90}Sr/^{90}Y$ beta source. Equivalent doses (D_E) were determined using the single aliquot regeneration (SAR) method of Murray and Wintle, (2000). A preheat at 240 °C for 10 s was used and the OSL signal was recorded for 40 s at 125 °C. OSL sensitivity of the samples had a high signal to noise ratio. Only aliquots that had a recycling ratio of <10% were used in determining the mean D_E for age calculation. Dose recovery tests (Wintle and Murray, 2006) were undertaken on the samples to check whether the laboratory dose could be recovered to within 2% using the SAR protocol. The mean and standard error of D_E and D_R and their associated uncertainty were used to calculate the OSL age (Table 2). The OSL ages were also determined using the weighted mean, which skews toward the lower D_E values that generally have lower uncertainties associated with them, and therefore provides a minimum estimate of the OSL ages. However, we use the ages determined by the mean and standard error of the D_E values to define the ages in our study.

Data used in the age calculations is presented in Table 2 and typical OSL characteristics are illustrated in Figure 6. All samples had dose recovery within 2% (Fig. 6). The shine down curves these samples showed the sharp decay, which confirm that the OSL signal is dominated by the fast component (Fig. 6). This provides confidence that the samples would have been rapidly bleached

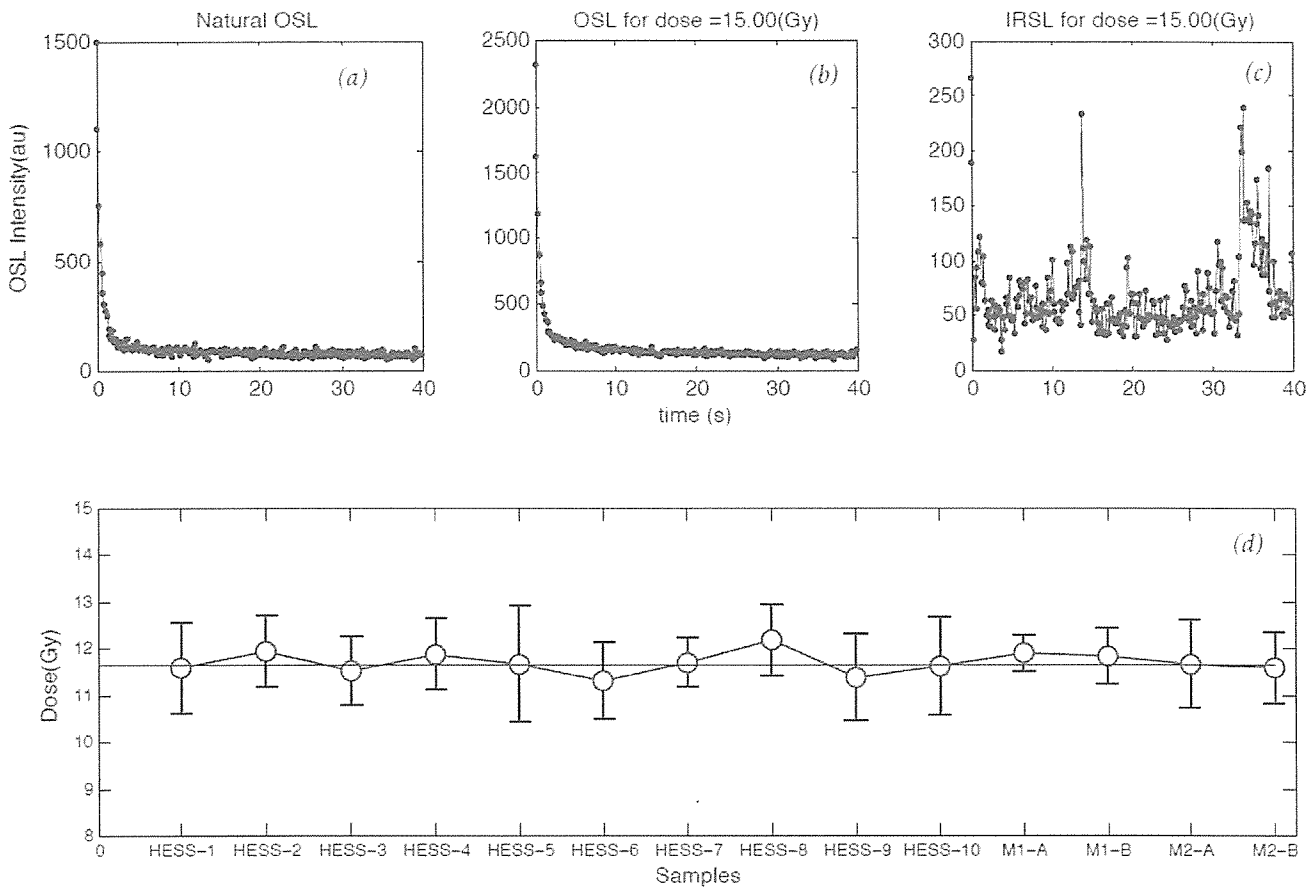

Fig. 6. Typical shine down curves for sample HESS 6. A) A typical natural blue optically stimulated luminescence (BLSL) shine down curve; B) a blue OSL shine down curve for 15 Gy beta dose; C) infrared stimulated luminescence (IRSL) for 15Gy beta dose that confirms the absence of any feldspar in the sample. D) Dose recovery test for sample, a dose of ~11.65 Gy was given to sample and recovered back using single aliquot regenerative-SAR method. The dose recovered for each sample is mean of 5 aliquots and error bars are standard deviation for these aliquots. This test shows almost every sample mean value for recovered dose within the range of 2-3% of uncertainty.

prior to deposition and would not result in an overestimation of the depositional age (Aitken, 1998). The spread of D_E values for individual samples is significant, but is fully expressed the mean and standard error and the fast shine down curves and low luminescence signals provide confidence in the ages and that they are not overestimates. Samples DALE 5 and DALE 6 provide similar ages to the radiocarbon ages, which provides further confidence in the OSL methodology and ages (see discussion below).

Radiocarbon dating

Materials for radiocarbon dating were retrieved from two localities within GLI shoreline deposits (Fig. 5C and Table 3). At these locations several meters of surficial aeolian dunes happened to have been removed by mechanized excavation, for road building and construction of a shooting range. This unique situation allowed access to subsurface gravels and sandy gravels via manual digging and bucket auger. Sediment was thus recovered to a maximum depth of about 2 m below the ground surface, down to and just below the water table (see, Hiscott, 2000, and Fadem, 2001a,b). However precise stratigraphic placement of each dated shell relative to each other was not possible, due to caving in of water- saturated sediment. A significant amount of shell material was recovered at both sites, which included complete half valves of fingernail clams (*Sphaerium similie*), larger unidentified clams, and gastropods. Most shell debris had evidence of partial dissolution and larger clams had well preserved pearly luster along interior surfaces. There was no evidence of secondary recrystallization upon examination beneath a binocular microscope. Only the best-preserved (minimal dissolution) shells were sent for radiocarbon analysis after cleansing in H_2O_2 and rising with distilled water. Samples were sent to Geochron Laboratories at Oxford University and the National Ocean Sciences Accelerator Mass Spectrometry Facility (NOSAMS) facility Woods Hole Oceanographic Institution, Woods Hole Road Woods Hole, MA, USA. Ages reported in Table 1

Table 3

Radiocarbon ages from mollusc shell debris recovered from two sites within paleo-beach deposits shown in Figure 3C (after Fadem, 2001).

Sample type	Sediment	$\delta^{13}C$	Radiocarbon age (years)	Calibrated Age 1 σ uncertainty (years BP)	Calibrated Age 2 σ uncertainty (years BP)
Locality 3a					
OL-0 *Sphaerium simile*	gravelly sand	-9.5‰	10,730 ± 85	12,570 – 12,700/12,530 – 12,870	12,680 – 12,990
OL-3 *Sphaerium simile*	gravelly sand	-10.2‰	10,800 ± 50	12,610 – 12,730	12,580 – 12,850
Locality 3b					
OL-23 *Sphaerium simile*	gravelly sand	-10.1‰	10,990 ± 40	12,740 – 12,940/13,000 – 13,070	12,680 -- 12,990
OL-28 *Helisoma companulatum c.*	gravelly sand	-6.7‰	10,200 ± 40	11,820 – 12,000	11,760 – 12,060 11,130 – 11,240
OL-29 *Helisoma companulatum c.*	gravelly sand	-6.9‰	9,760 ± 40	11,180 – 11,220	

are not corrected for any hard water effects but are adjusted for the $\delta^{13}C$ value of the carbonate shell, as included in Table 1. We report ages as calibrated following the CALIB 6.0 routine of Stuiver et al. (2011) (see: http://calib.qub.ac.uk/calib/; as discussed by Reimer et al., 2004).

At present there is no information on the hard water correction for fossil mollusks within the Oneida Lake basin and so we have declined to provide any correction to the radiocarbon ages. However, we wish to point out several observations which suggest that any such correction is not likely to be large in the case of the data reported in Table 1. Hard water corrections have been reported for other Great Lake fossil mollusks and these include: 250 years for Lake Michigan, 440 years for Lake Huron (Rea and Coleman, 1995), and 535 years for Lake Ontario (Anderson and Lewis, 2012). In the case of Oneida Lake there are important considerations to keep in mind. Among these is the fact that Oneida Lake is surrounded by less carbonate rock than the Great Lakes in general. Also the $\delta^{13}C_{carb}$ of the species in question (*Sphaerium similie*) is consistently isotopically lighter (~10‰) than one would expect, given a large role for DIC incorporation (usually close to 0 ‰; i.e. -3.0 ‰, Rea and Colman, 1995). Instead the relatively light carbon would indicate either an unusual vital effect and/or some incorporation of remineralized organic matter (i.e., soil carbon or algal carbon) during metabolism. Either way, the effect would be to make the ages somewhat younger, not older than expected. This would offset or diminish substantially any hard water (residual DIC) effect present within this system. The fact that modern fingernail clams from the region (but not this basin) still retain a moderately light $\delta^{13}C_{carb}$ signature (Wurster and Patterson, 2001) would suggest that a hard water correction may not be necessary. Unfortunately reports of hard water corrections in the Great Lakes do not utilize *Sphaerium similie* and in some cases do not even report $\delta^{13}C_{carb}$ values, or even pre-bomb specimens (Anderson and Lewis, 2012), thus making a more thorough comparison difficult. We prefer to present our ages without the hard water correction, until such a time when pre-1950 specimens of *Sphaerium similie* can be located for analysis—the search is ongoing.

Allegheny Escarpment

The southern border of our study area includes the prominent hills and valleys that collectively define the northern edge of the Allegheny escarpment. While the overall north-to-south orientation of the major drainages reflects the selective linear erosion of the Finger Lakes valleys and interfluves (Mullins and Hinchey, 1989) the most recent episode of glacial sculpting has marked a set of prominent west-to-east streamlined features (Fig. 2). This is due the shift in ice sheet flow from full Last Glacial Maximum (LGM) to the Late Glacial when the emergent Adriondacks bifurcated the SE Laurentide Ice Sheet into the Ontario Lobe and the Mohawk Lobe (Fig. 1). Hence, during the later stages of glaciation across the Ontario Lowland ice sheet flow was directed eastward from the west to northwest (Hess and Briner, 2009; Figs. 1 and 2).

The upland region is generally mantled with a sequence of ground moraines and scattered ice contact deposits of stratified drift and localized glacial lake muds and sands (Cadwell 1991). Across this forested and agricultural landscape distinct pre-LGM units can only be recognized within scattered and discontinuous exposures. In order to provide a relative age test of our OSL methods we identified one of the more persistent of these pre-LGM units near Clinton, New York for sampling and analyses. On the campus of Hamilton College we were afforded the opportunity for sampling fresh exposures of a locally widespread sand unit that can be found and traced to lie below the LGM till horizon at elevations of between 260-275 m. We obtained four samples for OSL dating from within adjacent exposures of a very well sorted, fine-grained sand unit, which lies below a red till. Between the till and the sand there is a thin discontinuous horizon of laminated clays and silts (presumably lake or pond deposits) that are distinctly deformed and partially incorporated in the basal portions of the till deposit. This provides clear evidence for ice over riding and partially eroding the stratigraphy, which in this case preserved a sand unit of undetermined thickness. This succession is nearly identical to other exposures found across the region, such as near Cortland and Auburn New

York (Friends of the Pleistocene field trip personal communication Dave Barclay and Andy Koslowski, 2014).

Our age results ranged from 48.6 ± 3.1 ka to 60.4 ± 4.0 ka (Table 2; Fig. 1 in Supplement item 1) thus confirming a Mid Wisconsinan age for the sand beneath the till and correlation to the Port Talbot Interstadial (Muller and Calkin, 1993; Dremanis et al., 1966). The utility of this observation is that it establishes the applicability and reliability of the OSL technique to resolving (within reason) numerical ages for sediments of interest in the study area.

Rome Sand Plains

The Rome Sand Plains comprise one of the better known landforms in the study area (Figs. 2 and 5A, B) and include a spectacular set of well-preserved parabolic dunes and associated ecosystems including pitch pine barrens and perched peat bogs that cover nearly 61 km^2. While the Rome Sand Plains have been studied for some time there is actually very little known about the age of the aeolian dunes. Most recently Kurczewski (1999) ascribed origin the aeolian dunes to having formed from sands that were washed into Glacial Lake Iroquois at its southeastern end as the lake level subsided following glacial recession. The dune forms themselves are only the most recent set of features which lie upon an elevated "terrace" that boarders the north eastern side of the Oneida Lake Lowland, below the limestone core of the Tug Hill Plateau that lies to the north (Figs. 1 and 2). The terrace core itself is at about 137 m asl in elevation and is cut by meanders of Wood Creek and as of yet unevaluated ridges that parallel the break in slope between the "sand plains" and the alluvial valley of Fish and Wood Creek (Figs. 2 and 5A, B). One of the dune forms is well exposed by an excavation into the southern prong of the parabola which reveals steep foresets (dipping towards 110°) overlain by laminated, well sorted, fine to medium sand and silty sand (Figs. 5A and 7). We obtained three samples for OSL dating across the facies, as illustrated in Figure 7 (see methods section for sampling protocol). From the top of the section (at 142 m asl) to the bottom the ages are

Supplemental Figure 1: Measured section observed on the Hamilton College Campus and location of four OSL samples (M1-A, -B and M2-A, -B). Excavation was for the construction of the Wellin Art Museum, as observed on 9/11/11.

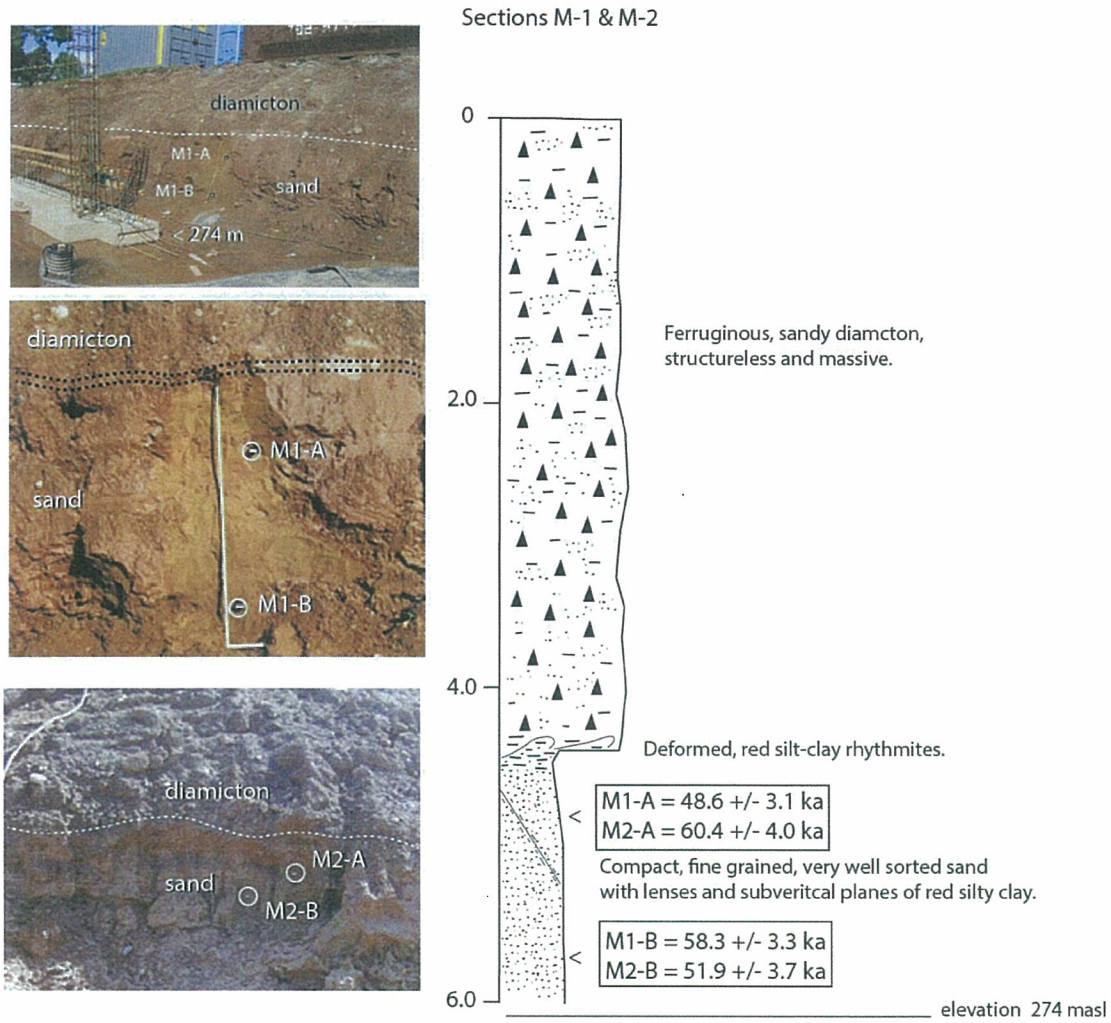

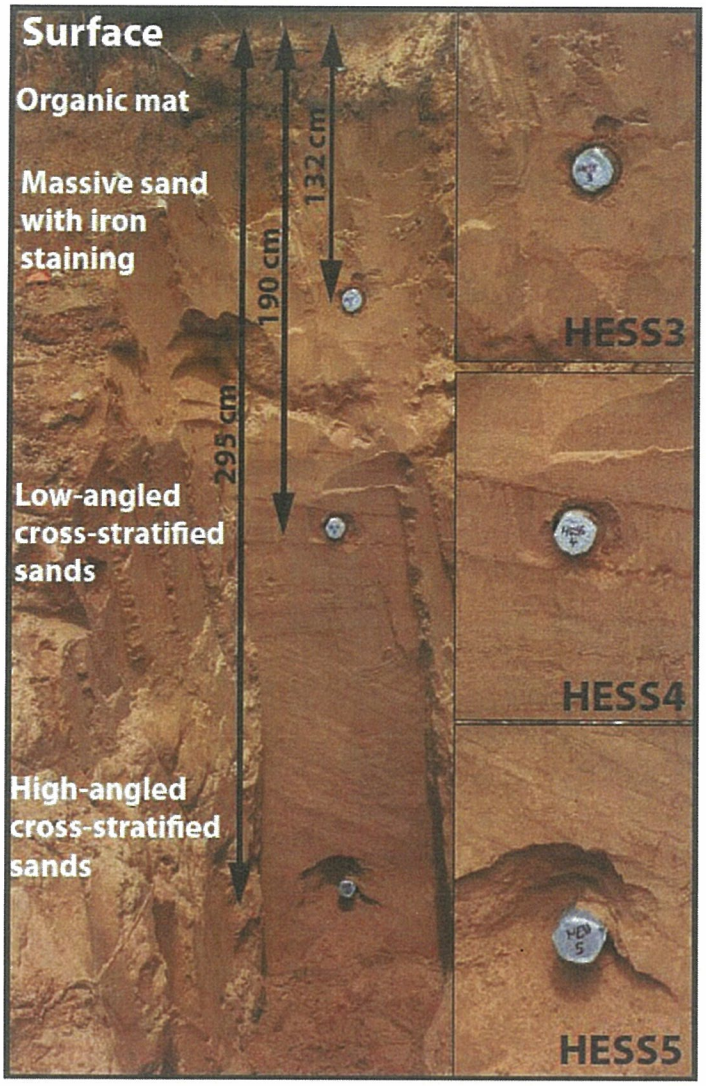

Fig. 7. View of section within parabolic dune located in Fig. 2 and 5A, with location and age result of OSL samples. Excavation into the dune form was completed by hand.

13.6 ± 0.4 ka, 11.8 ± 0.5 ka and 12.2 ± 0.8 ka (Table 2; Fig. 7). Although the top two ages appear stratigraphically reversed but they are overlapping within 2 σ uncertainty of each other and are therefore essentially the same age. There is a significant amount of dune sand yet to be examined and sampled for age control, particularly below this particular dune form (Fig. 5A, B) and its contact with the underlying "terrace".

An exposure within the top of the terrace, upon which the aeolian dunes formed, lies about 3.6 km to the west of the dated dune (Figs. 5B and 8). A mechanized excavation just off Route 49 reveals a sequence of stratified, subaqueously deposited sand that lies stratigraphically below parabolic dune forms found in close proximity (Fig. 5B). The succession of sand consists of two units: 1) a lower interbedded succession of climbing ripple drift, cross laminated, fine to medium grained sand and thin bedded silty, fine grained sand; and 2) an upper trough cross bedded succession of gravelly coarse sand and very coarse sand (Fig. 8). These units are separated by a prominent disconformity marked by channelization into the lower unit by the upper unit. The lower unit suggests continuous, subaqueous deposition, perhaps on a delta front, and the upper unit is more indicative of small braided channels related to shallow fluvial processes. Samples for OSL dating were collected across both units (Fig. 8) and from top to bottom yield ages of 22.5 ± 1.4 ka, 31.0 ± 1.1 ka and 27.4 ± 1.0 ka (Table 2 and Fig. 8). Although the lower two ages appear stratigraphically reversed they overlap within 2 σ uncertainty of each other and are therefore essentially the same age.

"Irish Ridge" System

Pertinent to our discussion of the development of the landscape east of Oneida Lake are the prominent set of irregular and discontinuous ridges exemplified by Irish Ridge Road (Figs. 2 and 3). Features such as these occur with crest elevations of between 137 and 143 m asl with significant variation in crest elevation along the linear trend of the ridgeline. These features also serve to separate a somewhat

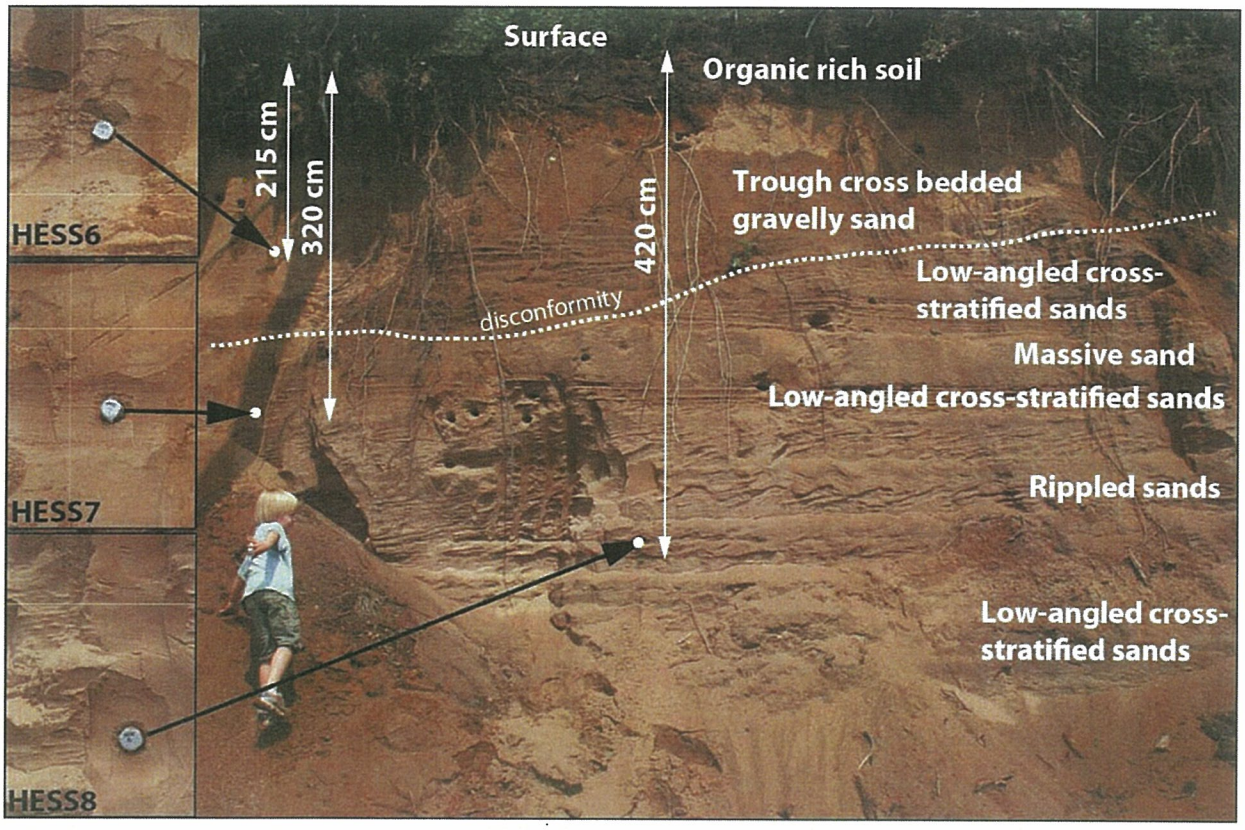

Fig. 8. Stratigraphic exposure of units exposed near top of the Rome Sand Plains "terrace" with locations and result of OSL samples and located in Fig. 5B.

irregular streamlined topography (to the west) and a strikingly flat terrain (to the east) across the Verona Test Site Military Reservation (Fig. 3). The trend of the ridges themselves are irregular and do not parallel any presumed shoreline and in fact the continuity of the "ridges" is rather more like a beaded system suggesting that those processes leading to their accretion were spatially variable along the trend line. The lateral distribution of the beaded ridges defines a salient and reentrant pattern such that a pronounced eastward bulge (salient) in the crest lines is present toward the axis of the Oneida Basin, toward the Rome divide. In contrast the southward extent of the ridge system defines a reentrant as the general elevation of the landscape increases (such as at Irish Ridge Road). This pattern is parallel to the pronounced set of ice marginal channels incised into the northern edge of the Allegheny escarpment, as seen along the southeastern portion of our study area (Fig. 2; Muller and Cadwell, 1986). Internally the ridge system is composed of sandy gravel and gravelly sand as seen in relict aggregate pits near Paradise Hill and Grove Cemetery (Fig. 3). A single ~50 m long ground penetrating radar line (run orthogonal to the ridge crest along the northern boundary of Grove Cemetery) demonstrated pronounced foresets with a uniform eastward dip (Hiscott, 2000). In cross section the ridges have a clear asymmetry with steeper westward slopes that are rather uniform and gentler eastward slopes that are irregular with bulges and depressions (Fig. 3). According to Wright (1972), and Muller and Cadwell (1986) ridges such as these, including Irish Ridge Road, were mapped as "lacustrine sand" with little elaboration.

Reticulate Ridges

Within the easternmost extension and axial depression of the Oneida Basin (east of Route 49, along the Rome New London Road) a peculiar set of reticulated ridges are present (Fig. 4; Clements, 2014; Domack et al., 2014). These features define a conjugate set of intersecting ridges that define a polygonal or reticulate network that covers a significant area (Fig. 2). The ridges are symmetric in

cross-section and in the single exposure, so far examined, are observed to consist of compact diamicton. The extent of the reticulated terrain is limited by erosion along the borders of Wood (to north), Stony (to northeast) and Fish Creeks (to west). The barge canal limits these features to the south. The eastern limit of this reticulated relief is limited by the Rome moraine complex which itself seems to correspond to the easternmost extension of the "Irish Ridge" line as described above.

These landforms did not figure prominently in the mapping done by Wright (1972) and Muller and Cadwell (1986) probably because the typical relief of most of these features was not discernable on topographic elevation maps of the time. In contrast, the recent Lidar data is present in our paper (Fig. 4), clearly demonstrating their continuity and unique character (Clements, 2014; Domack et al., 2014). There are features similar to this, but of far more subtle relief, found across the "till uplands" just SE of modern Oneida Lake (Fig. 2). Of additional importance is the clear change in relief of the rides and swales as the general elevation changes. As seen in Figure 4 the higher elevation regions appear to have lost all expression of the individual ridges and appear to have been beveled off while at lower elevations the swales seem to be flattened (as if filled-in) between the prominent crests of individual ridges.

Lake Shorelines

The most obvious set of shoreline features in our area are present ~26 m below the Rome Sand Plain "terrace" and 10 km to the southwest of the Rome Sand Plain (Figs. 2 and 5C). The most prominent of these features run in a northeast to southwest direction and display a northward splaying in their width (similar to spit morphology; Fig. 5C). Aeolian dunes of well-sorted fine to medium grained sand cap two of widest of these shorelines (3a, b in Fig. 5C). A younger set of shoreline ridges run parallel to the modern shoreline of Oneida Lake (Fig. 5C). These crosscut the youngest of the more prominent shorelines, as can be seen ~1.6 km east of the modern Oneida Lake shoreline (Fig. 5C). Both sets of shoreline ridges are delineated by the 114 m asl topographic contour, although capping

dunes in the beach ridges extend the elevation of these features by another 6 m (Fig. 9).

Excavations down into the higher shore deposits (Fig. 9) reveal coarse sandy gravel to gravelly sand, rich in mollusk fragments and whole valves, mostly *Helisoma* (a gastropod) and *Sphaerium* sp. (a fingernail clam; Fadem, 2001a,b). In contrast, the subdued parallel shorelines are dominantly fine to medium sand and lack shell material. Radiocarbon ages have been obtained from shell debris in two of the irregular, higher shorelines (Table 3, 3b in Figs. 5C and 9) and range in age from 10,990 + 40 ^{14}C years BP (*Spherium simile*) to 10,200 + 40 ^{14}C years BP and 9,760 + 40 ^{14}C years BP (on *Helisoma* c. c.; Table 3). A large set of aeolian dunes are present immediately above the most westward of the shorelines. The best preserved of these features are to be found in Verona Beach State Park, at the State Police gun range (Figs. 4C, and 8). Two samples were collected from this locality (3b in Fig. 5C) from within the aeolian dunes for OSL dating, which yielded ages of 10.3 + 0.9 ka to 11.6 + 1.3 ka (Tables 1 and 2, and Fig. 9). The OSL samples are offset laterally from the radiocarbon samples by less than 10 m. One other excavation was dug in the higher shorelines as located at 3c in Figure 5. Here a uniformly sorted medium grained sand was found with a prominent soil profile including a superimposed O horizon beneath a typical Spodosol profile of Fe enrichment (Fig. 10 A). Two samples were collected from within a clean unaltered quartz rich sand, about 1 m below the alteration horizons (Fig. 10A), with resultant OSL ages of 14.5±0.7 ka and 12.4±0.7 ka (Table 2).

The lower elevation, parallel, shoreline deposits were excavated at one locality-- located about 1 km from the NE corner of Oneida Lake (Fig. 2). Here, two samples for OSL dating were obtained from medium-grained sand. These were collected from distinctively different horizons (Fig. 10B), one within the zone of mineral leaching (HESS9) and the other within unaltered quartz rich sand, just above the water table (HESS10). Ages ranged from 6.2±0.4 ka to 14.0±0.3 ka (Table 2). We consider the 6.2 ka age more reliable because HESS 10 sample has abnormally low K concentration, which is

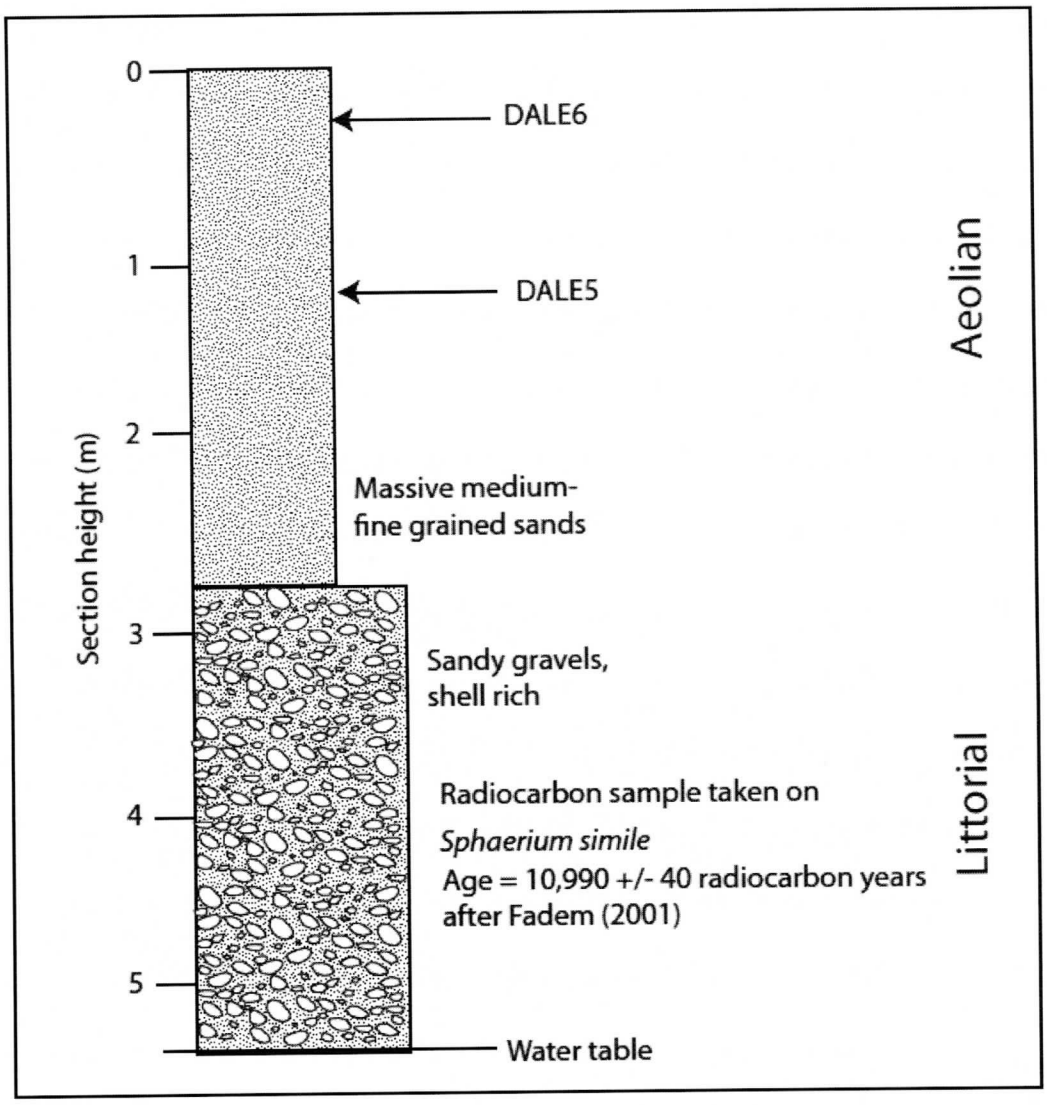

Fig. 9. Composite stratigraphic section of fossiliferous, shoreline deposit and overlying aeolian dune, located as location 3b, Figure 5C. Location and result of radiocarbon and OSL samples.

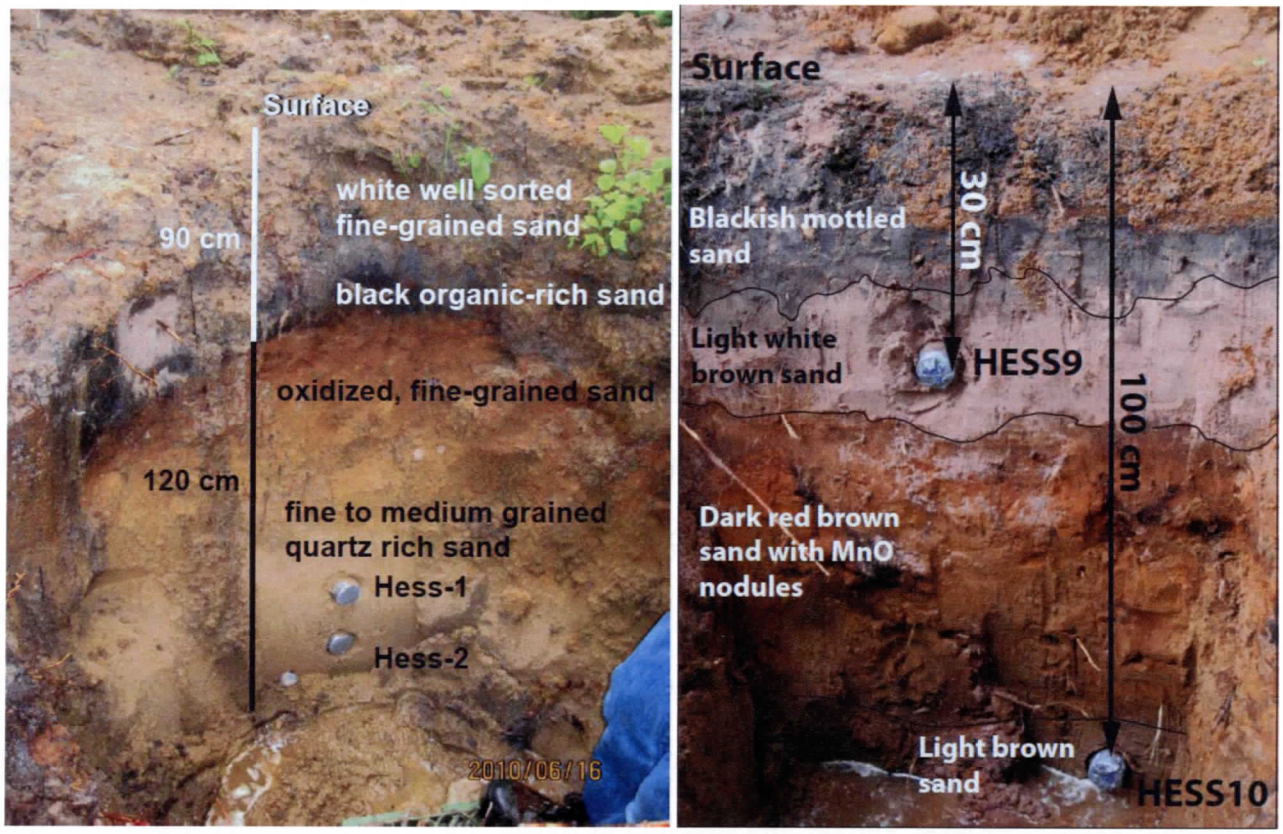

Fig. 10. A) Excavation of shoreline beach deposit located in Figure 5 C-c with location of OSL samples. B. Oneida Lake shoreline sands as located in Fig. 2.

5 times less than the upper sample. The low K concentration may be the result of leaching.

Other shoreline (SL) features are apparent from the Lidar data and these are located on Figure 2. Of these only a set of three discontinuous features can be found at elevations (~150 m asl) that would correspond to the main GLI shoreline, as defined by Pair and Rodrigues (1993).

Discussion and Interpretation

Our results define the ages on several sets of landforms around present day Oneida Lake representing the Late Glacial history of Glacial Lake Iroqois. Of particular note are our OSL ages that provide a minimum age for the formation of the Rome Sand Plain parabolic dune field, which is in the range of 11 to 12 ka. We interpret these ages as minimum because we only sampled the uppermost portions of one large parabolic dune. Deeper exposures within the dipping foresets of the dune field may provide slightly older ages. Further, the direction of foreset dip as we measured (110°) is in perfect alignment with the overall geometry of all the parabolic dune forms, indicating that our lowermost sample is representative of the majority of dune building winds. Therefore, our age control fixes aeolian dune development during the later part of the Younger Dryas Stadial, which is consistent with a cold and arid setting indicative of a dominance of aeolian process across the landscape. These ages are considered robust as aeolian processes (saltation transport) expose quartz sand grains to sufficient sunlight to reset (bleach) any prior signal accumulation. The thousand-year age range is well within the estimated uncertainty of the methods and analytical technique.

If cold and arid conditions dominated the landscape at this time it is strange that aeolian dune forms are not more widespread within the Oneida Lake basin. We suggest the reason for the limited distribution is the association of the dune field on top of a relict sand "terrace", which provided an ample source of unconsolidated sand, when conditions became conducive to aeolian transport. The origin of this terrace is problematic for several reasons but the upper portions of it are well exposed at our second

dated locality (Figs. 2, 5B, and 9). What we describe as a terrace has been mapped in various ways as lacustrine sand, outwash, and kame deposits (Muller and Cadwell, 1986). The "terrace" is defined by the 137 m asl contour, with only its southernmost edge covered by the Rome Sand Plain (Muller and Caldwell, 1991). As the 137 m flat surface is traced to the north it encroaches into indentations within the bedrock topography of the Tug Hill Plateau, with only a very slight increase in elevation. In total, the terrace covers a large area between the irregular topography of the Tug Hill Plateau and the lowland areas of the Oneida Lake basin (Fig. 2).

We propose that this feature is a composite accumulation of Quaternary sediment but consists mostly of ice-contact, water stratified sediment (that constitutes a kame). It may be possible that the extensive sand deposit is a delta built out into the highest stand of GLI (R. Dineen personal communication, 2012) and that subsequent lake lowering left the delta stranded, allowing aeolian action to sculpt the parabolic dunes. However, the elevation of the sand "terrace", at greater than 137 m asl is 6 m asl above the elevation of the Rome outlet (col), which is at most 131 m asl in elevation. Yet the 137 m asl elevation for the "terrace" is below the limit of the proposed spillway of 155 m asl at Moss Island, near Little Falls (Pair and Rodriquez, 1993; Fig. 3).

As an alternative hypothesis we suggest that the core of the sand "terrace" was developed by a combination of an over-extended Ontario lobe of the Laurentide Ice Sheet, early in its retreat phase from the Rome area. This would have allowed localized impoundment of melt water and/or lake conditions in the catchment between the ice sheet lobe (occupying the Oneida Lake basin) and the uplands of the Tug Hill Plateau (Fig. 11). The sharp change in elevation from the sand "terrace" to the Oneida Basin Lowland is then a reflection of its marginal position between the ice and the plateau and the clear lateral incision by Wood and Fish Creeks during their Holocene meanderings. The antiquity of alluvial erosion and deposition by these rivers is indicated by buried trees, which yield radiocarbon ages of at least 10 ka (Cleary, 2002; Panyushkina, et al., in preparation). There is also

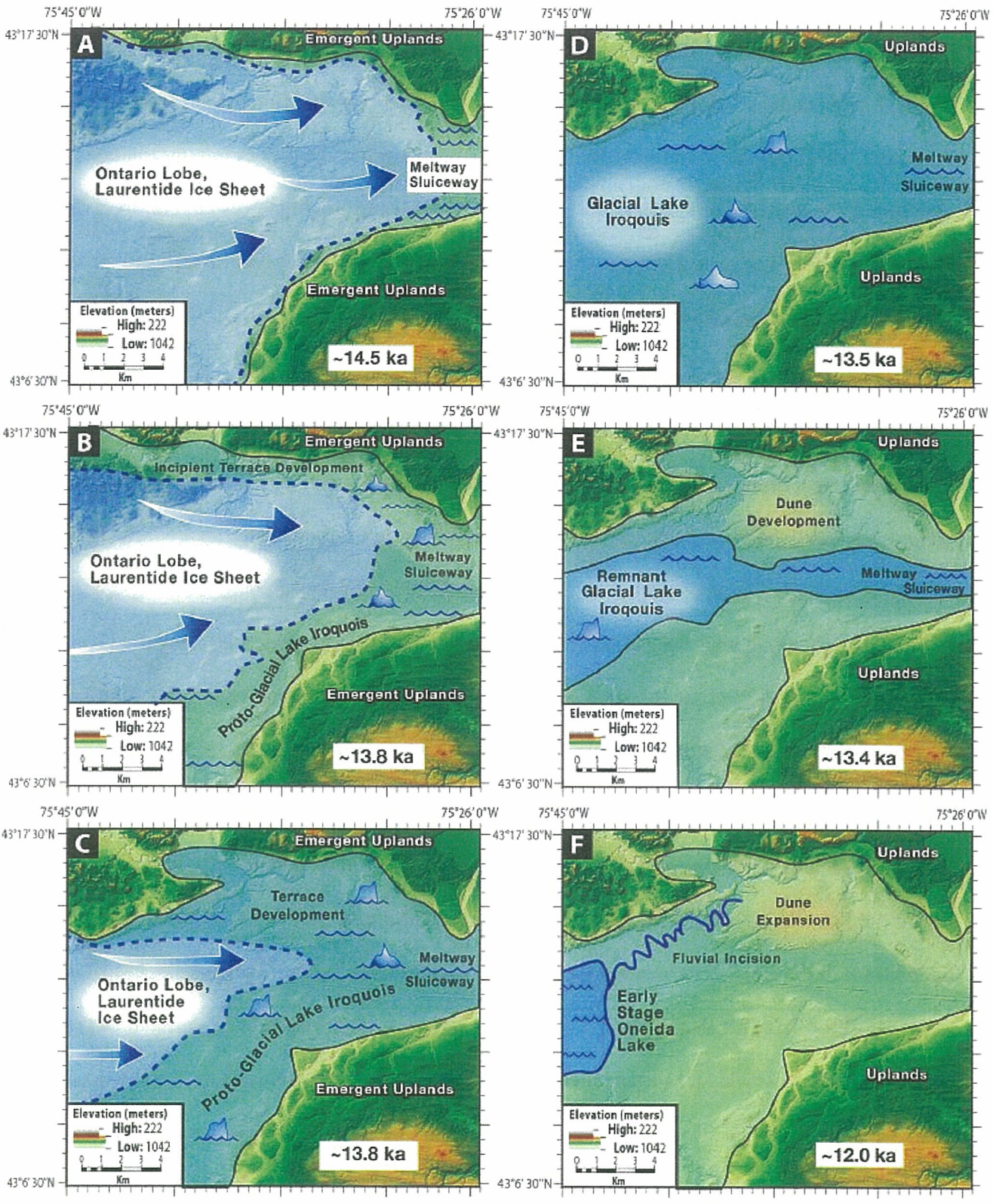

Fig. 11. Schematic of sequence of events leading to the evolution of landscape across the east Oneida Basin.

some evidence that parts of the sand terrace may be have accumulated as an esker fan, as narrow, sand- cored, ridges (beaded hills) can be seen to purge into the southwestern edge of the terrace, as they emanate out of the Oneida Lake basin (Fig. 2).

Our OSL ages from the upper portions of the sand "terrace" also add to the problem of its interpretation (Figs. 4B and 7). From our results there appear to be two sets of ages within the upper part of the terrace as exposed off Route 49. The upper unit is fluvial in origin as indicated by the large-scale cut and fill stratigraphy and tough cross-bedded gravelly sands and coarse sands. This fluvial stratigraphy is clearly separated from underlying deposits by a disconformity. The total age range is ~23 to ~31 ka (Table 2; Fig. 8). If the OSL ages we report are representative of the age of sediment aggregation, then the terrace is indeed quite complex and may include interstadial deposits that may be correlated to the Plum Point Interstadial of the Ontario Lowland (Morner, 1971). Interstadial conditions may have allowed ice surface lowering around the southern edge (lee) of the Tug Hill Plateau and localized emergence of terrain from beneath the ice sheet, without substantial retreat of the formal ice sheet margin that lay far to the south--beyond the Valley Heads.

Hence, we are left with the possibility that the "terrace" is indeed a composite feature composed a number of deposits, each contributing to its morphology and accumulation as landforms. The aeolian dunes are but one expression of this modification, but there are others such as the clear dendritic incision by localized streams and the formation of sandy alluvial fans out into the Oneida Lake Lowland, where such streams exit the terrace (Fig. 2).

The most definitive shoreline features found within the Oneida Lake basin are the prominent sets of linear ridges and swales present continuously from the modern shoreline of Oneida Lake toward the east, for over 2.5 km (Fig. 4C). Other ridges at 137 m asl elevation are present still further east and are mapped as lacustrine sands (Muller and Cadwell, 1986). These higher elevation ridges are clearly ice marginal deposits or subaqueous moraines, like Irish Ridge Road (Figs. 2 and 3; Domack

et al., 2012).

The Irish Ridge Road system actually comprises a set of discontinuous and arcuate features that roughly parallel the set of ice marginal channels found along the border of uplands in the SE part of our study area (Fig. 2). In particular the ice marginal channels can be mapped toward the NE where they translate, across the narrow saddle near Rome NY, to the Rome Moraine—a complex interpreted as ~14.6 ka in age (Ridge, 2004; Fig. 11A). This parallel arrangement to both groups of ice marginal features (the moraines and the channels) help to define the lobate nature of the Ontario Lobe as it receded to the west out of the Oneida Basin (Fig. 11A, B). The main axis of the Oneida Lowland provided sufficient focus for faster flow as documented by elongation ratios of streamlined features sculpted by ice flow (Briner 2007; Hess, and Briner, 2009). The asymmetry of the Irish Ridge features, their poorly sorted character, the eastward dipping foresets, and the transition into a flat terrain to the east indicate that they were formed by an active ice margin grounded in shallow water. We interpret this water body as proto-GLI (Fig. 11B, C) as it does not reflect the main phase of GLI as reconstructed by most workers (Pair and Rodrigues, 1993; Anderson and Lewis, 2012; Donnelly et al, 2005, and others). We wish to point out however that this impoundment could have been responsible for the higher elevation shorelines and parts of the sand "terrace" present along the edge of the Tug Hill Plateau in our study area (Figs. 2, 11B, and C) as we discuss below.

Additional support for the reconstruction shown in Figure 11 is demonstrated by the mapping of the Irish Ridge complex toward the NE where it lies just within the Rome moraine system (Fig. 2). Constrained within this set of ice marginal morainal banks are the unusual reticulated ground moraines, which cover an extensive area west of Rome on either side of the NY State Barge Canal (Figs. 2 and 4). These features are remarkably similar to crevasse squeeze ridges described and interpreted from tidewater ice lobes in Svalbard (Clemens, 2014; Domack et al., 2014; Ottesen et al, 2008; Solheim and Pfirman, 1985). The scale of the features and their orientation would reflect the

geometry of crevasses typically observed on surging glaciers which move out across a soft deformable bed in subaqueous settings. They are emplaced as sediment is squeezed into the basal crevasse openings preserved by the glacial ice, which lacks sufficient flow, following the surge, to reform and remove the squeeze ridges (Solheim and Pfirman, 1985). Such features, as observed in Svalbard, are typically associated with morainal banks which form basin-ward of the more interior crevasse squeeze ridges (Ottesen et al., 2008). Thus the features we describe and map from the Oneida Basin likely record a period of minor readvance (surge) of the Ontario Lobe, within a standing body of water (i.e. proto-GLI; Fig. 11A, B). The characteristic change in relief of ridges and swales with elevation reflects the consequent filling in of localized depressions (swales) by fine-grained lake sediments at greater depths and the beveling of the ridge surfaces by wave processes at shallower depths. That not all ridges and swales exhibit this character may reflect changes in the rate at which the level of GLI fell, such that early-on levels were falling slowly (conducive to erosion with lowering wave base) then later under a more rapid drawdown slightly deeper and intact features were left stranded.

Of importance to the overall landform association is the observation that both the ice marginal banks and associated reticulate ground moraine are masked by the sand "terrace" as they are traced to the north (Fig. 2), at least there is no expression of them along the northern border of the basin. While some of the absence can be explained by the erosion of Wood Creek (Fig. 4) the implication is that formation of the terrace was, in part, contemporaneous with and/or is younger than the ice marginal positions marked by the Irish Ridge Road "moraine system" (i.e., Fig. 11B, C).

Because of these map relationships described above the more prominent set of low elevation shorelines, observed east of Oneida Lake, post-date the earliest phases of GLI in the basin (Fig. 11E, F). We have determined ages (Tables 1 and 2) on three sets of these ridges, two illustrated

in Figure 3C (as a and b) and another, lower relief feature, also shown in Figure 3 as the easternmost ridge (c).

For a and b in Figure 5, we provide both radiocarbon and OSL ages because this composite chronology is internally consistent (Fig. 8), providing credence to our age assessment. Calibrated radiocarbon ages (Table 3) on the beach gravels and sands clearly place shoreline conditions in the core of the Younger Dryas Stadial, when the shoreline was at ~114 m asl. All the calibrated ages except one have overlapping distributions in time, between roughly 12 to 13 ka (Table 3), and thus spatial separation of these two ridges (3a and 3b in Fig. 3C) can be explained by rapid shoreline progradation toward the west, perhaps with a minor drop in lake level. Overlying aeolian deposition commenced fairly soon after, with OSL ages of 10.3 to 11.6 ka (Table 2; Fig. 9). Hence, the timing of aeolian dune formation is likely diachronous across the entire landscape with activity across the Rome Sand Plains having taken place some 1 ka earlier than coastal dunes on the last of the GLI shorelines.

Together, the ages and low elevation of these shorelines would suggest that they record the final emptying stage of GLI but they still record very energetic processes (a lake with a large fetch) and derivation from an immature source (tills). This is in accordance with the estimates of GLI drainage commencing as late as 13.2 ka (Rayburn et. al., 2011) but somewhat younger than the event as estimated at 13.5 ka by Anderson and Lewis (2012). The other shoreline recognized within this system (Fig. 3C-c) has two OSL ages, which indicate aggregation at 14.5± 0.7 to 12.4 ± 0.7 ka (Fig. 10A). Within 2 sigma uncertainty these ages converge at 13.8 – 13.1 ka, suggesting an association with the last drainage event of GLI, albeit slightly older than shorelines a and b, but in better agreement with the drainage events documented in Lake Ontario and the Champlain Valley (Anderson and Lewis, 2012; Rayburn et al., 2011).

The younger set of low energy shorelines, seen as parallel with the modern Oneida Lake shoreline

(Fig. 5C) were also excavated and two OSL ages obtained from a site north of NY State Barge Canal (Figs. 2 and 10B). Here two ages of 6.2±0.4 to 14.0±0.3 ka are in disagreement. The younger of the two ages would suggest that the low energy shorelines were emplaced in the middle Holocene. The discordant relationship between the low energy and older, higher energy ridges (Fig. 5C) would imply that the discordance itself was due to a second major drop in lake level, following the initial emptying of the GLI reservoir. But in this case it involved early stages of an isolated Oneida Lake (Fig. 11F). Assignment of this event to the early Holocene drawdown (arid) phase recognized across the Laurentian Great Lakes between 8.3 ka and 12.3 ka (Anderson and Lewis, 2012) would make sense and is in agreement with our chronology. A refilling of the Oneida Lake basin beginning in the middle Holocene would have allowed accretion of a new set of lower energy shorelines supplied by an abundance of sand now supplied by the Fish Creek drainage, which is known to have begun as early as 10.0 ka (Cleary, 2002).

Westward accretion of this system continued unabated until the 20th Century, when the construction of the NY State Barge Canal interrupted sand supply to the eastern shore of Oneida Lake and a renewed episode of shoreline erosion commenced (Domack et al., 2004).

Conclusion

Geomorphic mapping, sedimentological analysis, OSL and radiocarbon dating of landforms and sediments around the Oneida Lowland allow the Late Quaternary history of GLI, its drainage and the development of Onieda Lake to be reconstructed. We first demonstrate that use of the OSL dating method is a robust technique applicable to Late Quaternary sediments of broad age range in the study region, as we include results from interstadial (Port Talbot) sands that underlie the regional disconformity beneath till. Our work further shows that there was a minor readvance of the Ontario Lobe of the Laurentide ice sheet at ~14.5 ka. This advance and together with the retreat of the Ontario

Lobe at ~13.8 ka, helped produce the Irish Ridge Road moraine system and contributed to the formation of an extensive terrace system along the northern perimeter of the lowland. The extensive terrace, however, is a composite feature that began to form as early as 23-31 ka, during the Plum Point Interstadial. The prominent flat elevation of this 'terrace' does not directly reflect the highest stand of GLI, whose earliest shoreline expression is dated to between 12 to 15 ka within the study area. GLI likely began to drain at ~13.2 ka. Subsequent shoreline progradation and lowering of GLI toward the west continued into the Younger Dryas Stadial, as corroborated by a composite age model based upon both radiocarbon and OSL dating within a single straigraphic succession. The aeolian sands of the Rome Sand Plain, on the extensive terrace, formed by at least 12 ka, and provide a minimum age for the drainage of GLI. Dune formation continued to influence the landscape with aeolian features found to cap GLI beaches at 10 to 11 ka. Modern shorelines of Oneida Lake appear to be the latest of a set of shore-parallel features, which truncate, with disconformity, the youngest of the GLI shoreline features.

This work therefore suggests changes (lowering) in the level of GLI coincident with the Younger Dryas episode, roughly at 13.2 ka, consistent with revised models for outflow via the St. Lawrence drainage, which may have also drained glacial lakes within the larger Great Lakes Basin. Examination and continued dating of additional lanforms within the Oneida Lake Basin therefore have great potential to help us revise the timing and significance of events during the later stages of glaciation in New York State and surrounding regions.

Acknowledgements

MKM thanks the University of Cincinnati for supporting him while undertaking this research. We thank C.M. Fadem for her help during the early stages of this project when we ran the initial radiocarbon ages, which were presented in her senior thesis. We thank Dave Tewksbury (Hamilton

College) for his help with maps depicting the LIDAR topography of our study area, Dale Hess (Brock University), Scott Ingmire (Madison County Planning Office), and Todd Rayne (Hamilton College) for helpful discussions and assistance in the field. Financial support of this work was provided primarily via grants from the Levitt Public Policy Institute and the Dickson-Rodgers, Potter Fund (Hamilton College), and the Central New York Regional Planning and Development Board (via the NYS DEC). Participants in the NYSGA field trip of 2012 are thanked for their helpful input as these features and ages were discussed in the field (September, 2012). Managers of the Verona Beach State Park are thanked for their help in accessing several of our localities. Reviews of an earlier draft of this paper by A. Koslowksi and J. Rayburn were appreciated and their suggestions helped to improve this final version.

References

Aitken, M.J., 1998. An introduction to Optical dating: The Dating of Quaternary Sediments by the Use of Photon-stimulated Luminescence. Oxford University press, USA, New York.

Anderson, T.W., Lewis, C.F.M., 2012. A new water-level history for Lake Ontario basin: Evidence for a climate-driven early Holocene lowstand. J. Paleolimnol. 47, 513–530.

Arnold, K., 2004. Sediment Paticle Size of the Oneida Creek Delta, Senior Thesis. Hamilton College, Clinton, New York.

Barclay, D. and Koslowski, A 2014. Friends of the Pleistocene field trip (personal communication).

Benn, D.I., Evans, D.J.A. 2010. Glaciers and Glaciation. Hoder Arnold Publication, 2nd Edition.

Briner, J.P., 2007. Supporting evidence from the New York drumlin field that elongate subglacial bedforms indicate fast ice flow. Boreas 36, 143–147.

Cadwell, D.H., 1991. Surficial geology map of New York: New York State Museum Map and Chart Series 40, Scale 1:250 000.

Cleary, J.L., 2002. Chronology and Interpretation of Fluvial and Paleoflood Deposits along Lower Fish Creek, Oneida County NY. Senior thesis. Hamilton College, Clinton, New York.

Clements, T.J.C., 2014. Interpretation of a unique network of reticulated landforms in the Oneida Basin, Central New York, Senior thesis, Hamilton College, Clinton, New York 22 pp.

Cronin, T.M., Rayburn, J.A., Guilbault, J.-P., Thunell, R., Franzi, D.A., 2012. Stable isotope evidence for glacial lake drainage through the St. Lawrence Estuary, eastern Canada, 13.1–12.9 ka. Quat. Int. 260, 55–65.

Domack, E. W., Ingmire, S. , Arnold, K. 2004, Sediment dynamics of the Oneida Creek Delta, Oneida Lake, New York, final report to the Central New York Regional Planning and Development Board and N. Y. State Department of Environment and Conservation, 93 pp., see: http://www.cnyrpdb.org/oneidalake/pdf/SedimentDynamics[LR].pdf

Domack, E.W., 2010. Oneida Lake, a highly perturbed lake system in central New York, paper 29-4, Session 29, Annual Northeastern Section GSA meeting, Buffalo, New York.

Domack, E.W., Hess, D.P., Owen, L.A., Murari, M.K., Rayne, T., 2011. Landforms and surface geology of eastern Oneida Lake and Oneida County New York: new insights from matching bathymetry with Lidar topography, 46th GSA Annual Meeting Northeast and North Central Joint Meeting, Pittsburgh PA, paper 5-9.

Domack, E.W., Hess, D., Owen, L., Murari, M., Rayne, T., Tewksbury, D., 2012. Glacial history of the Oneida Lake basin. NYSGA field trip, A2.

Domack, E.W., Clements, T.J.C., and Tewksbury, D.A., 2014. LIDAR interpretation of a unique network of reticulated landforms in the Oneida basin, central New York. Abstracts with Program, Northeast Geological Society of America Section Meeting.

Donnelly, J.P., Driscoll, N.W., Uchupi, E., Keigwin, L.D., Schwab, W.C., Thieler, E.R., Swift, S.A., 2005. Catastrophic meltwater discharge down the Hudson Valley: A potential trigger for the Intra-Allerød cold period. Geology 33, 89.

Dremanis, A., Terasmae, J., and McKenzie, G. D., 1966. The Port Talbot interstade of the Wisconsin glaciation, Canadian Journal of Earth Sciences, 3, 305-325.

Fadem, C.M., 2001a. Chronology of landscape evolution at Oneida Lake, Northeastern Section -36th Annual, GSA meeting, Session No. 14- Poster #42.

Fadem, C.M., 2001b. Chronology of Landscape Evolution at Oneida Lake, New York. BA thesis Hamilton College, Clinton, New York. pp102.

Franzi, D., Rayburn, J., Knuepfer, P., Cronin, T., 2007. Late Quaternary History of Northeastern New York and Adjacent Parts of Vermont and Quebec, 70th Annual Northeast Friends of the Pleistocene Guidebook, Plattsburgh, New York. 70.

Fullerton, D. S., 1980, Preliminary correlation of post-Erie Interstadial events (16,000-10,000 radiocarbon years before present), central and eastern Great Lakes region, and Hudson, Champlain, and St. Lawrence Lowlands, United States and Canada: U.S. Geological Survey Professional Paper 1089,52 p.

Gruin, R. (2009). The "AGE" program for the calculation of luminescence age estimates. Ancient TL, 27, 45–46.

Hess, D.P., Briner, J.P., 2009. Geospatial analysis of controls on subglacial bedform morphometry in the New York Drumlin Field – implications for Laurentide Ice Sheet dynamics. Earth Surf. Process. Landforms 34, 1126–1135.

Hillaire-Marcel, C., Occhietti, S., 1977. Fréquence des datations Au 14C de faunes marines post-glaciaires de l'est du Canada et variations paléoclimatiques. Palaeogeogr. Palaeoclimatol. Palaeoecol. 21, 17–54.

Hiscott, E.C., 2000. Paleoenvironmental Development of Eastern the Shoreline of Oneida Lake, New York: Evidence from surficial mapping, aerial photography, and shallow geophysics. BA thesis. Hamilton College, Clinton, New York.

Jain, M., Singhvi, A.K., 2001. Limits to depletion of blue-green light stimulated luminescence in feldspars: implications for quartz dating. Radiat. Meas. 33, 883–892.

Kurczewski, F.E., 1999. Historic and Prehistoric Changes in the Rome, New York Pine Barrens, Northeast. Nat. 6, 327–340.

Michael Lewis, C.F., King, J.W., 2012. Introduction to "Holocene water levels and paleo-hydrology of the Laurentian Great Lakes". J. Paleolimnol. 47, 293–297.

Morner, N.-A., 1971. The Plum Point Interstadial: age, climate, and subdivision. Can. J. Earth Sci. 8, 1423–1431.

Muller, E.H., Caldwell, D.H., 1986. Surficial geologic map of New York State, Museum Map and Chart Series 40, scale 1:250 000, Finger Lakes Sheet.

Muller, E.H., Calkin, P.E., 1993. Timing of Pleistocene glacial events in New York State. Can. J. Earth Sci. 30, 1829–1845.

Muller, E.H., Prest, V.K., 1985. Glacial lakes in the Ontario Basin., Quaternary evolution of the Great Lakes. Geological Association of Canada, Toronto; Special Paper 30.

Mullins, H. T., and Hinchey, E. J., 1989, Erosion and infill of New York Finger Lakes: Implications for Laurnetide Ice sheet deglaciation. Geology, 17, 622-625.

Murari, M.K., Domack, E.W., Hess, D.P., Owen, L.A., 2011. Timing of esker and dune formation at the eastern end of Oneida Lake, New York State, defined by optically stimulated luminscence dating. 46th GSA Annual Meeting Northeast and North Central Joint Meeting, Pittsburgh PA Paper.

Murray, A.S., Olley, J.M., 2002. Precision and accuracy in the optically stimulated luminescence dating of sedimentary quartz: a status review 21, 11–16.

Murray, A.S., Wintle, A.G., 2000. Luminescence dating of quartz using an improved single-aliquot regenerative-dose protocol. Radiat. Meas. 32, 57–73.

Ottesen, D.; Dowdeswell, J. A.; Benn, D. I.; Kristensen, L.; Christiansen, H. H.; Christensen, O.; Hansen, L.; Lebesbye, E.; Forwick, M.; Vorren, T. O., 2008. Catastrophic meltwater discharge down the Hudson Valley: A potential trigger for the Intra-Allerød cold period. Quaternary Science Reviews, vol. 27, issue 15-16, pp. 1583-1599.

Pair D., Rodrigues, C. G, 1993, Late Quaternary deglaciation of the southwestern St. Lawrence Lowland, New York and Ontario. Geol Soc Amer Bull 105:1151–1164.

Panyushkina, I.P., Leavitt, S.L., Domack, E.W., Wiedenhoeft, A.C., 2015. First tree-ring study of ancient wood deposits from the Lake Oneida watershed, NY (in revision).

Parent, M., Occhietti, S., 1988. Late Wisconsinan deglaciation and Champlain sea invasion in the St. Lawrence valley. Géographie Phys. Quat. 42, 215–246.

Porat, N., 2006. Use of magnetic separation for purifying quartz for luminescence dating. Anc. TL 24, 33–36.

Prescott, J.R., Hutton, J.T., 1994. Cosmic ray contributions to dose rates for luminescence and ESR dating: Large depths and long-term time variations. Radiat. Meas. 23, 497–500.

Rayburn, J., Verosub, K., Franzi, D., Knuepfer, P., 2006. A preliminary Paleomagnetic Study of the Glacial Lacustrine/Champlain Sea Transition in Cores from the Northern Champlain Valley., in: Geological Society of America, New York. Abstracts with Programs, Northeastern Section 38, # 2.

Rayburn, J.A., Cronin, T.M., Franzi, D.A., Knuepfer, P.L.K., Willard, D.A., 2011. Timing and duration of North American glacial lake discharges and the Younger Dryas climate reversal. Quat. Res. 75, 541–551. doi:10.1016/j.yqres.2011.02.004

Rayburn, J.A., Franzi, D.A., Knuepfer, P.L.K., Cronin, T.M., Berke, M.A., 2005. Evidence for a series of large freshwater discharge events from eastern North America to the North Atlantic immediately preceding the Younger Dryas. In: Program with Abstracts, American Geophysical Union Fall Meeting.

Rea, D. K., and Colman, S. M., 1995. Radiocarbon ages of pre-bomb clams and the hard-water effect in Lakes Michigan and Huron. Journal of Paleolimnology, 14, 89-91.

Reimer, P.J., Baillie, M.G.L., Bard, E., Bayliss, A., Warren Beck, J., Bertrand, C.J.H., Blackwell, P.G., Buck, C.E., Burr, G.S., Cutler, K.B., Damon, P.E., Lawrence Edwards, R., Fairbanks, R.G., Friedrich, M., Guilderson, T.P., Hogg, A.G., Hughen, K.A., Kromer, B., McCormac, G., Manning, S., Ramsey, C.B., Reimer, R.W., Remmele, S., Southon, J.R., Stuiver, M., Talamo, S., Taylor, F.W., van der Plicht, J., Weyhenmeyer, C.E., 2004. IntCal04 terrestrial radiocarbon age calibration, 0-26 cal kyr BP. Radiocarbon 46, 1029–1058.

Ridge, J.C., 2004. Quaternary Glaciations-Extent and Chronology - Part II: North America, in: Ehlers, J., Gibbard, P.L. (Eds.), Developments in Quaternary Sciences, Elsevier, pp. 169–199.

Solheim, A., and Pfirman, S. L., 1985, Sea-floor morphology outside a grounded, surging glacier: Bråsvelbreen, Svalbard, Marine Geology, 85, 127-143.

Stuiver, M., Reimer, P.J., and Reimer, R., 2011, Calib Radiocarbon Calibration Routine 2011. (http://calib.qub.ac.uk/calib/)

Wintle, A.G., Murray, A.S., 2006. A review of quartz optically stimulated luminescence characteristics and their relevance in single-aliquot regeneration dating protocols. Radiat. Meas. 41, 369–391.

Wright, F.M.I., 1972. The Pleistocene and Recent Geology of the Oneida-Rome district, New York. Ph.D. thesis. Syracuse University.

Wurster, C. M., and Patterson, W. P., 2001. Seasonal variation in stable oxygen and carbon isotope values recovered from modern lacustrine freshwater molluscs: paleclimatological implications for sub-weekly temperature records. Journal of Palelimnology, 26, 205-218.

TREE-RING RESEARCH, *Vol. 71(2), 2015, pp. 83–94*
DOI: http://dx.doi.org/10.3959/1536-1098-71.2.83

TREE-RING INVESTIGATION OF HOLOCENE FLOOD-DEPOSITED WOOD FROM THE ONEIDA LAKE WATERSHED, NEW YORK STATE

IRINA P. PANYUSHKINA[1]*, STEVEN W. LEAVITT[1], EUGENE W. DOMACK[2,3], and ALEX C. WIEDENHOEFT[4]

[1]Laboratory of Tree-Ring Research, University of Arizona, Tucson, AZ, 85721, USA

[2]Department of Geosciences, Hamilton College, Clinton, NY, 13323, USA

[3]College of Marine Science, University of South Florida, St. Petersburg, FL, 33701, USA

[4]Center for Wood Anatomy Research, USDA Forest Products Laboratory, Madison, WI, 53726, USA

ABSTRACT

Glacial deposition and fluvial/lacustrine sedimentation interact over terrains in central New York State to preserve a history of geological and hydrological events as well as hydroclimatic transitions. The lower reach of Fish Creek draining the eastern watershed of Oneida Lake, NY, is an area with prominent wood remains. This study explores a collection of 52 logs encased in organic-rich deposits exposed by bank erosion at three locations along Fish Creek near Sylvan Beach, NY, with respect to radiocarbon ages, species, and the crossdating potential of tree rings. Radiocarbon ages and successful tree-ring crossdating document what we interpret as seven major hydrologic episodes *ca.* 10 ka (*i.e. ca.* 10,000 cal yr BP), 7.4 ka, 6.8 ka, 6.4 ka, 5.5 ka, 3.1 ka and 2.2 ka cal BP, during which channel aggradation and tree burial may have been associated with abruptly increased flood frequency and/or high water tables. This pilot study establishes four floating tree-ring records: [1] early Holocene hemlock (*Tsuga*), mid-Holocene [2] walnut (*Juglans* sp.) and [3] sycamore (*Platanus*), and [4] late Holocene elm (*Ulmus* sp.), with sample sizes of 8–14 series of 55–135 years length. Despite the complexity of distribution of radiocarbon ages at each site, the wealth of well-preserved wood demonstrates great promise for understanding the paleoflood history of the Oneida watershed by documenting the magnitude, location, and timing of floods. Further additional systematic sampling can add and strengthen tree-ring dating and tree-ring based flood records, confirm results, and contribute to the Holocene hydrological history of the region.

Keywords: paleoflood, paleohydrology, riparian forest, U.S. Northeast, Fish Creek, dendrochronology.

INTRODUCTION

Significant increases in flood discharge and frequency in recent decades across the densely populated U.S. Northeast (Baldigo 1999; Knox 2000; Collins 2009; Smith *et al.* 2011) can be put into long-term context with hydrological proxies resolving Holocene flood history at local and regional scales (Changnon and Kunkel 1995). Instrumental records of runoff recorded since 1890 provide some historical measure of flood events and offer insights into linkages of large-scale climate modes with continental rainfall and streamflow in the eastern U.S. (Enfield *et al.* 2001). For pre-instrumental events, with proper dating control, lacustrine sediments provide the primary proxy record for frequency and magnitude of large Holocene runoff events (Kochel 1988; Brown *et al.* 2000; Ward *et al.* 2007), but uneven availability of such records in space and time supports the need for as many flood proxies as possible. Additionally, correspondence between pollen climatic proxies and discrete radiocarbon-dated chronologies of extreme runoff and paleoflood events is often weak (Brown *et al.* 2000). Consequently, new proxies with higher spatial and temporal resolution are needed to improve the dating control and correspondence of coarsely resolved proxies and to advance our understanding of paleohydroclimate of this region.

*Corresponding author: ipanyush@email.arizona.edu

The U.S. Northeast landscape underwent profound changes in climate, hydrology and vegetation over the last 20,000 years, shaping the environment and imprinting on plant growth and preservation. Forests previously occupying belts and isolated refugia south of the Laurentide ice sheet were gradually able to expand into newly exposed terrain as the glacier retreated (Williams *et al.* 2001; Shuman *et al.* 2002; Panyushkina and Leavitt 2012). In addition to abrupt climate fluctuations during deglaciation up to the beginning of the Holocene, such as the Younger Dryas event *ca.* 12,900 to 11,600 cal BP (henceforth "cal BP" denotes cal yr BP, *i.e.*, calibrated radiocarbon ages in years before AD 1950), significant changes of hydroclimates occurred throughout the North Atlantic sector during cold events dating back at *ca.*11.5 ka cal BP (the Preboreal Oscillation), 10.2 ka cal BP, 9.3 ka cal BP, 8.2 ka cal BP, 5.9 ka cal BP, 4.2 ka cal BP, 2.8 ka cal BP, 1.4 ka cal BP and 0.4 ka cal BP (the Little Ice Age) (Mayewski *et al.* 2004; Wang *et al.* 2013).

Pollen has been the key plant fossil for unraveling North American climate evolution and vegetation changes of the past 20,000 years (*e.g.* Shane and Anderson 1993; Grimm 2001; Jackson *et al.* 2006), supplemented by other measurements (*e.g.* charcoal, ostracodes, isotope composition) from sediment cores (*e.g.* Yu 2000; Curry and Filippelli 2010; Moos and Cumming 2012). Nevertheless, the best potential for annually-resolved insight into environmental variability lies with tree rings, and fortunately wood in the Great Lakes area has been widely preserved in glacial, lacustrine, alluvial and bog deposits (*e.g.* Kaiser 1994; Griggs and Kromer 2008; Panyushkina and Leavitt 2010). The Great Lakes Tree-Ring Network (http://greatlakes.ltrr.arizona.edu/) has been developing annually-resolved floating tree-ring records suitable for interpretation of environmental/hydrological changes (*e.g.* Panyushkina *et al.* 2008).

A large amount of wood has been previously observed in fluvial sediments along Fish Creek in the Oneida Lake watershed in north-central New York (Cleary 2002). This paper describes the first dendrochronological sampling of ancient wood from this location in a pilot study to determine its (1) taxa and age, (2) characteristics and suitability for crossdating and tree-ring analysis, and (3) potential value for the Holocene hydrological studies and our initial interpretations.

SITE SETTING

Oneida Lake is located *ca.* 25 km northeast of Syracuse, New York. The lake is oriented east to west, *ca.* 30 km (20 mi) long, *ca.* 8 km (5 mi) wide, and an average depth of *ca.* 7 m (22 ft). The lake is a remnant of Glacial Lake Iroquois, which existed in the Late Pleistocene when the flow of the St. Lawrence River from the Great Lakes to the Atlantic Ocean was dammed by the Laurentide Ice Sheet (Bloomfield 1978). Fish Creek drains from the Tug Hill Plateau (main source of rainfall for surface runoff in the area) north-northeast of Oneida Lake. The Fish Creek watershed is one of seven primary sub-watersheds of Oneida Lake. Fish Creek meanders across an extensive alluvial plain that includes the lower Wood Creek watershed whose drainage delivers water westward toward Fish Creek from further east. Within the plain are at least four sets of meanders, each characterized by distinctive channel widths and meander radii. These likely reflect long-term changes in water discharge and/or hydroclimate during the Holocene (Cleary 2002). Exposed along the cut banks of the modern channel are various sequences representing (1) point bar lateral accretion, and (2) floodplain and oxbow lake vertical accretion. Within these latter two facies, buried large-diameter logs are found in abundance (Figure 1). The majority of these are clearly transported, and no *in situ* buried trees have yet been discovered, although peat layers rich in wood may indicate some sequences of floodplain paleosoils (Cleary 2002).

The alluvial plain succession of Fish and Wood Creeks cuts though a prograded beach ridge and dune landscape of eastern Oneida Lake, which yields ages of *ca.* 12,800 cal BP, indicating contemporaneous development of both landscapes as the shoreline of Oneida Lake built westward (Hiscott 2000; Fadem 2001). The shoreline and fluvial facies themselves rest upon an older glacial landscape of sculpted (west to east) ridges (ground

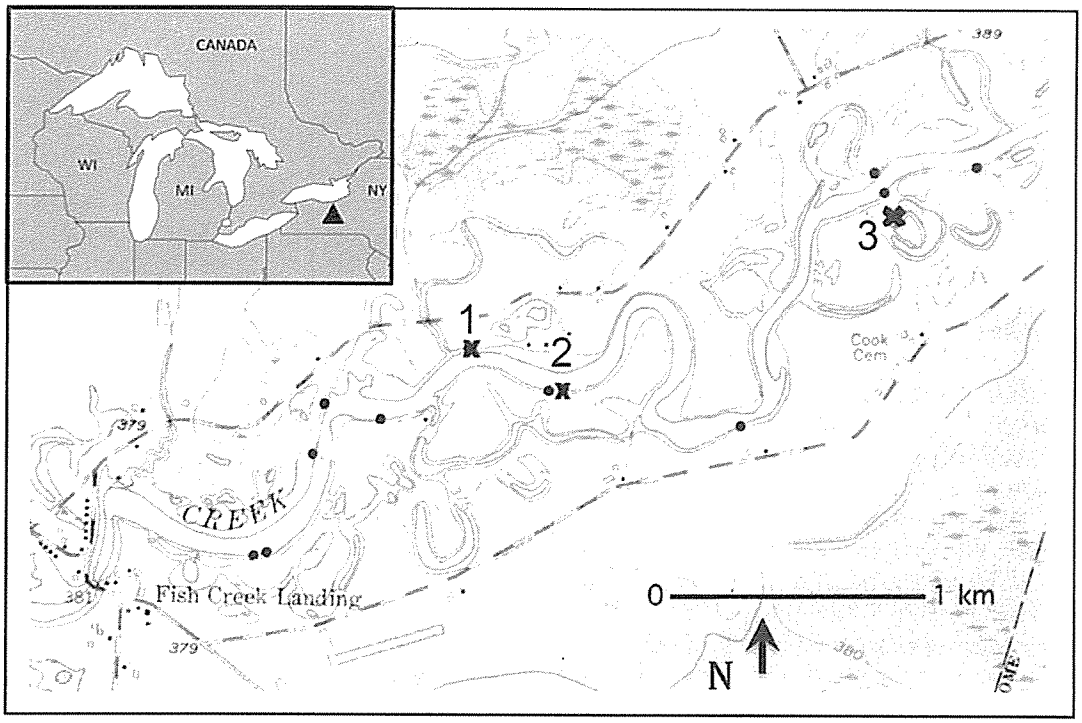

Figure 1. Map showing exposures of buried wood (•) documented by Cleary (2002) and sites sampled for this study (X) on the banks of the low reach of Fish Creek near Sylvan Beach, Oneida County, New York State. See triangle on the left insert map indicating the location of the studied area in the Great Lakes watershed.

moraine), ice marginal banks, and older shorelines of Glacial Lake Iroquois, the latter of which yield ages of *ca.* 14,600 cal BP (Hiscott 2000; Fadem 2001).

MATERIALS AND METHODS

With help of the Hamilton College Dept. of Geosciences pontoon research vessel we traversed a stretch of Fish Creek *ca.* 7–9 km upstream from its mouth at Sylvan Beach, NY, on the eastern flank of Oneida Lake. Along this stretch we sampled three locations with abundant wood, designated as Sites #1 (*ca.* 43.228127N, 75.686264W), #2 (*ca.* 43.226688, 75.682230W) and #3 (*ca.* 43.233036, 75.668626W) (Figure 1). The sites fall within an elevation range of *ca.* 113–114 m a.s.l. (370–375 feet a.s.l.), *ca.* 1–2 m above the average recent elevations of Oneida Lake. Fifteen, 25 and 12 samples were obtained from the three sites, respectively, at positions both just above and just below the water level (Figure 2). Logs at Site 1 were mainly situated in a peaty muck layered with yellowish brown sand. At Sites 2 and 3, the logs were found buried in a yellowish brown sandy silt of the modern riverbank. Cross-sections were cut from the logs with a handsaw in the field. In most cases, the cross-sections were complete, with pith, the outermost rings and even bark preserved for many. Samples were tightly covered in plastic wrap and shipped to the University of Arizona for analysis.

Wood taxonomy of 17 specimens from Sites 1 and 2 was determined at the Center for Wood Anatomy Research, USDA Forest Products Lab, Madison (WI). Thin-sections prepared along the grain from the radial and tangential surfaces were analyzed under high magnification of a reflecting light microscope to identify diagnostic anatomical features. Taxonomy at the species level could not be determined with certainty for any of the samples because of the condition of the wood, but genus identification was made for most. Genus

Figure 2. Buried logs at Sites 1, 2 and 3 inundated by past floodwaters. The logs likely were transported downstream and deposited as congested assemblages in ancient channels along Fish Creek.

assignment of the other wood samples was made through visual comparison with wood structure/microanatomy attributes of the 17 identified wood specimens.

Tree-ring widths were measured on slightly wet wood that was surfaced by freshly cutting with a razor blade. The tree-ring series were crossdated visually by plotting the tree-ring width measurements and matching the patterns. First, crossdating was performed among tree-ring series from the same tree genus within a site. Second, the floating tree-ring records from the same genus were overlapped between sites where possible (Figure 3). Accuracy of the crossdated data was checked with the COFECHA program (Holmes 1983). Dates of the outermost rings from the crossdated series were tabulated and employed to develop a mortality record of trees buried in the Fish Creek sediments.

For radiocarbon dating, the outer 10 rings of specimens from Sites 1, 2 and 3 were subsampled and processed to isolate the alpha-cellulose component using the sodium chlorite delignification method (Leavitt and Danzer 1993) followed by sodium hydroxide removal of hemicelluloses (Sternberg 1989). The α-cellulose samples were submitted to the NSF-Arizona Accelerator Mass Spectrometry (AMS) Laboratory at the University of Arizona for radiocarbon dating. The ^{14}C dates were calibrated and plotted with OxCal 4.2 software (https://c14.arch.ox.ac.uk/) that utilizes the IntCal13 calibration curve (Reimer *et al.* 2013).

RESULTS AND DISCUSSION

Anatomy and tree genus identification of wood specimens from Fish Creek indicate a collective suite of hemlock (*Tsuga*), sycamore (*Platanus*), elm (*Ulmus*), walnut (*Juglans sp.*), beech (*Fagus grandifolia*) and maple (*Acer*). The buried wood collected at the sites largely comprised hemlock and elm (28% and 30% of total collected specimens, respectively), and fewer sycamore (20%) and walnut (18%). Beech and maple representation was much less (4% and 2%, respectively). Spatial distribution of tree genera among the three sampled locations is not uniform. All identified tree genera appear at Site 1 and the adjacent Site 2 (except for beech). Site 3, located about one kilometer eastward from the other two sites, has only elm and hemlock (Table 1, Figure 1).

Regionally, the pre-settlement forest on the Oneida watershed was transitional between boreal and broadleaf deciduous, with mixed stands of hardwoods (yellow birch, sugar maple and American beech), Appalachian oak, pine, and occasionally eastern hemlock (Küchler 1964), so the collective suite of sampled trees does not match this potential modern-forest species composition. Major land-cover changes since AD 1650 (European settlement period) have significantly modified the vegetation in the Great Lakes area, drastically reducing the coverage of the old growth conifer forest on river watersheds and riparian corridors (Steyaert and Knox 2008). Heavy logging prior to 1929 (USDA 1994), and insect outbreaks, pathogens, and urban development over the late 20th Century have removed or replaced original natural vegetation (Cole *et al.* 1998). This could also explain the genus differences between the ancient and the Modern-era riparian forests. Additionally, the suite we collected may be biased taxonomically by field sampling

Table 1. Distribution of tree-ring specimens among sites (Sites 1, 2 and 3) collected at the lower reach of Fish Creek. The total number of samples (51) is less by one because #216 disintegrated during inadvertent rapid drying prior to tree species being identified.

	Number of Trees				Total Length of Series		
Tree Species	Site 1	Site 2	Site 3	Radii Range (cm)	Site 1	Site 2	Site 3
Hemlock	1	6	7	3–19	129	104	124
Elm	5	5	5	5–15	92	96	98
Walnut	4	5	0	5–25	50	47	-
Sycamore	3	7	0	3–21	55	100	-
Maple	1	1	0	8–9	61	75	-
Beech	1	0	0	10	103	-	-

of large embedded logs expected to have many rings, which were readily accessible for cutting from the boat or the shore.

Crossdating of specimens within genus per site was successful but not straightforward in some cases because there are some specimens with fewer than 50 rings (years) (Table 2). From a statistical point-of-view, the low ring number (24 in one case), especially for walnut specimens, could confound the crossdating, but we found the tree-ring variance had distinct patterns that visually matched well. Furthermore, the short time series have similar growth rates and a few very distinctive pointer years, which further favor the trees most likely being contemporaneous. Forty-five out of 52 specimens were crossdated. One hemlock specimen (#208, 116 rings) and one elm specimen (#105, 93 rings) could not be matched with the groups. One walnut sample had only 12 rings (#213), and specimen # 216 (53 rings) disintegrated during inadvertent rapid drying. One beech (#108, 103 rings) and two maple (#109, 61 rings and #219, 75 rings) specimens were not included in the pilot dating because of low sample replication even though the maple tree-ring series overlapped. Overlapping tree-ring series from the same genus between sites resulted in four floating tree-ring records of hemlock, walnut, sycamore and elm spanning 55 to 135 years (Table 3). These crossdating results support contemporaneity among trees of a genus buried together within and between sites along the Fish Creek riverbanks near Sylvan Beach.

Four ^{14}C dates measured on outer rings of the studied specimens (Table 4) provide ages of the crossdated assemblages at *ca.* 10,000 cal BP (hemlock), 7400 cal BP (walnut), 5500 cal BP (sycamore) and 3100 cal BP (elm). Radiocarbon dating on wood specimens from earlier studies (Fadem 2001; Cleary 2002), which had not been crossdated and were collected at other locations of along Fish Creek near Sylvan beach, reveals three additional episodes of wood deposition occurring *ca.* 6400 cal BP, 6800 cal BP and 2200 cal BP (Table 4, Figure 4A). Cumulative distribution of all calibrated ^{14}C ages (Figure 3B) dates the earliest deposition of hemlock soon after the 10.2 ka cal BP cold event abrupt climate excursion (Mayewski *et al.* 2004). Next, a cluster of four radiocarbon ages emerged during the Mid-Holocene between 7.4 ka and 5.5 ka cal BP. The final two events in the wood record occurred at *ca.* 3.1 ka and 2.2 ka cal BP in the Late Holocene. Overall, the dating establishes seven major discrete wood deposition episodes during the Holocene and documents gaps in wood deposition during *ca.* 2000-year intervals before and after the Mid-Holocene and in the most recent 2200 years.

The age of ^{14}C-dated trees and their range of radial growth rates may provide some clues about geomorphological evolution of the Fish Creek valley. Even though all identified groups of trees include young and/or near-maturity trees, their growth rates vary widely as regulated by a combination of edaphic and climatic factors. The group of 10 ka cal BP hemlock trees with a 139-year span had much slower growth than trees from other intervals. The 120- to 130-year-old hemlocks formed 20- to 30-cm diameter stems (Table 1, 3). The trees growing during the mid-Holocene intervals have more than twice the growth rate of the hemlock.

Table 2. Tree-ring crossdating results for the Fish Creek specimens. The first digit of the 3-digit specimen ID number corresponds to the site number. Bold sample ID indicates radiocarbon-dated specimen. Length (years) and correlation coefficient of tree-ring series (R) shorter than 45 years are designated with italic font. Span is fit into floating chronologies.

Group	Sample ID	Length	Span	*r* with Master
Hemlock 10,000 cal BP	#106	129	6–135	0.42
	#305	115	1–115	0.48
	#214	104	14–117	0.37
	#309	77	39–115	0.52
	#210	75	34–108	0.42
	#308	73	51–123	0.58
	#302	72	50–121	0.51
	#310	54	69–122	0.44
	#303	49	75–123	0.45
	#218	*44*	33–76	0.57
	#221	*43*	70–112	0.41
	#220	*37*	78–114	0.44
	#304	*27*	63–89	*0.40*
Walnut 7400 cal BP	**#103**	50	1–50	0.55
	#201	47	9–55	0.46
	#217	45	1–45	0.53
	#206	*42*	5–46	*0.50*
	#100	*39*	17–55	*0.33*
	#215	*32*	16–47	*0.53*
	#101	*28*	15–42	*0.75*
	#111	*27*	16–42	*0.59*
Sycamore 5500 cal BP	#200	100	32–100	0.39
	#203	95	34–86	0.54
	#211	69	5–99	0.50
	#202	64	48–71	0.51
	#102	55	42–93	0.49
	#212	53	36–99	0.57
	#205	52	22–76	0.47
	#114	45	1–100	0.39
	#104	*42*	29–74	*0.34*
	#222	*24*	56–97	*0.64*
Elm 3100 cal BP	#301	98	1–98	0.58
	#204	97	1–97	0.60
	#107	92	8–100	0.50
	#113	59	43–101	0.49
	#112	55	25–79	0.36
	#207	55	24–78	0.38
	#311	53	37–90	*0.55*
	#300	51	44–94	0.63
	#223	46	26–71	0.53
	#306	46	47–92	0.40
	#209	*44*	51–94	*0.52*
	#307	*42*	49–90	*0.60*
	#110	*37*	43–79	*0.32*
	#224	*32*	44–75	*0.46*

Sycamores formed *ca.* 20-cm diameter trunks in 90 years of growth. Diameter of *ca.* 55-year-old walnut trees was nearly 0.5 m (Table 1, 3). American walnut is sensitive to soil conditions and grows best on deep, well-drained and moist alluvial soils like those of the Appalachian Piedmont (Williams 1990). It is likely that the large walnut logs dated *ca.* 7.4 ka cal BP came from a well-established part of floodplain formed during a prolonged period of stability and soil development. Alternatively, low growth rate of hemlock may indicate growth on shallow muck soils corresponding to a shorter period of stability, *ca.* 10 ka cal BP.

The pattern of studied tree mortalities in dated episodes seems to provide further insight into paleoflooding history of the area. The position of buried logs and the crossdating results support the hypothesis that most trees were not falling randomly but rather entrained and deposited by profound hydrologic events. The relatively young age of studied trees and lack of pith rot (that commonly develops when aging trees naturally die) may indicate a sudden fall, and rapid transport and burial of trees in the fluvial sediments. Buried wood from the fluvial deposits can document high-magnitude flood disturbances that remove floodplain trees and transport floating wood downstream in channels (Johnson *et al.* 2000). Additionally, high water adversely affects the vegetative and reproductive growth of trees, alters plant anatomy, and induces plant mortality (Kozlowski 1997). Comparison of tree-ring growth patterns (Figure 3) and distribution of tree mortality dates (Figure 5) suggests that prolonged wet conditions may be contributing to decadal deteriorating growth conditions for some species just prior to the *coup de grâce* flood(s) that removes the trees. The slow growth rates and reduced variance over the final decade or so of several of the records may reflect effects of water-table rise and oxygen-deficiency on the tree roots across the Fish Creek alluvial plain (Figure 3), possibly indicating pluvial periods with substantial increase in rainfall in the phases when the extreme flooding occurred. A large range of termination dates for individual trees within cross-site records (Figure 5) suggests subsequent occurrence of large floods and river aggradation during which the trees were likely toppled or uprooted and buried.

Table 3. Group statistics of averaged tree-ring width series from the Fish Creek wood collection.

Chronology	Length	# Trees	Site	Mean, mm	Mean Sensitivity	Interserial Correlation
10,000 cal BP						
Hemlock	135	13	1, 2, 3	1.04	0.28	0.43
7400 cal BP						
Walnut	55	8	1, 2	2.15	0.31	0.48
5500 cal BP						
Sycamore	100	10	1, 2	1.31	0.29	0.48
3100 cal BP						
Elm	101	14	1, 2, 3	1.32	0.30	0.48

Modern Fish Creek runoff is strongly influenced by the seasonal distribution of precipitation, with maximum river discharge in spring from melted snow and prominent rainstorms (Matonse and Frei 2013). The increase in the number of extreme floods across the U.S. Northeast in the last decade is attributed to the highest frequency of extreme warm-season precipitation events in the last 100 years (Collins 2009; Matonse and Frei 2013), particularly associated with high-precipitation events promoted by tropical cyclones and organized extratropical systems (Smith *et al.* 2011; Dai 2013). The dated episodes of wood deposition may result from a similar increase in frequency of such extreme summer precipitation events in the area. Overall, all ^{14}C dates derived from the tree rings may be associated with periods of significant changes in the fluvial process and hydrological regime of the Fish Creek catchment. If our accumulations of wood from discrete periods represent flooding events, as is generally the inference in a number of such studies (*e.g.* Jílek *et al.* 1995; Kukulak *et al.* 2002), our results suggest that the fluvial stability of the Creek has been interrupted by frequent flooding events followed by an intensification of channel aggradation processes dated *ca.* 10 ka cal BP, 7.4 ka cal BP, 6.8 ka cal BP, 6.4 ka cal BP, 5.5 ka cal BP, 3.1 ka cal BP and 2.2 ka cal BP. High flood recurrence is highly sensitive to climate change, and increased flood frequency occurs abruptly at various timescales from decadal to millennial (Baker *et al.* 1992; Knox 2000). These dated episodes may indicate increased frequency and/or magnitude of floods, which could be coupled with generally higher variability of rainfall.

Because the sites are only *ca.* 1–2 m above the elevation of Oneida Lake and the terminus of Fish Creek at Oneida Lake may effectively also function as a delta, the hydrology of sampling sites may have also been affected by lake level. Studies of sediment sequences in neighboring lakes

Table 4. ^{14}C dating of wood buried along Fish Creek near Sylvan Beach, NY. Fadem (2001) and Cleary (2002) are sources of ^{14}C dates measured on bulk wood marked with asterisks.

Lab ID	Site	Tree Species	^{14}C Age, yr BP	Cal Age Range, 2 Sigma Cal yr BP	Material
FCIP-103	1	Walnut	6513 ± 48	7320–7500	10 outer rings
*GX-28622	1	n/a	6000 ± 40	6740–6940	bulk wood
*GX-28623	1	n/a	5510 ± 50	6260–6400	bulk wood
FCIP-107	1	Elm	2910 ± 40	2950–3200	10 outer rings
*GX-28624	1	n/a	2280 ± 40	2160–2260	bulk wood
*GX-28624	2	n/a	4900 ± 43	5590–5730	10 outer rings
FCIP-202	2	Sycamore	4826 ± 45	5470–5560	10 outer rings
*GX-28621	2	n/a	2970 ± 40	3000–3260	bulk wood
FCIP-308	3	Hemlock	8964 ± 55	9910–10,100	10 outer rings

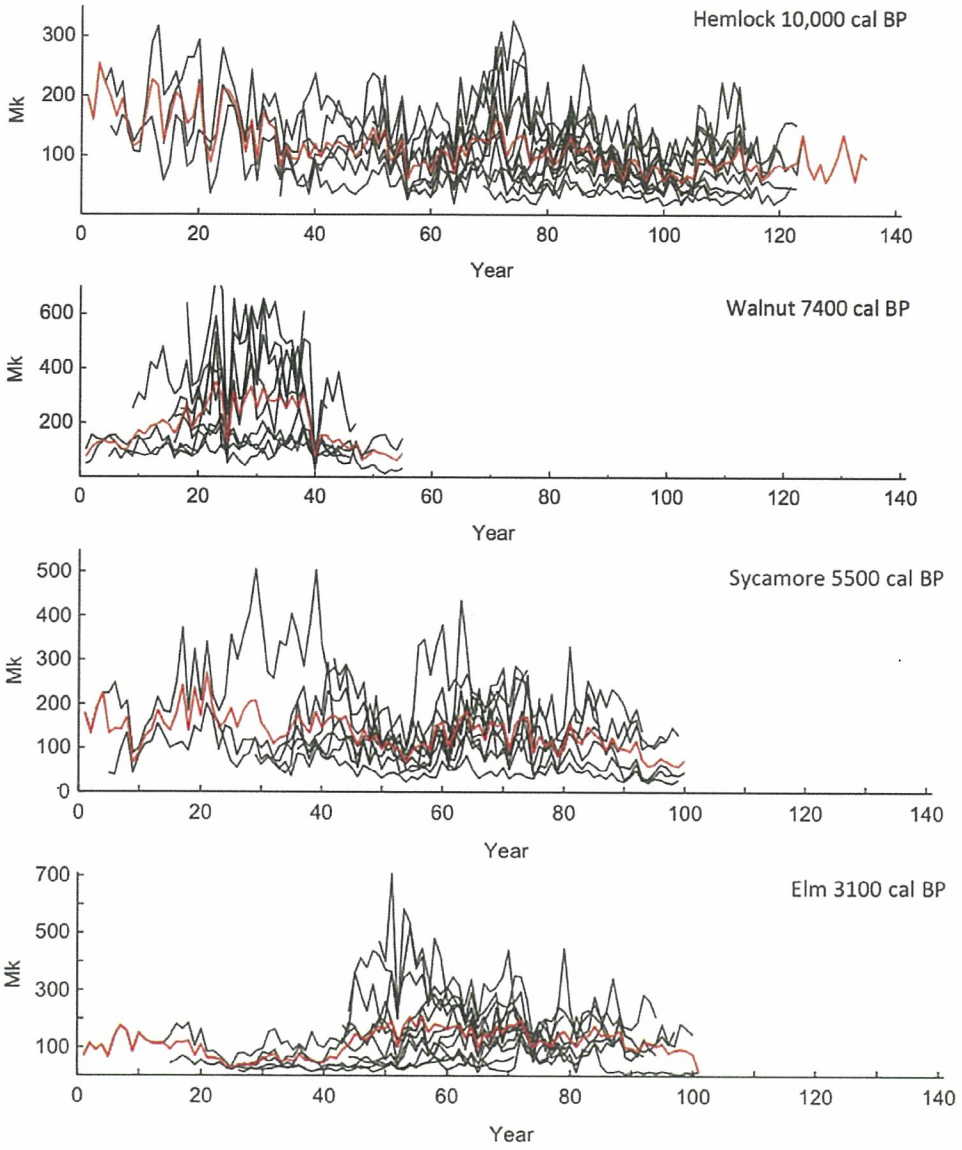

Figure 3. Curves of tree-ring width measurements (raw data) showing the crossdating positions of trees. Red line is the mean, and y-axis units of "Mk" are microns.

suggests higher lake levels between ca. 6000 and 9000 cal BP despite warming of the mid-Holocene climate optimum (Mullins 1998; Mullins and Halfman 2001). Although we did not consider this in the analysis, more careful future sampling may also help in understanding variations in Oneida Lake levels.

CONCLUSIONS

In the Holocene, the riparian landscape of the Fish Creek floodplain transformed from cold-mesic conifer forest dominated by hemlock in the early Holocene to a broad-leaf deciduous forest of the warm and more humid mid-Holocene, which

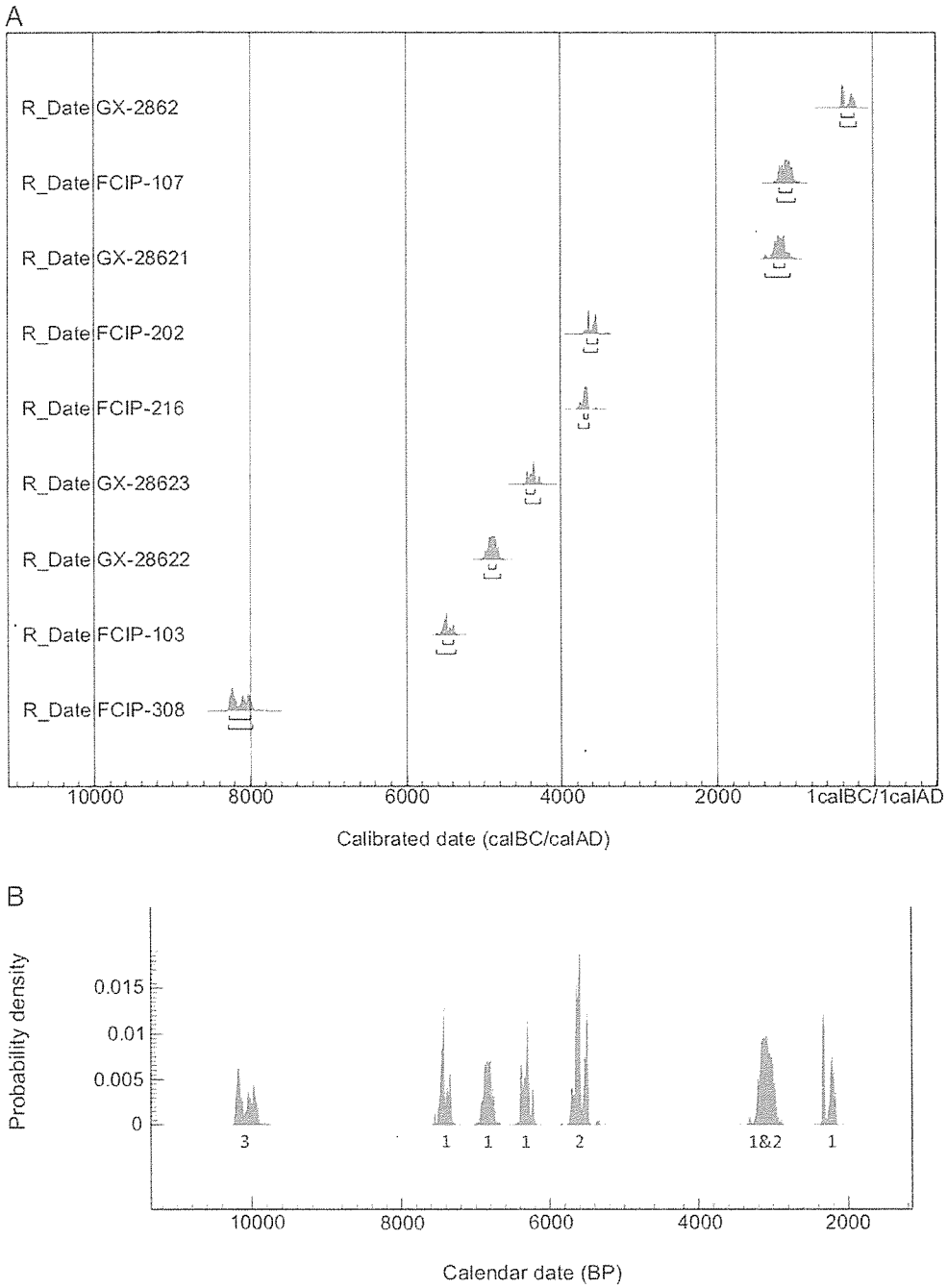

Figure 4. Radiocarbon dating summary of the Fish Creek wood. (A) Individual calibrated radiocarbon dates (data from Table 4). Probability distribution is shown in shaded area. The bars under the probability distribution denote 68.2% and 95.4% ranges. (B) Cumulative probability density function (PDF) plot of calibrated ^{14}C ages of Fish Creek wood. The numbers immediately below each PDF refer to the contributing site(s).

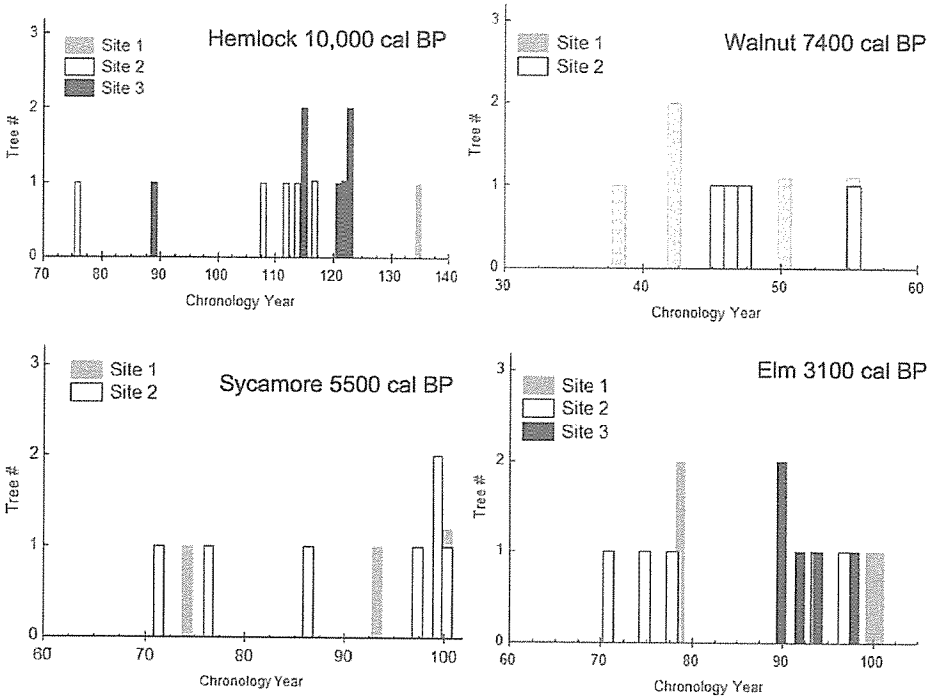

Figure 5. Tree mortality records of studied intervals and sites based on crossdating results of the outermost preserved rings often with bark.

included walnut (7.4 ka cal BP) and sycamore (5.5 ka cal BP), and later hardy elms (3.1 ka cal BP). The fluvial disturbance of the riparian forest has resulted in major deposition of wood in levees along meandering creek channels in the lower reach of the Fish Creek. The promising results of this pilot study of buried wood in Fish Creek riverbanks show that wood is abundant and can be crossdated, and that the preserved wood and tree rings are suitable for (1) developing records of paleofloods and fluvial geomorphic activity in the lower reach of Fish Creek, and (2) providing details of the Holocene history of U.S. Northeast hydrology and its response to climate change.

The crossdating of various tree species from multiple locations and a high number of contemporaneous trees suggests that wood buried by the floods is a good diagnostic tool for understanding temporal and spatial patterns of large paleofloods in the area. Thus far, based on the tree rings alone, the Holocene history of Fish Creek encompasses seven major episodes of increased flood frequency dating back to *ca.* 10 ka cal BP, 7.4 ka cal BP, 6.8 ka cal BP, 6.4 ka cal BP, 5.5 ka cal BP, 3.1 ka cal BP and 2.2 ka cal BP driven by increased precipitation over the Tug Hill Plateau and/or at the larger scale of the U.S. Northeast.

Amplified concern about recent extreme floods across New York State motivates interest in long well-dated paleoflood records from this area. The good crossdating potential of tree rings from the fluvial deposits provide a framework for linking tree-ring flood evidence to a fluvial sediment chronology of Fish Creek, which would be a rich, well-dated archive of flooding history at various temporal and spatial scales. To fully exploit this paleoenvironmental archive, however, a large-scale wood sampling campaign with a more sophisticated sampling protocol will be needed to verify and expand on our results.

ACKNOWLEDGMENTS

We are thankful to C. Griggs, N. Pederson and D. Barkley for their helpful comments and discussion of an early version of the manuscript.

The thoughtful comments of two reviewers and Associate Editor G. Wiles greatly helped in improving the final paper. The radiocarbon dating was done at the NSF-Arizona Accelerator Mass Spectrometry (AMS) Laboratory at the University of Arizona. This research was sponsored by the National Science Foundation, P2C2 Program award #AGS-1003483.

REFERENCES CITED

Baker, R. G., L. J. Maher, C. A. Chumbley, and K. L. Van Zant, 1992. Patterns of Holocene environmental change in the midwestern United States. *Quaternary Research* 37: 379–389.

Baldigo, B. P., 1999. *Trends in base flows and extreme flows in the Beaver Kill Basin, Catskill Mountains, New York, 1915–94.*, U.S. Geological Survey Open-File Report 98–65; 23 pp.

Bloomfield, J. A., 1978. *Lakes of New York State*, Volume 2. Academic Press, New York; 499 pp.

Brown, S. L., P. R. Bierman, A. Lini, and J. Southon, 2000. 10,000 yr record of extreme hydrologic events. *Geology* 28: 335–338.

Changnon, S. A., and K. E. Kunkel, 1995. Climate-related fluctuations in midwestern floods during 1921–1985. *Water Resources Planning and Management* 121:326–334.

Cleary, J. L., 2002. *Chronology and Interpretation of Fluvial and Paleoflood Deposits along Lower Fish Creek, Oneida County NY.*, Senior thesis, Hamilton College, Clinton, NY; 94 pp.

Cole, K. L., M. B. Davis, F. Stearns, G. Guntenspergen, and K. Walker, 1998. Historical land cover changes in the Great Lakes region. In *Perspectives on the Land-use History of North America: A Context for Understanding Our Changing Environment*, edited by T. D. Sisk, pp. 43–50. Biological Sciences Report. USGS/BRD/BSR 1998-0003, U.S. Geological Survey: Biological Resources Division, Reston, VA.

Collins, M. J., 2009. Evidence for changing flood risk in New England since the late 20th century. *JAWRA*. 45(2):279–290. doi:10.1111/j.1752-1688.2008.00277.x.

Curry, B. B., and G. M. Filippelli, 2010. Episodes of low dissolved oxygen indicated by ostracodes and sediment geochemistry at Crystal Lake, Illinois, USA. *Limnology and Oceanography* 55(6):2403–2423.

Dai, A., 2013. The influence of the inter-decadal Pacific oscillation on U.S. precipitation during 1923–2010. *Climatic Dynamics*. 41(3–4):633–646. doi:10.1007/s00382-012-1446-5.

Enfield, D. B., A. M. Mestas-Nunez, and P. J. Trimble, 2001. The Atlantic multidecadal oscillation and its relation to rainfall and river flows in the continental U.S. *Geophysical Research Letters* 28:2077–2080.

Fadem, C. M., 2001. *Chronology of Landscape Evolution at Oneida Lake, New York*. BA thesis, Hamilton College, Clinton, NY; 102 pp.

Griggs, C. B., and B. Kromer, 2008. Wood macrofossils and dendrochronology of three mastodon sites. In *Mastodon Paleobiology, Taphonomy, and Paleoenvironment in the Late Pleistocene of New York State: Studies on the Hyde Park, Chemung, and North Java Sites* (Chap. 5), edited by W. D. Allmon, and P. L. Nester, *Palaeontographica Americana* 61: 49–61.

Grimm, E. C., 2001. Trends and palaeoecological problems in the vegetation and climate history of the northern Great Plains, USA. *Proceedings of the Royal Irish Academy* 101B: 47–64.

Hiscott, E. C., 2000. *Paleoenvironmental Development of Eastern the Shoreline of Oneida Lake, New York: Evidence from Surficial Mapping, Aerial Photography, and Shallow Geophysics*, BA thesis, Hamilton College, Clinton, NY; 52 pp.

Holmes, R., 1983. Computer-assisted quality control in tree-ring dating and measurement. *Tree-Ring Bulletin* 43:69–78.

Jackson, S. T., R. K. Booth, Y. Huang, E. G. Pendall, J. E. Nichols, T. A. Minckley, and M. Taylor, 2006. Late Holocene hydrological variability in ombrotrophic peatlands of eastern North America. *PAGES News* 14:26–28.

Jílek, P., J. Melková, E. Růžičková, J. Šílar, and A. Zeman, 1995. Radiocarbon dating of Holocene sediments: Flood events and evolution of the Labe (Elbe) River in central Bohemia (Czech Republic). In *Proceedings of the 15th International ^{14}C Conference*, edited by Cools, G. T., D. D. Harkness, B. F. Miller, and E. M. Scott. *Radiocarbon* 37(2):131–137.

Johnson, S. L., F. J. Swanson, G. E. Grant, and S. M. Wondzell, 2000. Riparian forest disturbances by a mountain flood – the influence of floated wood. *Hydrological Processes* 14:3031–3050.

Kaiser, K. F., 1994. Two Creeks interstade dated through dendrochronology and AMS. *Quaternary Research* 42: 288–298.

Knox, J. C., 2000. Sensitivity of modern and Holocene floods to climate change. *Quaternary Science Reviews* 19:439–457.

Kochel, R. C., 1988. Geomorphic impact of large floods: review and new perspectives on magnitude and frequency. In *Flood Geomorphology*, edited by V. R. Baker, R. C. Kochel, and P. C. Patton, pp. 169–187. John Wiley & Sons, New York.

Kozlowski, T. T., 1997. Responses of woody plants to flooding and salinity. *Tree Physiology Monograph 1*, Heron Publishing, Canada; pp. 1–29.

Küchler, A. W., 1964. *Manual to Accompany the Map of Potential Natural Vegetation of the Conterminous United States (with separate map at scale 1:3,168,000)*. Special Publication 36, American Geography Society, Princeton, NJ; 154 pp.

Kukulak, J., A. Pazdur, and T. Kuc, 2002. Radiocarbon dated wood debris in floodplain deposits of the San River in the Bieszczady Mountains. *Geochronometria*. 21:129–136.

Leavitt, S. W., and S. R. Danzer, 1993. Method for batch processing small wood samples to holocellulose for stable-carbon isotope analysis. *Analytical Chemistry* 65:87–89.

Matonse, A. H., and A. Frei, 2013. A seasonal shift in the frequency of extreme hydrological events in southern New York State. *Climate*. 26:9577–9593. doi:10.1175/JCLI-D-12-00810.1.

Mayewski, P. A., E. E. Rohling, J. C. Stager, W. Karlén, K. A. Maasch, L. D. Meeker, E. A. Meyerson, F. Gasse, S. van

Kreveld, K. Holmgren, J. Lee-Thorp, G. Rosqvist, F. Rack, M. Staubwasser, R. R. Schneider, and E. J. Steig, 2004. Holocene climate variability. *Quaternary Research*. 62:243–255. doi:10.1016/j.yqres.2004.07.001.

Moos, M. T., and B. F. Cumming, 2012. Climate–fire interactions during the Holocene: A test of the utility of charcoal morphotypes in a sediment core from the boreal region of north-western Ontario (Canada). *International Journal of Wildland Fire*. 21(6):640–652, doi:10.1071/WF10117.

Mullins, H. T., 1998. Holocene lake level and climate change inferred from marl stratigraphy of the Cayuga Lake Basin, New York. *Journal of Sedimentary Research* 68:569–578.

Mullins, H. T., and J. D. Halfman, 2001. High-resolution seismic reflection evidence for Middle Holocene environmental change, Owasco Lake, New York. *Quaternary Research* 55:322–331.

Panyushkina, I. P., and S. W. Leavitt, 2010. Ancient tree-ring archives in the U.S. Great Lakes region. *Eos, Transactions of the American Geophysical Union* 91(50):489–490.

———, 2012. Ancient boreal forests under the environmental instability of the glacial to post-glacial transition in the Great Lakes region (14,000–11,000 years BP). *Canadian Journal of Forest Research*. 43:1032–1039, dx.doi.org/10.1139/cjfr-2012-0339.

Panyushkina, I. P., S. W. Leavitt, T. A. Thompson, A. F. Schneider, and T. Lange, 2008. Environment and paleoecology of a 12 ka mid-North American Younger Dryas forest chronicled in tree rings. *Quaternary Research* 70:433–441.

Reimer, P. J., E. Bard, A. Bayliss, J. W. Beck, P. G. Blackwell, C. Bronk Ramsey, C. E. Buck, H. Cheng, R. L. Edwards, M. Friedrich, P. M. Grootes, T. P. Guilderson, H. Haflidason, I. Hajdas, C. Hatta, T. J. Heaton, A. G. Hogg, K. A. Hughen, K. F. Kaiser, B. Kromer, S. W. Manning, M. Niu, R. W. Reimer, D. A. Richards, E. M. Scott, J. R. Southon, C. S. M. Turney, and J. van der Plicht, 2013. IntCal13 and MARINE13 radiocarbon age calibration curves 0–50000 years cal BP. *Radiocarbon* 55:1869–1887.

Shane, L. C. K., and K. H. Anderson, 1993. Intensity, gradients, and reversals in late-glacial environmental change in east-central North America. *Quaternary Science Reviews* 12:307–320.

Shuman, B. N., T. Webb III, P. J. Bartlein, and J. W. Williams, 2002. The anatomy of a climatic oscillation: Vegetation change in eastern North America during the Younger Dryas chronozone. *Quaternary Science Reviews* 21:1777–1791.

Smith, J. A., G. Villarini, and M. L. Baeck, 2011. Mixture distributions and the hydroclimatology of extreme rainfall and flooding in the Eastern United States. *Journal of Hydrometeorology*. 12:294–309. doi:10.1175/2010JHM1242.1.

Sternberg, L. S. L., 1989. Oxygen and hydrogen isotope measurements in plant cellulose analysis. In *Modern Methods of Plant Analysis V. Plant Fibres*, edited by H. F. Linskens, and J.F. Jackson, pp. 1089–1099. Springer-Verlag, New York.

Steyaert, L. T., and R. G. Knox, 2008. Reconstructed historical land cover and biophysical parameters for studies of land-atmosphere interactions within the eastern United States. *Journal of Geophysical Research*. 113: D02101, doi:10.1029/2006JD008277.

USDA Forest Service, 1994. *Ecological Subregions of the United States: Section Descriptions*. WO-WSA-5. U.S. Department of Agriculture, Forest Service, Washington, DC.

Wang, S., Q. Ge, F. Wang, X. Wen, and J. Huang, 2013. Abrupt climate changes of Holocene. *Chinese Geographical Science* 23(1):1–12. doi:10.1007/s11769-013-0591-z.

Ward, P. J., J. C. J. H. Aerts, H. de Moelb, and H. Renssen, 2007. Verification of a coupled climate-hydrological model against Holocene palaeohydrological records. *Global and Planetary Change* 57:283–300.

Williams, J. W., B. N. Shuman, and T. Webb, III, 2001. No-analog conditions and rates of change in the climate and vegetation of eastern North America. *Ecology* 82: 3346–3362.

Williams, R. D., 1990. *Juglans nigra* L.: Black walnut, In *Silvics of North America: Volume 2, Hardwoods*, edited by R.M. Burns and B.H. Honkala (tech. coordinators), pp. 391–399. Agricultural Handbook 654, U.S. Department of Agriculture Forest Service, Washington, DC.

Yu, Z., 2000. Ecosystem response to Lateglacial and early Holocene climate oscillations in the Great Lakes region of North America. *Quaternary Science Reviews* 19:1723–1747.

Received 5 October 2014; accepted 28 May 2015.

Green Lakes (Dead Man's Point) and Oneida Lake Marl Section, Sky High Farms

75°52'18.65"W and 43° 7'14.90"N

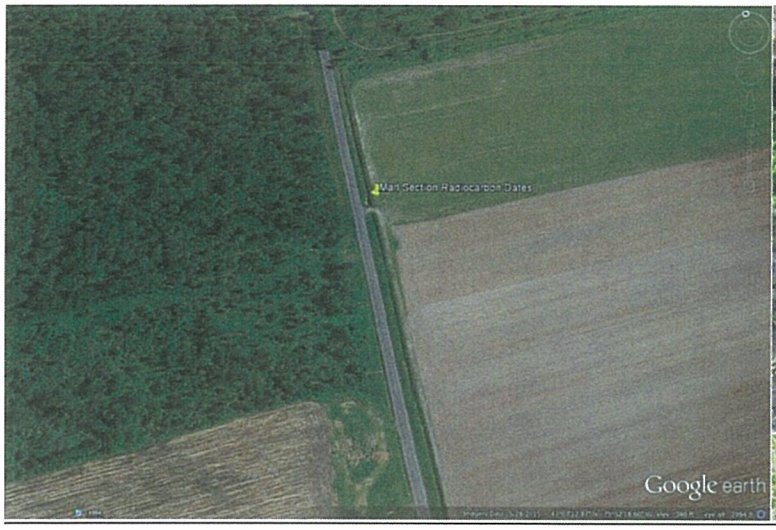

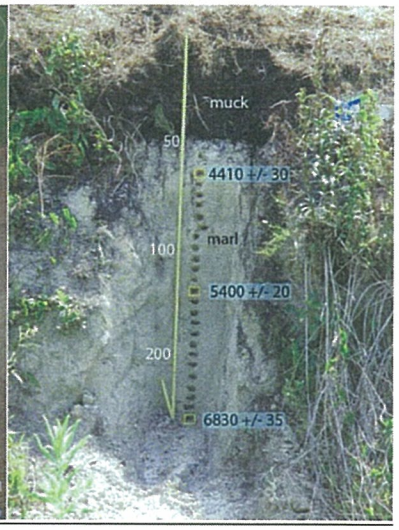

Lab Number	Sample Type	Section	Depth	13d C	Radiocarbon age +/-	error
NOSAMS 125434	quagga mussel	modern (live)		nm	390	15
CAMS 171666	gastropods	OL-'15-1	52-54 cm	nm	4410	30
NOSAMS 133138	gastropods	OL-'15-1	122-124 cm	-8.68	5400	20
CAMS 171667	gastropods	OL-'15-1	177-179 cm	nm	6830	35
GX-23937	wood	DM Point	mid section	-26.2	4810	85
GX-23938	wood	DM Point	mid section	-26.3	4040	180

Current Archaeological Research on Paleoindian Sites in Central New York

Jonathan C. Lothrop, New York State Museum
Michael Beardsley, Beauchamp chapter, NYSAA
Mark Clymer, Beauchamp chapter, NYSAA
Susan Winchell-Sweeney, New York State Museum
Meredith H. Younge, New York State Museum

In: *Oneida Basin, Glacial Lake Iroquois and Archaeological Contexts*, edited and compiled by Eugene Domack, pp. 1-33. Guidebook for 79th Annual Reunion of the Northeastern Friends of the Pleistocene Field Conference, June 3-5, 2016, Verona, New York (http://www2.newpaltz.edu/fop/).

Introduction

This chapter describes ongoing archaeological research on earliest human occupations of Central New York during the late Pleistocene and early Holocene. These early Native Americans, hunter-gatherers known to archaeologists as Paleoindians, settled the eastern Great Lakes from circa 13,000 to about 10,800 calendar years before present (Cal BP) (or 11,000-9500 radiocarbon years before present (RCYBP) (Ellis and Deller 1990, 1997, Ellis et al. 2011). Following Lothrop et al. (2014), this paper examines archaeological evidence for early human settlement of Central New York, but focuses on data from three newly discovered Paleoindian sites in the Oneida basin.

Because of the dynamic nature of New York's late Pleistocene and early Holocene landscapes and environments, we rely on the research of our earth scientist colleagues to provide a physical context for studying early Native American settlement of Central New York. In this regard, ongoing Quaternary studies of (1) the Ontario basin (Anderson and Lewis 2012; Bird and Kozlowski 2016), (2) the Oneida Basin and Ontario Lowland (reported in this guidebook), and (3) the Finger Lakes region (Kozlowski and Graham 2014), plus paleontological studies of the broader New York region (Feranec and Kozlowski 2016), offer key insights on the evolution of landscapes, environments and potential terrestrial prey species associated with human settlement of Central New York. In addition, recent research on Devonian stratigraphy in the New York region sheds new

light on some of the toolstone sources exploited by Paleoindian populations in the New York region (e.g., Ver Straeten and Brett 2006).

Archaeological research on the first peoples of Central New York is proceeding on two tracks. The first involves the New York Paleoindian Database (NYPID) project, with a primary focus on recording diagnostic stone weapons tips of these first peoples for the New York region (Lothrop 2009). Lothrop et al. (2014) describe data collected on fluted and unfluted Paleoindian points to broadly model early human settlement of the Central New York region. Here, we review these 2014 findings, but focus on our second research track, ongoing field investigations and preliminary analysis of three newly discovered Paleoindian sites, located in the Oneida basin between Oneida Lake and the Onondaga escarpment. These three sites – Glass Factory, Owlville South, and Owlville Pine South – lie in close proximity, and together, comprise the Owlville Paleoindian site cluster.

Background

We first provide physical contexts for early Native American occupation of Central New York, summarizing the region's setting and post-glacial lake sequence, paleoenvironments and regional resources, and then review previous Paleoindian research in Central New York.

Setting and Postglacial Lake Sequence

Our Central New York study area encompasses the Ontario Lowlands or lake plain, and the Appalachian (or Allegheny) Plateau to the south, subdivided by the Onondaga escarpment (see Figure 1). Terrain on the Ontario Lowlands consists of mostly low-lying landscapes punctuated by drumlins and other glacial features, with elevations ranging from 80 to 180 m above sea level (ASL). The Oneida basin consists of a shallow, bedrock trough in this Ontario Lowland landscape (Figure 2); the modern Oneida Lake footprint measures 33 km east-west and 9 km north-south. Along the southern border of the Ontario Lowland, the Onondaga (or Portage) escarpment rises abruptly to elevations of 360 to 550 m, marking the northern edge of the Plateau. Further east, the Tug Hill Plateau and the Adirondack Highlands flank the northern margins of the Oneida basin and Mohawk Valley.

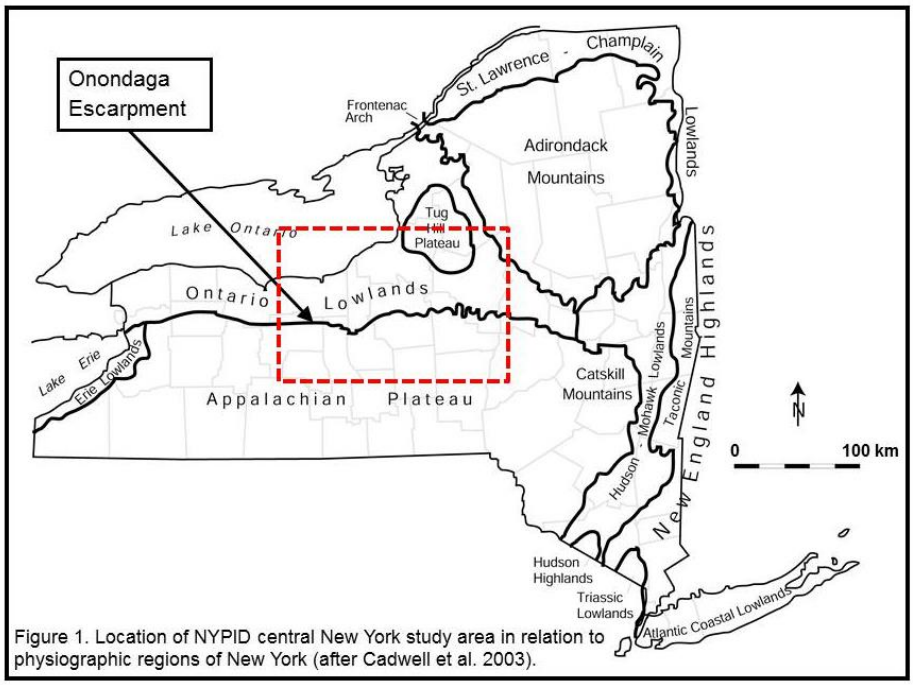

Figure 1. Location of NYPID central New York study area in relation to physiographic regions of New York (after Cadwell et al. 2003).

Major stream drainages on the Ontario Lowlands include the east-flowing Seneca River and the west-flowing Oneida River; their confluence forms the Oswego River, which flows north to Lake Ontario. East of Oneida Lake, the Mohawk River rises at Rome, flowing southeast to the Hudson Valley. To the south, the Chenango River and its tributaries drain south across the Plateau to the Susquehanna River.

Late Pleistocene landscapes for early Native American colonization of Central New York were formed by the sequence of deglacial events in the Ontario basin. The Mapleton Moraine marks the Port Huron readvance in Central New York, and is dated from circa 15,249 to 14,749 Cal BP (Kozlowski and Graham 2014). With ice retreat from this position, glacial melt waters began pooling in the Oneida basin, forming the earliest footprint of proglacial Lake Iroquois. Anderson and Lewis (2012: 522-523) propose that, with continued meltwater input, Lake Iroquois continued to expand south of the Laurentide ice sheet, reaching its maximum footprint at circa 13,500 Cal BP (11,700 RCYBP) and inundating the Ontario Lowlands and the Cayuga Lake basin (Bird and Kozlowski 2016) (see Figure 2). Lake Iroquois initially drained down the Iro-Mohawk Valley, but beginning 13,500 Cal BP, Laurentide ice retreat from the northern

Adirondacks opened a series of lower drainage outlets via the St. Lawrence, leading to progressively lower lake levels in the Ontario basin and culminating with Early Lake Ontario at circa 12,900 Cal BP (see Figure 2).

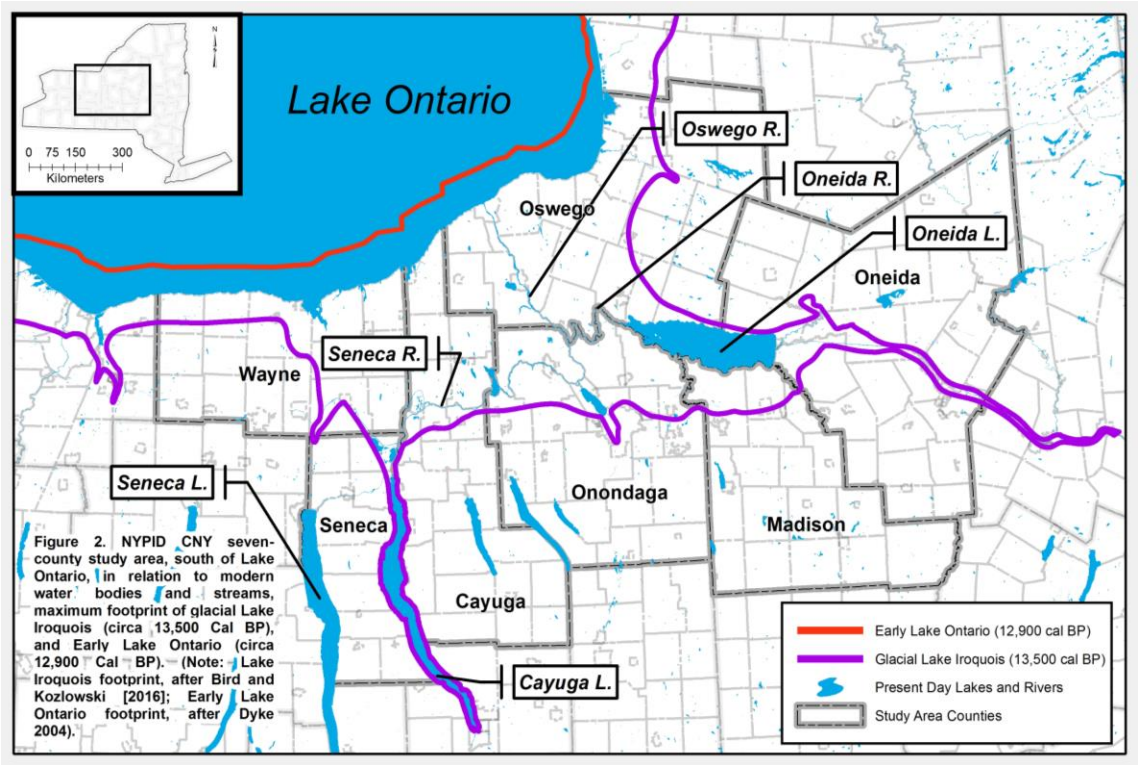

Figure 2. NYPID CNY seven-county study area, in relation to modern water bodies and streams, footprints of proglacial Lake Iroquois (circa 13,500 Cal BP) and Early Lake Ontario (circa 12,900 Cal BP). (Note: Lake Iroquois footprint, after Kozlowski and Bird 2016; Early Lake Ontario footprint, after Dyke 2004).

Anderson and Lewis (2012: 522-523) date Early Lake Ontario from 12,900 to 12,300 Cal BP (11,000-10,400 RCYBP), when this water body was likely confluent with the newly formed Champlain Sea. In Central New York, the shoreline of Early Lake Ontario lay 5-10 km north of the shoreline of modern Lake Ontario (see Figure 2). Thereafter, the combination of rising basin outlet sills (due to isostatic rebound) and warmer, drier early Holocene climate (beginning circa 11,600 Cal BP), resulted in a closed-basin, low-stand in the Ontario basin between 12,300 and 8,300 Cal BP (10,400-7500 RCYBP). Figure 3 illustrates the temporal overlap of Paleoindian occupations in Central New York (circa 13,000-10,800 Cal BP) with the smaller, lower footprint of Early Lake Ontario. Importantly, recent sediment coring in Oneida Lake suggests a contemporaneous low-

stand occurred in the Oneida basin during the late YD and early Holocene, indicating a water body with a smaller footprint than modern Oneida Lake (Domack, personal communication, 2016).

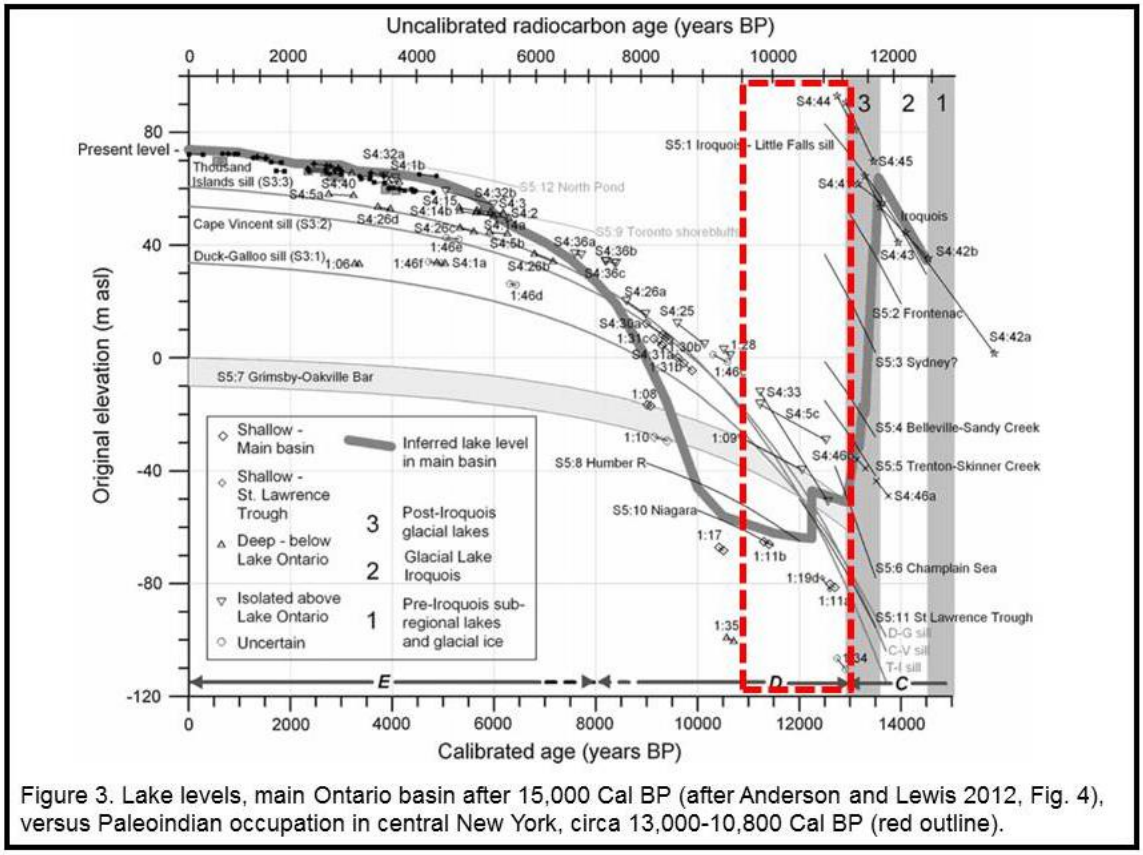

Figure 3. Lake levels in the main Ontario basin since 15,000 Cal BP (after Anderson and Lewis 2012, Figure 4, *versus* time span of early Native American occupation in central New York (outlined in red).

Paleoenvironments

Tree and plant communities of the late glacial and early Holocene in Central New York were conditioned by climatic factors. To the east, in the New England and Canadian Maritimes region, climate proxies document a strong signal of the post-Allerod Younger Dryas (YD) climatic reversal, with abrupt declines in temperature and moisture at circa 12,900 Cal BP (Hou et al. 2006; Shuman et al. 2004). After the YD onset, the Allerod trend towards mixed coniferous-deciduous tree communities was reversed, resulting in expanded tundra settings to the north and spruce parklands and spruce forests to the

south. With the abrupt advent of warmer, drier conditions in the early Holocene, at 11,600 Cal BP, closed pine and pine-oak forests rapidly expanded across New England, and most of the Canadian Maritimes (Newby et al. 2005).

In the eastern Great Lakes, some pollen sequences show a short-lived spruce peak at the YD onset, followed by declines in spruce, ash, and nonarboreal pollen and an increase in pine during the YD (Ellis et al. 2011; Karrow 2004; McCarthy et al. 2015). Notably, faunal remains of arctic fox, found at the Udora site in the Georgian Bay region of Ontario, document open tundra-like environments during the site's Early Paleoindian, Gainey phase occupations in the early YD (Storck and Spiess 1994). Post-YD, tree communities in the lower Great Lakes are dominated by pine and mixed pine-deciduous species.

In Central New York, early pollen core studies of bogs and wetlands around Oneida Lake document transitions from spruce to pine-dominated tree taxa (Cox 1959; Durkee 1960), but chronological control for these sequences is poor. Anderson and Lewis (2012) analyzed pollen and radiocarbon dated macro botanicals from sediment cores that were originally extracted in Lake Ontario between 1966 and 1974. These cores were situated at former subaerial and subaqueous (shallow and deep-water) settings around the margins of Early Lake Ontario. Pollen stratigraphy in cores from eastern Lake Ontario generally document spruce maxima correlated with the YD, and pine dominance during the early Holocene (Anderson and Lewis 2012:517-521 and ESM). The nature and variation of open versus closed forest landscapes over the course of the YD remains unclear for the eastern Ontario basin, although we suspect a transition from parkland-like settings in the early YD to more closed forests towards the end of the YD (Table 1) (Ellis et al. 2011; Newby et al. 2005).

Table 1. Paleoindian point sequence for Eastern Great Lakes (after Ellis and Deller 1990, Deller and Ellis 1992, Jackson and Hinshelwood 2004), climatic episodes and probable central New York environments and Ontario basin Lake levels (after Anderson and Lewis 2012).

Paleoindian Chronology	**Paleoindian Point Types**	**Climatic Episode**	**C. New York Environments**	**Ontario Basin Lake Levels**
Early Paleoindian ~12900-12,200 Cal BP (~11,000-10,300 RCYBP)	Gainey [1]	↑ Younger Dryas (Dry, Cold) ↓	Spruce Parklands? ↓ Spruce Forest?	Early Lake Ontario (12,900-12,300 Cal BP) ↓ E. Lake Ontario: Closed basin low-stand (12,300-11,600 Cal BP)
Middle Paleoindian ~12,200-11,600 Cal BP (~10,300-10,100 RCYBP)	Barnes			
	Crowfield			
	Holcombe			
Late Paleoindian ~11,600-10,800 (?) Cal BP (~10,100-9500 RCYBP)	Plano (Agate Basin-like) & Hi-Lo	Early Holocene (Dry, Warm)	Pine Forest	E. Lake Ontario: Closed basin low-stand (11,600-8300 Cal BP)
	Plano (Eden-like)			

Note 1: Earlier Clovis-affiliated populations may be present in the Eastern Great Lakes slightly earlier, circa 13,250-12,900 Cal BP and associated with Spruce-Pine-Oak Forests of the late Bolling-Allerod (Lothrop et al., 2016).

Regional Resources

Against the backdrop of these postglacial environmental settings, Ice Age terrestrial fauna have figured prominently in debates over potential prey species for YD-era Paleoindian populations in the New England-Maritimes and eastern Great Lakes. Limited faunal recoveries from Paleoindian sites most often record caribou and equivalent sized large mammal (Lothrop et al., 2016). Especially in the New England-Maritimes, the YD-era mix of tundra to the north and spruce parklands and forests to the south is projected as ideal habitat for long-distance migratory caribou herds (Newby et al. 2005). Mastodon is the most common of fossil proboscidea in the Northeast and New York, although published archaeological evidence for Paleoindian exploitation of this species is presently limited to possible scavenging (rather than hunting) at the Hiscock site in western New York (Laub 2003).

Feranec and Kozlowski (2016) report Bayesian analysis of AMS dates on paleontological specimens from New York, providing regional indicators of species colonization and extirpation. This study projects that caribou colonized the postglacial tundra of southern New York between 17,970 and 16,450 Cal BP, while American mastodon likely entered the region between 14,540 and 14,090 Cal BP (when spruce parklands and forests were common). Although caribou survived locally in New York until the 19th century, this analysis suggests that mastodon were likely extirpated from the region *during* the YD, circa 12,460 to 11,930 Cal BP, while optimal spruce habitats for this species are proposed to have still prevailed. Because of the chronological overlap of several centuries for mastodon and early Native American populations, this study implicates humans and not habitat change in the extirpation of mastodon from New York – a working hypothesis for which we as yet have no clear archaeological evidence.

Devonian cherts were perhaps the dominant regional toolstone source for Paleoindian populations in Central New York during the late Pleistocene and early Holocene. Chert-bearing limestones are present along the north-facing Onondaga escarpment, locally 15 to 20 km south of Oneida Lake (Lothrop 1989) (see Figure 1). Best known are the cherts of the middle Devonian Onondaga formation members, outcropping along the Onondaga escarpment across New York (Fisher et al. 1970) (see Figure 1). To the southeast, outcrops of the Esopus Shale formation (Lower Devonian) contain chert beds, beginning in the town of Richfield Springs (Otsego County) and extending east along the south side of the Mohawk Valley and south along west side of the Hudson Valley (Fisher 1980; Ver Straeten and Bell 2006; Ver Straeten, personal communication, 2014).

In the mid-Hudson Valley of eastern New York, Paleoindian groups exploited chert-bearing shales of the Ordovician Normanskill group (Funk 2004). Outside of New York, Native American populations also mined Cambro-Ordovician jasper from the Hardyston formation in the Reading Prong district of the middle Delaware Valley and extracted cherts from the upper Mercer and Vanport limestones in east-central Ohio (Lothrop and Bradley 2012: 14-15).

Previous Paleoindian Research in Central New York

Lothrop et al. (2014) summarize previous archaeological research on Paleoindian occupations in the New York region, and review current models of Paleoindian lifeways in New York and the broader Northeast (Ellis 2008, 2011; Ellis et al. 2011; Lothrop et al. 2011). With respect to Central New York, this overview also makes clear that our current interpretations of Paleoindian occupations south of Lake Ontario are influenced by and dependent on the far more advanced archaeological research conducted by our Canadian colleagues over the last four decades (e.g., Ellis and Deller 1990, 1997; Ellis et al. 2011; Jackson and Hinshelwood 2004). Ontario researchers have played pivotal roles in defining (1) the relative chronology of diagnostic bifaces for the eastern Great Lakes (Deller and Ellis 1992, 2011; Ellis 2004; Jackson 2004), (2) changes in flaked stone tool technologies over time (Ellis and Deller 1988; Jackson 1998), and (3) temporal variation in Paleoindian mobility and land-use (Ellis 2011; Ellis and Deller 1990; Jackson and Hinshelwood 2004). These models offer context for approaching the archaeology of contemporaneous Paleoindian populations "south of the border," but also raise fundamental questions as to how closely the evidence for Paleoindian lifeways and material culture in Central New York hews to models developed for southern Ontario.

Table 1 compares the Paleoindian chronology and diagnostic point forms for the eastern Great Lakes, with contemporaneous climates, environments and lake levels for Central New York. Figure 4 illustrates diagnostic Paleoindian biface types.

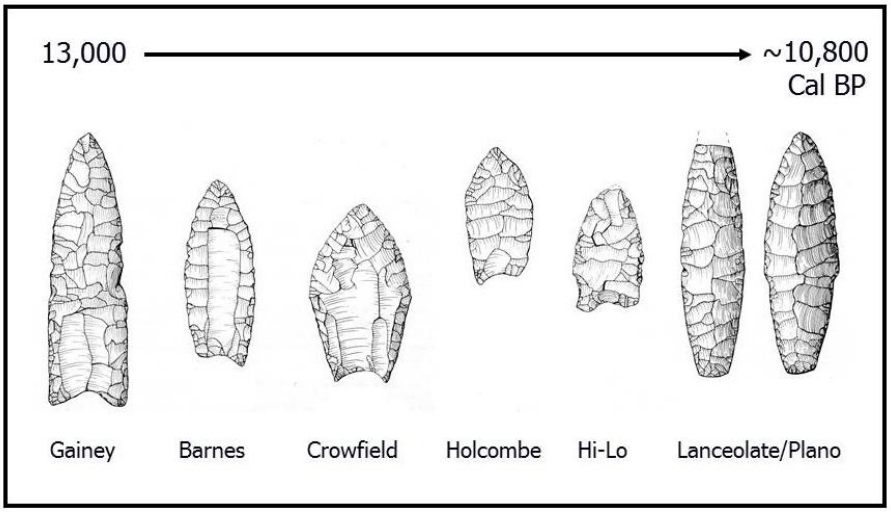

Figure 4. Paleoindian biface sequence for eastern Great Lakes region, estimated at circa 13,000-10,800 Cal BP (after Ellis and Deller 1990, Fig. 3.1).

Although several Paleoindian sites have been investigated in western New York (Gramly 1988, 1999; Laub and Spiess 2003), and eastern New York (e.g., Funk 2004; Funk and Steadman 1998; Lothrop and Bradley 2012; Lothrop et al., in press), archaeological research on Paleoindian occupations in Central New York has been limited (Table 2). In the 1930s, William A. Ritchie's excavations at the Oberlander #1 site, situated on the north shore of the Oneida Lake outlet (Ritchie 1940), documented Archaic Brewerton point components dating to circa 5000 Cal BP, but also recovered unfluted Late Paleoindian points, including parallel-flaked "Plano" Agate Basin-like and Eden-like forms. In 1963, Ritchie tested the Early Paleoindian Potts site, located west-northwest of Oneida Lake (Ritchie 1969). In 1982 and 1983, archaeologists from the Buffalo Museum of Science revisited the Potts site, excavating three Paleoindian occupation areas on the northern nose of the drumlin host landform. This fieldwork documented a predominantly Early Paleoindian Gainey phase occupation (Gramly and Lothrop 1984; Lothrop 1989), represented by a stone tool assemblage likely made on Esopus shale chert (with closest outcrops in the mid-Mohawk Valley) (Ver Straeten, personal communication, 2014).

Several researchers have reported distributional data on Paleoindian bifaces for New York, beginning with Ritchie (1957, 1965), who noted a major concentration of points in the central part of the state. In 2002, Bradley and Funk (n.d.) assembled additional data on Paleoindian bifaces for Central New York. Lothrop et al. (2014) combined these unpublished data with more Paleoindian bifaces recorded for a seven-county study area (see Figure 2), generating an updated chronological and geographic overview of Paleoindian occupations in Central New York.

Chronologically, Paleoindian bifaces recorded for Central New York include early (Gainey), middle (Barnes, Crowfield), and late (Agate Basin-like, Eden-like) Paleoindian point forms (Table 1), documenting occupations during both the late Pleistocene YD and early Holocene. GIS mapping by township of Paleoindian point densities per 100 km^2, revealed that Paleoindian bifaces were far more common within the footprint of former proglacial Lake Iroquois, as compared to higher elevation terrain on the Appalachian plateau, south of the Onondaga escarpment (Figure 5). Within the Ontario Lowland, Paleoindian biface density is highest in townships that front southern and western shores

of Oneida Lake and the east-west traces of the Oneida and Seneca rivers. Likewise, all but one of the Paleoindian sites documented in the Central New York study area lie within the former footprint of proglacial Lake Iroquois on the Ontario Lowlands (see Figure 5, Table 2).

Undeniable biases exist in these distributional data, including (1) collector bias (e.g., fortuitous discoveries of Paleoindian points during surface survey of known late prehistoric sites along the Seneca and Oneida drainages), and (2) absence of data for now-inundated shorelines of Early Lake Ontario and Oneida Lake that were exposed by lake low-stands during the YD and early Holocene (see Figure 5). Recognizing these biases, the present data set nevertheless documents seasonal Paleoindian use of the Iroquois bottomlands that included a focus on localities proximal to the Seneca and Oneida drainages.

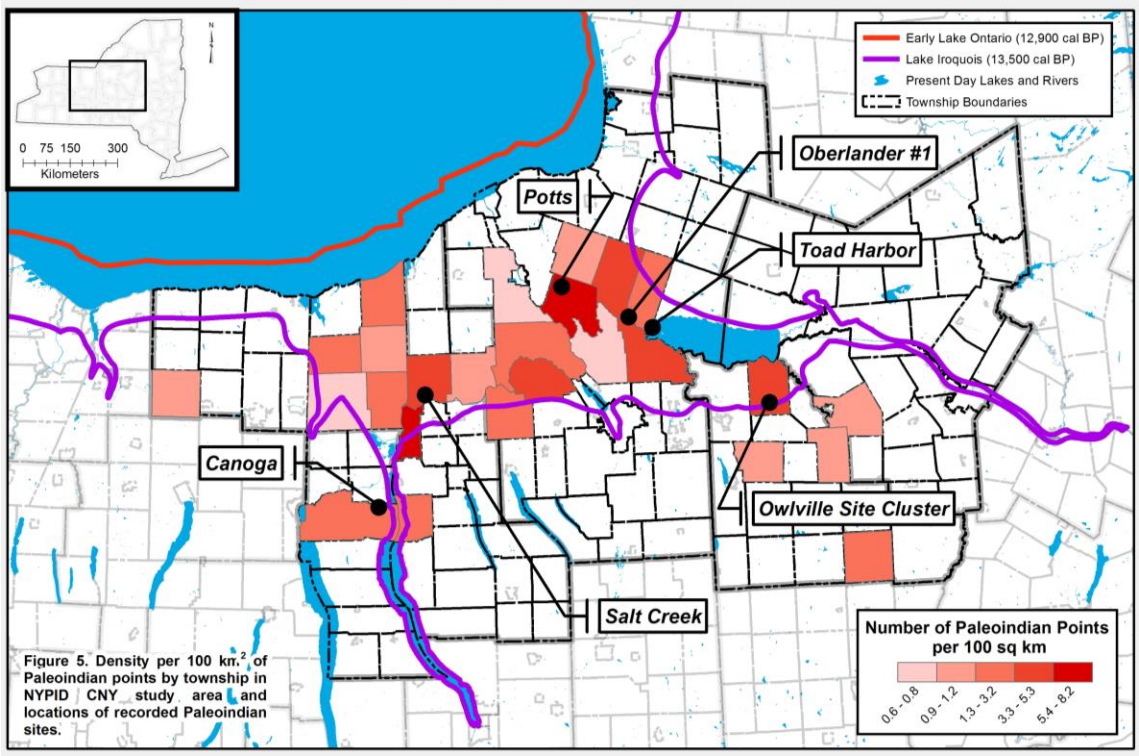

Figure 5. Density per 100 km² of Paleoindian points by township in NYPID CNY study area and locations of recorded Paleoindian sites.

Table 2. Settlement characteristics of Paleoindian sites in central New York.

Site	County	Drainage	Investigation	Component/ Point form	Toolstone	Assemblage	References
Canoga	Seneca	Seneca	Surface collection	MP/Barnes	PA Jasper; Normanskill; Vanport?	Points Endscrapers	Lothrop et al. 2014
Salt Creek	Cayuga	Seneca	Surface collection	EP or MP	Jasper; Silicified sandstone	Points	Lothrop et al. 2014
				LP/Eden-like?	Chert (Devonian?)	Point	
Potts	Oswego	Oneida	Excavation	EP/ Gainey	Esopus; Normanskill	Points Bifaces Unifaces	Gramly and Lothrop 1984; Lothrop 1988, 1989
				MP/Barnes	W. Onondaga	Point	
Oberlander #1	Oswego	Oneida	Excavation	LP/Agate Basin-like	Gray chert (Devonian?)	Point	Ritchie 1940
				LP/Eden-like	W. Onondaga; Gray chert (Devonian?)	Points Knife	
Toad Harbor	Oswego	Oneida	Surface collection	EP/Gainey	Jasper; Normanskill; Red chert or jasper	Points Unifaces *Pieces Esquillees*	Bradley and Funk n.d.
Owlville Site Cluster							
Glass Factory	Madison	Oneida	Surface collection & STPs	MP/Crowfield	Esopus; Brown chert (Devonian?)	Points Bifaces Unifaces	Lothrop et al. 2014
Owlville South	Madison	Oneida	Surface collection & STPs	MP/Crowfield ?	Esopus	Point Unifaces	This Paper
Owlville Pine South	Madison	Oneida	Surface collection & STPs	MP/Crowfield	Esopus; Brown chert – Devonian?	Point Unifaces	This Paper

Component Key: EP = Early Paleoindian; MP = Middle Paleoindian; LP = Late Paleoindian

Preliminary Archaeological Investigations of the Owlville Site Cluster

Here we summarize ongoing investigations at three fluted point Paleoindian sites – Glass Factory, Owlville South, and Owlville Pine South – that together make up the Owlville Paleoindian site cluster. These sites are situated on the Ontario Lowland between Oneida Lake and the Onondaga escarpment. Between 2007 and 2015, co-authors Beardsley and Clymer identified and systematically surface collected these three Paleoindian sites, along with eight other undated, or later Holocene-age lithic scatter sites within a 35-acre study area on private property. In 2014 and 2015, New York State Museum archaeologists began collaborating with Beardsley and Clymer on field investigations, beginning with GPS recording of surface collected artifacts to provide high resolution provenience mapping. Subsequent test excavations were carried out to gauge the stratigraphic context of these sites, and to collect systematic excavated samples. As of June, 2016, we have conducted minimal shovel testing at Glass Factory and Owlville South, and more extensive testing at Owlville Pine South. Shovel test pits (STPs) measured 50x50-cm, and were excavated by soil horizons, passing soils through three-millimeter mesh for systematic artifact recovery. Although analysis of surface collected and excavated artifacts is ongoing, preliminary study has tentatively identified Crowfield type fluted bifaces at all three sites, indicating occupations likely dating to circa 12,000 Cal BP, in the latter portion of the YD.

Surficial mapping shows that the Owlville cluster sites are situated on lacustrine silt and clay of proglacial Lake Iroquois (Muller and Cadwell 1986). Extensive swamp deposits are mapped to the north and northwest, consisting of peat-muck and poorly drained organic silt and sand. Known locally as "Black Beach," immigrant Italian-American farmers cleared and cultivated these Canastota mucklands, making Canastota the "Onion Capital of the World" for a time in the early 20th century (Barbagallo 2005). More localized muck deposits are present in lower elevation settings around Oneida Lake, and recent AMS dating indicates that underlying marl deposits formed during the mid-Holocene, followed by muck formation in the late Holocene (Domack, personal communication, 2016). During the YD and early Holocene (contemporaneous with the associated low-stand in the Oneida basin), we suspect that these low settings were

probably dry much or most of the year. New mapping of the maximum footprint of Lake Iroquois (Bird and Kozlowski 2016) shows that the Owlville cluster sites lie near and probably just north of the former southern shore of Lake Iroquois. Further south, Muller and Cadwell (1986) map the foot slopes of the Onondaga escarpment as glacial till. Canaseraga Creek and its tributaries (Cowaselon, Owlville and Canastota creeks) head on the dissected north face of the Onondaga escarpment, and drain the vicinity of the Owlville site cluster before flowing north to Oneida Lake at Lakeport.

Glass Factory

The Glass Factory site is situated on terrain that slopes gently westward and northward to a low-order stream. Based on GPS mapping of surface collections in 2014 and 2015, the overall site measures approximately 120x100 m. An erosional scarp flanks the western margin of the site, and may constitute a wave-cut beach scarp formed when Lake Iroquois was dropping to lower levels between 13,500-12,900 Cal BP (Gene Domack, personal communication, 2014).

Beardsley discovered the Glass Factory site in the spring of 2007, during surface survey of plowed fields. The site name derives from historic glass cullet (waste) observed on the surface, along with prehistoric Native American stone tools and flaking debris. This glass waste likely represents discard from the 18th-century Peterboro Glass Factory.

Early on, surface-collected stone artifacts indicated that Glass Factory contained several Native American archaeological components. The western portion of the site is dominated by Holocene-era projectile points and other bifaces, including stemmed Neville, Lamoka and Susquehanna broad points, and most commonly, broad blade, stemmed Snook Kill bifaces. These diagnostic bifaces document periodic reoccupation of this western sector of Glass Factory between circa 8500 and 3000 Cal BP. Other artifacts found in this portion of the site and not associated with the site's Paleoindian component include two endscrapers manufactured on projectile point segments, a quartzite flaked adz bit, and waste flakes from biface reduction. Excluding the adz, toolstones for these Holocene-age artifacts consist of a wide variety of cherts, at least some of which likely derive from outcrops at the nearby Onondaga escarpment to the south.

Surface collection at Glass Factory also produced artifacts reflecting older, late Pleistocene occupation. In 2010, 2011 and 2012, Beardsley and Clymer recovered four fluted preforms that represent fluted point manufacturing failures (Figure 6), documenting a YD-era Paleoindian component.

The four fluted bifaces from Glass Factory include (1) the basal fragment of a preform with a single flute on one face (Figure 6, A); (2) a preform base with multiple flutes on both faces, and lateral edges that expand markedly from the base (Face angle, a measure of whether biface hafting margins are parallel [= 90°], or expanding [>90°], equals 102.5° for this biface) (Figure 6, B); (3) a preform fluted from the tip (Figure 6, C); and (4) a lateral edge fragment of a fluted preform with a distinct shoulder outline on the blade margin adjoining the remnant flute scar (Figure 6, D).

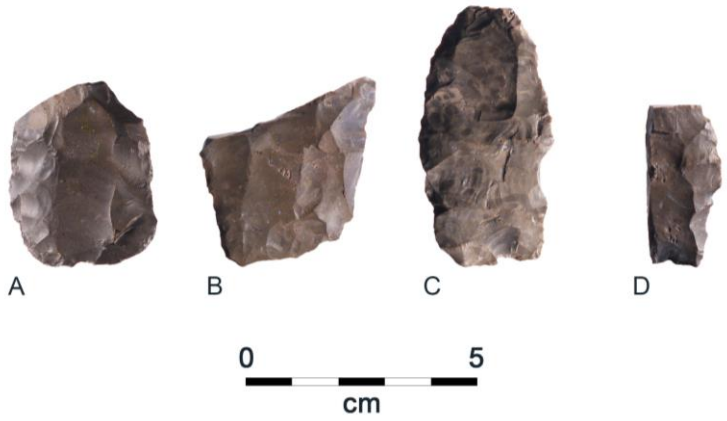

Figure 6. Glass Factory site, fluted bifaces. A: Preform base, single flute; B: Preform base, three flutes; C: Preform, tip flute; D: Preform, right lateral/proximal fragment, showing partial channel scar and "shoulder" on adjoining blade edge.

Detailed technological studies of Crowfield points found in southwestern Ontario (Deller and Ellis 1992: 41-51; Deller and Ellis 2011:67-68, 74) document the following distinguishing attributes on finished Crowfield fluted bifaces:

- Straight hafting margins (lower lateral edges) that expand markedly from the base (face angle range = 100° to 111°);
- Maximum width located at or above the midline of the point;
- Multiple (or less commonly) single flute scars extending from the base on one or both faces, and occasional fluting downward from the tip;

- Biconvex cross-sections averaging less than 5 mm thick, with high width-to-thickness ratios averaging 6:1;
- Bases measuring between 13.1 and 22.8 mm wide, with shallowly concave to flat basal margins;

Additionally, Deller and Ellis (2011: 73-75) also note that a distinct, pointed shoulder is often present on Crowfield points whose blade edges *have not been resharpened* (as would be the case for very late-stage manufacturing failures).

Based on these attributes, the three fluted preforms illustrated in Figure 6, B, C, and D, likely represent unfinished Crowfield points. As a type, Crowfield bifaces constitute the last of the long-fluted point forms in the biface sequence for the eastern Great Lakes (see Table 2, Figure 4), and date to the latter portion of the YD, likely after circa 12,000 Cal BP (Bradley et al. 2008; Deller and Ellis 1992; Lothrop et al., 2016).

Lithic types for Paleoindian artifacts at Glass Factory appear to consist of two types. The first toolstone is tentatively identified as lower Devonian, Esopus Shale formation chert (Fisher 1980; Ver Straeten and Bell 2006). Fisher (1980) describes this formation as consisting of 10- to 25-cm-thick beds composed of naturally fractured blocks of silicified argillite, with dark gray shale inter-beds. Vertical variation in silica content, visible in individual blocks, results in irregular banding that parallels individual beds. From the top down, these individual blocks are square, rectangular, or triangular in shape, and rectangular to square in side view. Lithic replication experiments show that the geometry of individual blocks in the silicified argillite beds would have facilitated standardized blank production (Lothrop 1988, Appendix C). As noted, the Potts site in Oswego County documents Early Paleoindian use of this toolstone, comprising well over 95% of the lithic assemblage at that early Paleoindian site (Lothrop 1989). The second toolstone in the Paleoindian component at Glass Factory consists of a brown limestone chert. Artifacts of this material sometimes display joint faces, suggesting it also derives from a bedded outcrop source, perhaps from Devonian formations in the nearby Onondaga escarpment.

Other Paleoindian artifacts in the Glass Factory assemblage are dominated by unifacial tools (that is, manufactured by percussion or pressure flaking on only one face of a tool

blank). Most common are endscrapers, a frequent tool form on most Paleoindian fluted point sites. In plan view, these tools are triangular in form, having been shaped by unifacial flaking of the lateral and distal edges of the original tool blank (Figure 7, A-F). All examples display convex distal bits or working edges. Lateral margins taper to the proximal end, indicating these tools were hafted in a socketed handle to increase leverage during use. Microscopic use-wear analysis of endscrapers from Paleoindian sites indicates that they were most commonly used to process hides for skin clothing manufacture (Loebel 2013).

Other flake tools in the Glass Factory assemblage do not show hafting modifications, and were probably hand-held during use. The largest of these is a palm-sized backed uniface, refitted from two fragments (Figure 7, J). Manufactured from a blank driven off the side face of a quarry block, the irregular, unifacially flaked left margin is denticulated (toothed). The flat, unworked surface on the right edge, oriented perpendicular to the plane of the tool, may constitute backing to facilitate prehension during use of this heavy-duty cutting or scraping tool. The collection also includes a second possible backed tool (Figure 7, I): steep unifacial retouch on the left margin, and flat block cortex on the right side, suggest a hand-held, cutting or scraping function for this tool. A third uniface with a concave working edge may have been used for working shafts of wood or bone (Figure 7, H). Finally, a flake tool with a refined bifacial edge on the right margin was likely used for cutting (Figure 7, G).

Flaking debris surface collected at Glass Factory, of Esopus and brown chert, is limited to small, late-stage biface reduction flakes, as well as indeterminate flake types. The absence of cores and early-to-middle-stage flaking debris is expected, because archaeological evidence for the glaciated northeast shows that fluted point groups routinely reduced toolstone at or near source outcrops, producing a transported tool kit of blanks and finished implements. This segmenting of the reduction sequence served to reduce weight of a transported tool kit that included finished implements and tool blanks. Transport of both blanks and finished tools permitted the flexibility to produce tools of different forms and functions at use locations, on an as-needed basis (Ellis 2008; Lothrop and Bradley 2012).

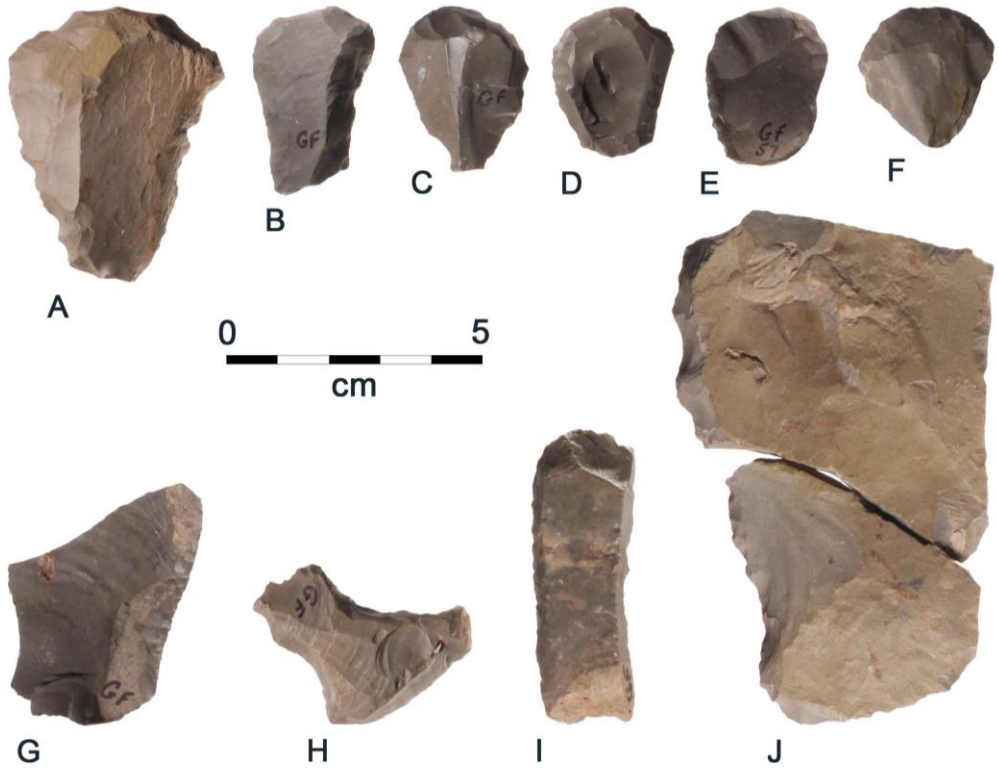

Figure 7. Glass Factory site, flake tools. A through F: Endscrapers, with unifacial retouch on dorsal surfaces (proximal ends of B and F broken off); G: Flake tool with refined bifacial flaking on right lateral edge; H: Uniface with distal, concave bit; I: "Backed" uniface, with steep scraper retouch on left edge and flat block cortex backing on right margin; J: Large "backed" uniface, with denticulated scraper retouch on left margin and unretouched flat surface on right margin (refitted from two fragments).

Owlville South

Situated several hundred meters southwest of Glass Factory, Owlville South is located on an interfluve dissected by two low-order streams. Beardsley discovered Owlville South in 2014; subsequent limited shovel testing and ongoing surface collection indicate this site consists of a very low density near-surface lithic scatter measuring about 60x40 meters.

As with Glass Factory, two pre-contact Native American components are present at Owlville South. The first is represented by a basal fragment of an Archaic stemmed Lamoka point, and the tip section of a probable second stemmed biface. These points were fashioned from a brown chert that is indistinguishable from artifacts of brown chert in the Paleoindian component at the Glass Factory site. A tested cobble core of the same

material is likely also associated with this Late Archaic occupation, dating to circa 4500 Cal BP.

Paleoindian stone tools at Owlville South were manufactured from Esopus chert (Figure 8). The fluted point from this location consists of a small, thin basal fragment whose lateral edges expand markedly from the base (face angle = 100°). A single channel scar is present on the obverse face. Lateral margins display light edge grinding. Based on these attributes, we tentatively identify this fluted biface as a Crowfield point (Figure 8, A).

Other Paleoindian tools recovered at Owlville South include two endscrapers, one complete (Figure 8, B) and a distal bit fragment (Figure 8, C). In addition, Figure 8, D, illustrates a narrow-bitted unifacial tool. Due to steep unifacial flaking on the lateral edges of the dorsal face and invasive flaking on the ventral surface, the lower two-thirds of this tool tapers toward the base in plan and profile. These features, coupled with edge grinding applied to the lateral edges after flaking, indicate that the proximal end of this tool was likely mounted in a socket or binding haft. On the distal end, steep unifacial retouch defines a thick unifacial point or beak that could have been used for heavy-duty grooving or slotting of wood or bone. Some features of this tool resemble the hafted perforator tool type described by Ellis and Deller (1988:136), but it differs in its straight, tapering (rather than convex) lateral margins.

Figure 8. Owlville South site, artifacts. A: Probable small Crowfield point base (single flute on obverse face); B: Endscraper; C: Endscraper bit fragment (thermal fracture); D: Hafted perforator or beak.

Debitage of Esopus chert at Owlville South includes small numbers of biface reduction flakes and two uniface retouch flakes. Of note, the debitage sample includes a single biface thinning flake of probable Pennsylvania jasper, whose likely source would be in the Hardyston formation in the Delaware Valley of eastern Pennsylvania.

Owlville Pine South

The Owlville Pine South (OPS) site is situated on featureless terrain, between Owlville South and Glass Factory. In April 2015, while returning from surface survey of another site, Beardsley walked through the OPS locality and discovered a convergent scraper of Esopus chert (Figure 9, E). Subsequent surface finds by Beardsley and Clymer in 2015 included a Crowfield point and other Paleoindian tools (Figure 9). During shovel testing the fall of 2015, we recovered artifacts in 21 of 24 STPs, at counts of one to three specimens per STP. This fieldwork confirmed that OPS consists of a near-surface lithic scatter with low artifact densities, measuring perhaps 70x30 meters.

Figure 9. Owlville Pine South site, artifacts. A: Crowfield point with distal impact fracture (left lateral edge reworked/truncated by scraper retouch onto reverse face); B: Endscraper (cavity on right lateral margin due to plow nick); C: Hafted perforator; D: Graver (distal point defined by unifacial retouch); E: Convergent scraper with unifacial retouch on distal and right lateral margins.

Esopus chert makes up 98% of the artifact sample at OPS, providing further evidence of a Paleoindian preference for this toolstone at sites in the Oneida basin. In 2016, Beardsley and Clymer surface collected two flakes of a brown chert, indicating that this toolstone

(macroscopically similar to artifacts of brown chert in the Glass Factory Paleoindian assemblage) was also used at OPS.

Artifact recoveries to date at OPS indicate the site consists exclusively of a Paleoindian component cultural component. Across the glacial Northeast, single-component Paleoindian sites are uncommon because later pre-contact Native American groups often occupied the same locality (as at Glass Factory and Owlville South). Where this occurs, these later cultural lithics can introduce "background noise" into a palimpsest multicomponent archaeological assemblage. In such cases, while it is often possible to segregate artifacts of Paleoindian and later components based on raw material type, lingering uncertainty as to the cultural affiliation of some artifacts can make behavioral interpretations more difficult. This does not appear to be the case at OPS, highlighting the interpretive potential of this site.

Features of the fluted point found at OPS reveal a complex use history. Two flutes are present on each face (see Figure 9, A), and light edge grinding on the lower right edge indicates this point was finished and ready for hafting. A spinoff- type, distal impact fracture (Clarkson 2016; Iovita et al. 2014), consisting of a concave, transverse break and associated deep ripple scar, documents damage during use as a projectile. Unifacial retouch on the left blade margin (scars extending onto the reverse face), suggests that after the impact fracture and removal from the foreshaft mount, this point was apparently recycled as a hand-held tool for cutting or scraping. Despite breakage and reworking, this point's surviving attributes of (1) multiple fluting on each face, (2) a straight hafting margin (right side) that expands markedly from the base (right edge face angle = 109°), and (3) shallow basal concavity and maximum width above the midpoint, clearly qualify this point as a Middle Paleoindian Crowfield form (Deller and Ellis 2011:67-68).

Other formal Paleoindian artifacts recovered to date at OPS consist of unifacial tools, all of Esopus chert. The first surface find – the convergent sidescraper (Figure 9, E) – displays unifacial retouch on the dorsal face (distal and right lateral margins), and would have been used as a hand-held, cutting or scraping tool. The lone endscraper displays the thick, triangular cross-section of the parent tool blank (Figure 9, B), likely intended to

minimize transverse breakage from downward force transmitted through the endscraper's socket haft during scraping use (Iceland 2013; Lothrop 1989).

The tool illustrated as Figure 9, C, displays unifacial retouch that defines wider convex margins on the proximal end, and a narrow distal segment that tapers to an acute point. The proximal end of this tool was almost certainly hafted to allow increased load application on the pointed tip, perhaps during slotting of wood or bone. This artifact resembles the hafted perforator tool type described by Ellis and Deller (1988:136) for Middle Paleoindian sites in southern Ontario.

Surface collection at OPS also produced two flake gravers. These artifacts display small unifacial spurs created by delicate pressure retouch, made on thin flake blanks from biface reduction. The first example displays two spurs, both broken during use, while the second graver (Figure 9, D) exhibits a single complete spur. Researchers have debated the functions of these delicate graver tools at Paleoindian sites. Tomenchuk and Storck (1997) propose that coronet gravers were used in a rotary fashion for boring or cutting thin discs of bone or wood. More recently, Osborne (2014) argues that, based on their co-occurrence with preserved bone needles at Paleoindian sites in western North America, stone gravers may have been used to produce eyes on bone needles – a critical tool for hide clothing manufacture to reduce YD-era cold stress.

Preliminary analysis of flaking debris recovered during surface collection and shovel testing at OPS reveals late-stage debitage types expected at a Paleoindian residential camp not associated with a lithic source. Biface reduction debris includes larger thinning flakes produced by direct percussion, small pressure flakes, and three channel flake fragments – all products of late-stage fluted point manufacture. Other flake types include small uniface retouch flakes, generated during manufacture or resharpening of scraper bit edges. Taken together, these flake types document stone tool manufacture and maintenance during a Paleoindian encampment.

Discussion and Preliminary Conclusions

Recording and GIS mapping of Paleoindian points across the Central New York study area informs us on some cumulative patterns of human land-use during the late

Pleistocene and early Holocene. Documentation and investigation of individual archaeological sites and artifact assemblages provides complementary insights on early Native American occupations of specific landforms, site activities, mobility and technology. Below, we summarize preliminary insights gained from the ongoing investigation of the recently recorded Owlville cluster sites.

Land-Use and Settlement

As shown in Figure 5, GIS density mapping of Paleoindian points across our Central New York study area serves to reveal some aspects of repetitive land-use. Despite significant sources of bias, these data do suggest seasonal use of former Iroquois Lake bottom lands as one aspect of Native American settlement from the late Pleistocene into the early Holocene (Lothrop et al. 2014).

Locations of individual Paleoindian sites in this Central New York study area generally mirror the overall trends from density mapping (see Figure 5). Sites are found on terraces along the Seneca and Oneida rivers (Salt Creek, Oberlander #1), and on shoreline settings of Cayuga Lake (Canoga) and Oneida Lake (Toad Harbor). Importantly, we also have site locations in interior settings removed from these main drainages, including the Potts and Owlville cluster sites. Situated on a drumlin, the Potts site may represent a strategic game overlook for early Paleoindians. By contrast, the Middle Paleoindian Owlville cluster sites lie on bottomland proximal to low-order tributaries of Canaseraga Creek. These contrasting settings may be telling us that earliest Native American settlement in Central New York was perhaps more nuanced and complex, in ways that we do not fully understand.

Artifacts of Esopus chert and other likely Devonian cherts (the former found at all three Owlville cluster sites), point to yet-to-be-discovered contemporaneous Paleoindian quarry sites at outcrops for these toolstones. For Esopus chert, quarry locations are most likely present to the southeast in the mid-lower Mohawk Valley, while one or more quarry locations for the brown chert found at Glass Factory and OPS could lie along the Onondaga escarpment to the south. Judging from Funk's evidence for Paleoindian residential occupations at the West Athens Hill quarry site (2004), we might expect that

sites projected for these Devonian source outcrops would reflect not just toolstone extraction, but actual encampments of Paleoindian bands (Lothrop and Bradley 2012).

Looking north to southern Ontario, researchers there have noted the frequent (but not exclusive) association of fluted point sites in the Huron basin with southern strandlines of proglacial Lake Algonquin, and the inference that this may reflect site encampments strategically located to facilitate intercept hunting of migrating caribou herds (Ellis and Deller 1990, 1997; Ellis et al. 2011; Storck 1984). Underwater archaeological investigations of the now-submerged Alpena-Amberley Ridge (exposed during the Lake Stanley low-stand in the Huron basin), have revealed abundant evidence of probable stone hunting blinds, located to intercept seasonal caribou herd migrations along this landform (Sonnenburg et al. 2015). By extension, we can project the possible former presence of seasonal fluted point encampments, perhaps located for similar reasons along or near the now-submerged shorelines of Early Lake Ontario and the contemporaneous Oneida basin lake (see Figure 5).

Perhaps most striking about the discovery of the Owlville site cluster is the finding of three Middle Paleoindian sites (represented by Crowfield bifaces), situated on different landforms in an area measuring less than 500 linear meters across. Elsewhere, archaeologists have documented geographic clusters of Paleoindian sites in the New England-Maritimes (e.g., Boisvert 2012; Lothrop et al. 2011; Spiess et al. 2012), and in the Huron basin of southern Ontario (Ellis and Deller 1990, 1997). Where found, these site clusters represent repeated visits to distinct geomorphic landscapes, likely related in part to the presence of fixed resources like toolstone outcrops and/or the seasonal occurrences of prey species or other resources. For both the eastern Great Lakes and New England-Maritimes, site clusters are most common for Middle Paleoindian Barnes/Michaud-Neponset point sites, thus predating the Owlville site cluster.

For Crowfield point sites, there are no documented clusters of sites on record for the Northeast, and the low archaeological visibility and small size of the few excavated single component residential sites (Deller and Ellis 1996; Ellis et al. 1991; Timmins 1994) may indicate atomized Paleoindian settlement patterns during the late YD. If our

typological assessments of recovered bifaces are correct, then Glass Factory, Owlville South, and OPS may represent the first case of multiple Crowfield point sites found in close proximity. Indeed, our recording to date of *only two other Crowfield points in Central New York* (isolated finds, Wayne and Onondaga counties), makes the discovery of this Crowfield component site cluster all the more remarkable. Going forward, this raises the question as to whether the Owlville site cluster is unique in Central New York, or reflects discovery bias due to low archaeological visibility of these late fluted point sites.

Toolstone and Mobility

Northeastern archaeologists have had a long-standing interest in geologic sourcing of stone tools found on Paleoindian sites because of attendant implications for these peoples' seasonal movements and land-use. Current evidence indicates Paleoindian populations in the glaciated Northeast routinely mined toolstone at primary (bedrock) outcrop lithic sources during seasonal movements in the late Pleistocene and early Holocene, and rarely exploited secondary sources of cobble toolstone, found as lag deposits in stream gravels. Consequently, geologic source attribution of stone tools found at Paleoindian sites can provide measures of range mobility practiced by these peoples (Burke 2006; Lothrop and Bradley 2012). Synthesizing such data, Ellis (2011) documents evidence for seasonal movements by YD-era Paleoindian groups in the Northeast that routinely covered several hundred kilometers in straight-line distances between sites and lithic sources – exceptionally high levels of mobility that were not matched by Native American groups in later prehistory. The reasons for this high mobility are not fully understood, but likely reflect (1) a highly seasonal, subarctic resource base that included migratory prey species, as well as (2) low human population densities during the late Pleistocene that fostered periodic interaction between bands in different sub-regions for information and mate exchange (Ellis 2008).

The presence of Esopus chert as a dominant toolstone in the Potts and Owlville cluster site assemblages can inform us on seasonal range movements across Central New York by early and middle Paleoindian groups (see Table 2). The closest outcrops of this toolstone are found in the middle Mohawk Valley, circa 65 km to the east-southeast,

suggesting seasonal movements from this source area, up the Mohawk Valley, to encampments in the Oneida basin. Notably, artifacts of Ordovician Normanskill chert as a less common raw material at the Early Paleoindian Potts and Middle Paleoindian Canoga sites could reflect seasonal travel down the Mohawk to Hudson Valley outcrops such as West Athens Hill. Finally, the presence of probable Pennsylvania jasper in the Middle Paleoindian Canoga and Early Paleoindian Toad Harbor collections suggests seasonal movements to (or connections with resident Paleoindian groups in) Hardyston source areas in the middle Delaware Valley to the south. These preliminary data on toolstone at Paleoindian sites in Central New York hint at temporal variation in both source use and implied directions and distances of seasonal travel.

Stone Technology

Organizational studies of early and middle Paleoindian technology for the glaciated Northeast use assemblages of discarded tools and flaking debris found at sites to reconstruct the acquisition and reduction of raw toolstone, and the design and manufacture of transported stone toolkit. These analyses document a rigidly segmented reduction sequence, and the manufacture of standardized tools and tool blanks. Ellis (2008) argues that the high seasonal range mobility of these peoples may have necessitated time budgeting, that in turn governed the structure of the transported tool kit. In particular, the routine transport of tool blanks as well as finished tools allowed Paleoindian flintknappers to manufacture tools of specific form and function on an as-needed basis during seasonal travels.

In this view, the use of Esopus chert as a primary toolstone at the Early Paleoindian Potts and Middle Paleoindian sites of Glass Factory, Owlville South, and OPS, makes sense. Unlike cherts in several members of the Onondaga limestone formation, Esopus chert occurs in beds that yield blocks of consistent thickness and predictable geometries. Experimental reduction of Esopus chert shows that corners on blocks of this raw material provide ready-made core striking platforms to produce tool blanks of standardized size and shape using direct percussion flaking (Lothrop 1988, Appendix C). In short, the consistent package size and form of Esopus chert made it easy to produce standardized

blanks of sufficient size for tool manufacture, making this toolstone attractive to Paleoindian flintknappers.

Deller and Ellis (1988, 1996, 2011) offer provisional definitions of stone technology associated with Crowfield sites in southern Ontario. These are seminal contributions to understanding late YD-era Paleoindian technology, largely based on three single-component artifact collections from the Crowfield type site (a ritual feature, Deller and Ellis 2011), and two residential sites – Bolton (Deller and Ellis 1996) and Alder Creek (Timmins 1994). For Central New York, the absence of prior investigations of Crowfield point sites means that we know far less about the stone technology of these peoples, and the degrees of similarity between this region and southern Ontario. Preliminary analysis of artifacts from the Owlville cluster sites – the first Crowfield point sites investigated in New York state – suggest some broadly comparable tool forms such as hafted perforators and backed bifaces. With continued investigation, artifact samples from these sites will facilitate additional cross-regional comparisons.

Acknowledgments

We thank Gene Domack for inviting us to participate in the 2016 Friends of the Pleistocene field trip to the Oneida basin, and for sharing his insights and unpublished data on evolution of the basin's Late Pleistocene and Holocene landscapes. Thanks also to our NYSM geology colleagues, Andrew Kozlowski and Brian Bird, for unpublished data from their research on the post glacial geology of Central New York and for providing their unpublished GIS shapefiles of Lake Iroquois in the Ontario basin. Bob Feranec, NYSM curator of vertebrate paleontology, shared his unpublished research on postglacial colonization and extirpation of mammals in the New York region. Chuck Ver Straeten, NYSM curator of Devonian stratigraphy, examined the Potts and Glass Factory artifact assemblages and concluded the likely presence of Esopus chert in these collections.

Thanks to Drs. T.W. Anderson and C.F.M. Lewis for information on their seminal studies on water level histories in the Ontario basin. Mr. Tim Ruhren, New York State Office of Information Technology Services, kindly provided liDAR mapping for areas south of Oneida Lake. We owe many thanks to archaeology colleagues Christopher Ellis and Jim

Bradley for sharing their expertise on early Native American settlement of southern Ontario and Central New York.

We are indebted to Tom and Joyce Bush for their support of this research by permitting access to their property for archaeological field investigations, for many other kindnesses, and for granting property access for the 2016 visit by the Friends of the Pleistocene field tour. Thanks to steadfast fieldworkers in the investigation of the Owlville cluster sites, including Lisa Anderson, Bernadette Giardina, Andrea Lain, Roger Longfield, Michael Lucas and Zachary Singer. Finally, thanks to John Hart, NYSM Director of Research and Collections, and Mark Schaming, NYSM Director, for their support of this research.

References Cited

Anderson, T.W., and C.F.M. Lewis
2012 A New Water-Level History for Lake Ontario Basin: Evidence for a Climate-Driven Early Holocene Low Stand. *Journal of Paleolimnology* 47:513-530.

Barbagallo, Tricia A.
2005 Black Beach. *New York Archives* 5(1): 18-22.

Bird, Brian, and Andrew Kozlowski
2016 *Late Quaternary Reconstruction of Glacial Lake Iroquois in the Ontario Basin of New York*. New York State Museum, Map and Chart Series Number 80.

Boisvert, Richard A.
2012 The Paleoindian Period in New Hampshire. In: *Late Pleistocene Archaeology and Ecology in the Far Northeast*, edited by Claude Chapdelaine, pp. 77-94. Texas A&M University Press, College Station.

Bradley, James W., Arthur Spiess, Richard Boisvert, and Jeff Boudreau
2008 What's the Point?: Modal Forms and Attributes of Paleoindian Bifaces and the New England-Maritimes Region. *Archaeology of Eastern North America* 36:119-172.

Bradley, James W., and Robert E. Funk
n.d. Paleoindian Find Spots in Central New York State: An Update. Unpublished manuscript in possession of senior author.

Burke, Adrian
2006 Paleoindian Ranges in Northeastern North America Based on Lithic Raw Materials Sourcing. In: *Notions De Territoire Et De Mobilité: Exemples De L'Europe Et Des Premières Nations En Amérique Du Nord Avant Le Contact Européen*, edited by C. Bressy, A. Burke, P. Chalard, H. Martin, pp. 77-89. Études et Recherches Archéologiques de l'Université de Liège, Liège.

Cadwell, Donald H., Ernest H. Muller, and P. Jay Fleischer
2003 Geomorphic History of New York State. In: *Geoarchaeology of Landscapes in the Glaciated Northeast*, edited by David L. Cremeens and John P. Hart, pp. 7-14. New York State Museum Bulletin 497.

Clarkson, Christopher
2016 Testing Archaeological Approaches to Determining Past Projectile Delivery Systems Using Ethnographic and Experimental Data. In: *Multidisciplinary Approaches to the Study of Stone Age Weaponry*, edited by Radu Iovita and Katsuhiro Sano, pp. 1-13. Springer Science+Business Media, Dordrecht.
Cox, D.D.
1959 *Some Postglacial Forests in Central and Eastern New York State as Determined by the Method of Pollen Analysis*. New York State Museum and Science Service, Bulletin 377.
Deller, D. Brian, and Christopher J. Ellis
2011 *Crowfield (AfHj-31): A Unique Paleoindian Fluted Point Site from Southwestern Ontario.* Memoirs of the Museum of Anthropology, University of Michigan, Number 49.
1996 The Bolton Site (AfHj-89): A Crowfield Phase Early Paleoindian Site in Southwestern Ontario. *Ontario Archaeology* 61:5-44.
1992 *Thedford II, A Paleo-Indian Site in the Ausable River Watershed of Southwestern Ontario,* Memoirs Museum of Anthropology, University of Michigan No. 24, Ann Arbor, Michigan.
1988 Early Paleoindian Complexes in Southwestern Ontario. In: *Late Pleistocene and Early Holocene Paleoecology and Archaeology of the Eastern Great Lakes Region*, edited by R. S. Laub, N.G. Miller, and D.W. Steadman, pp. 251-263. Bulletin of the Buffalo Society of Natural Sciences 33.
Durkee, L.H.
1960 Pollen Profiles from Five Bog Lakes in New York State. Unpublished PhD dissertation, Syracuse University.
Dyke, A. S.
2004 An Outline of North American Deglaciation with Emphasis on Central and Northern Canada. In: *Quaternary Glaciations - Extent and Chronology, Part II: North America, Developments in Quaternary Science 2*, edited by J. Ehlers, and P.L. Gibbard, pp.201-207. Elsevier: Amsterdam.
Ellis, Christopher
2011 Measuring Paleoindian Range Mobility and Land Use in the Great Lakes/Northeast. *Journal of Anthropological Archaeology* 30:385-401.
2008 The Fluted Point tradition and the Arctic Small Tool tradition: What's the connection? *Journal of Anthropological Archaeology* 27:298-314.
2004 Hi-Lo: An Early Lithic Complex in the Great Lakes Region. In: *The Late Paleoindian Great Lakes: Geological and Archaeological Investigations of Late Pleistocene and Early Holocene Environments*, edited by Lawrence J. Jackson and Andrew Hinshelwood, pp 57-84. Mercury Series Archaeology Paper 165. Canadian Museum of Civilization, Ottawa.
Ellis, Christopher J., and D. Brian Deller
1997 Variability in the Archaeological Record of Northeastern Early Paleoindians: A View from Southern Ontario. *Archaeology of Eastern North America* 25:1-30.
1990 Paleoindians. In: *The Archaeology of Southern Ontario to A.D. 1650,* edited by Christopher Ellis and Neil Ferris, pp. 37-63. Occasional Publications, London Chapter, Ontario Archaeological Society, Number 5.

1988 Some Distinctive Paleoindian Tool Types from the Lower Great Lakes Region. *Midcontinental Journal of Archaeology* 13(2): 111-158.

Ellis, Christopher J., D. Brian Deller, and Lawrence Jackson

1991 Investigations at Small, Interior, Early Paleoindian Sites in Southwestern Ontario. *Annual Archaeological Report, Ontario* 2: 92-96.

Ellis, Christopher J., Dillon H. Carr, and Thomas J. Loebel

2011 The Younger Dryas and Late Pleistocene Peoples of the Great Lakes Region. *Quaternary International* 242:534-545.

Feranec, Robert S., and Andrew L. Kozlowski

2016 Implications of a Bayesian radiocarbon calibration of colonization ages for mammalian megafauna in glaciated New York State after the Last Glacial Maximum. *Quaternary Research* 85:262-270.

Fisher, Donald W.

1980 *Bedrock Geology of the Central Mohawk Valley, New York*. New York State Museum, Map and Chart Series Number 33. The University of the State of New York, State Education Department, Albany.

Fisher, Donald W., Yngvar W. Isaachsen, and Lawrence V. Rickard

1970 *Geologic Map of New York, Hudson Mohawk Sheet*. University of the State of New York, State Education Department, Albany.

Funk, Robert E.

2004 *An Ice Age Quarry-Workshop: The West Athens Hill Site Revisited*. New York State Museum Bulletin 504.

Funk, Robert E., and David W. Steadman

1994 *Archaeological and Paleoenvironmental Investigations in the Dutchess Quarry Caves, Orange County, New York*. Persimmon Press, Buffalo.

Gramly, R.M.

1999 *The Lamb Site: a Pioneering Clovis Encampment*. Persimmon Press, Buffalo.

1988 Paleoindian Sites South of Lake Ontario, Western and Central New York State. In: *Late Pleistocene and Early Holocene Paleoecology and Archaeology of the Eastern Great Lakes Region*, edited by R. S. Laub, N.G. Miller, and D.W. Steadman, pp. 265-280. Bulletin of the Buffalo Society of Natural Sciences 33.

Gramly, R.M., and Jonathan C. Lothrop

1984 Archaeological Investigations of the Potts Site, Oswego County, New York. *Archaeology of Eastern North America* 12: 122-158.

Hou, J., Y. Huang, Y. Wang, B. Shuman, W.W. Oswald, E. Faison, and D.R. Foster

2006 Postglacial Climate Reconstruction Based on Compound-Specific D/H Ratios of Fatty Acids from Blood Pond, New England. *Geochemistry Geophysics Geosystems* 7: 1–7.

Iovita, Radu, Holger Schönekeß, Sabine Gaudzinski-Windheuser, and Frank Jäger

2014 Projectile impact fractures and launching mechanisms: Results of a controlled ballistic experiment using replica Levallois points. *Journal of Archaeological Science* 48:73-83.

Jackson, Lawrence J.
2004 Changing Our Views of Late Paleoindian in Southern Ontario. In: *The Late Paleoindian Great Lakes: Geological and Archaeological Investigations of Late Pleistocene and Early Holocene Environments*, edited by Lawrence J. Jackson and Andrew Hinshelwood, pp. 25-56. Mercury Series Archaeology Paper 165. Canadian Museum of Civilization, Ottawa.
1998 *The Sandy Ridge and Hallstead Paleoindian Sites: Unifacial Tool Use and Gainey Phase Definition in South-Central Ontario.* Memoirs of the Museum of Anthropology, University of Michigan, Number 32.
Jackson, Jackson and Andrew Hinshelwood
2004 *The Late Paleoindian Great Lakes: Geological and Archaeological Investigations of Late Pleistocene and Early Holocene Environments*, edited by Lawrence J. Jackson and Andrew Hinshelwood. Mercury Series Archaeology Paper 165. Canadian Museum of Civilization, Ottawa.
Karrow, Paul S.
2004 Ontario Geological Events and Environmental Change in the Time of the Late Paleoindian and Early Archaic Cultures. In: *The Late Palaeo-Indian Great Lakes: Geological and Archaeological Investigations of Late Pleistocene and Early Holocene Environments,* edited by Lawrence J. Jackson and Andrew Hinshelwood, 1-24. Mercury Series Archaeology Paper 165. Canadian Museum of Civilization, Ottawa.
Kozlowski, Andrew, and Brandon L. Graham
2014 *Glacial Geology of Cayuga County of the Eastern Finger Lakes: Lakes, Lore and Landforms*. Guidebook for 77th Annual Reunion of the Northeastern Friends of the Pleistocene Field Conference, June 7-8, 2014, Auburn, New York, pp. 90-101. The New York State Geological Survey, New York State Museum and New York State Education Department, Albany.
Laub, Richard S., and Arthur E. Spiess
2003 What Were Paleoindians Doing at the Hiscock Site? In: *The Hiscock Site: Late Pleistocene and Holocene Paleoecology and Archaeology of Western New York* State, edited by R.S. Laub, pp. 261-271. Bulletin of the Buffalo Society of Natural Sciences 37.
Loebel, Thomas
2013 Endscrapers, Use-Wear and Early Paleoindians in Eastern North America. In: *In the Eastern Fluted Point Tradition,* edited by Joseph A.M. Gingerich, pp. 315-330. University of Utah Press, Salt Lake City.
Lothrop, Jonathan C.
2009 The New York Paleoindian Database Project: a Call for Data. *New York State Archaeological Association Newsletter* 5(3): 6.
1989 The Organization of Paleoindian Lithic Technology at the Potts Site. In: *Eastern Paleoindian Lithic Resource Use,* edited by Christopher J. Ellis and Jonathan C. Lothrop, pp. 99-138. Westview Press, Boulder.
1988 The Organization of Paleoindian Lithic Technology at the Potts Site. Ph.D. Dissertation, Department of Anthropology, State University of New York at Binghamton.

Lothrop, Jonathan C., and James Bradley
2012 Paleoindian occupations in the Hudson Valley, New York. In: *Late Pleistocene Archaeology and Ecology in the Far Northeast*, edited by Claude Chapdelaine, pp. 9-47. Texas A&M University Press, College Station.
Lothrop, Jonathan C., Philip C. LaPorta, Joseph Diamond, Meredith H. Younge, and Susan Winchell-Sweeney
In press New Data on Paleoindian Sites and Isolated Finds in the Wallkill/Rondout Valley of New York and New Jersey. In: *In the Eastern Fluted Point Tradition II*, edited by Joseph Gingerich. University of Utah Press, Salt Lake City.
Lothrop, Jonathan C., Darrin L. Lowery, Arthur E. Spiess, and Christopher J. Ellis
2016 Early Human Settlement of Northeastern North America. *PaleoAmerica* 2(3):1-61 (DOI: http://dx.doi.org/10.1080/20555563.2016.1212178).
Lothrop, Jonathan C., James W. Bradley, Susan Winchell-Sweeney and Meredith H. Younge
2014 Paleoindian Occupations in Central New York. In: *Glacial Geology of Cayuga County of the Eastern Finger Lakes: Lakes, Lore and Landforms*, compiled by Andrew Kozlowski and Brandon Graham. Guidebook for 77th Annual Reunion of the Northeastern Friends of the Pleistocene Field Conference, June 7-8, 2014, Auburn, New York, pp. 90-101. The New York State Geological Survey, New York State Museum and New York State Education Department, Albany (http://www2.newpaltz.edu/fop/).
Lothrop, Jonathan C., Paige Newby, Arthur Spiess, and James W. Bradley
2011 Paleoindians and the Younger Dryas in the New England-Maritimes Region. *Quaternary International* 242: 546-569.
McCarthy, F., J. McAndrews, and E. Papalangelakis
2015 Paleoenvironmental Context for Early Holocene Caribou Migration on the Alpena-Amberley Ridge. In: *Caribou Hunting in the Upper Great Lakes: Archaeological, Ethnographic, and Paleoenvironmental Perspectives*, edited by E. Sonnenburg, A. Lemke, and J. O'Shea, pp. 13-30. Museum of Anthropology, University of Michigan, Memoir 57.
Muller, Ernest H. and, Donald H. Cadwell
1986 *Surficial Geological Map of New York, Finger Lakes Sheet*. University of the State of New York, State Education Department, Albany.
Newby, Paige, James Bradley, Arthur Spiess, Brian Shuman, Philip Leduc
2005 A Paleoindian Response to Younger Dryas Climate Change. *Quaternary Science Reviews* 24:141-154.
Osborne, Alan
2014 Eye of the Needle: Cold Stress, Clothing, and Sewing Technology during the Younger Dryas Colder Than in North America. *American Antiquity* 79 (1): 45-68.
Ritchie, William A.
1969 *The Archaeology of New York State* (revised). The Natural History Press, Garden City, New York.
1957 *Traces of Early Man in the Northeast*. New York State Museum and Service, Bulletin 358.
1940 *Two Prehistoric Village Sites at Brewerton, New York*. Research Records of the Rochester Museum of Arts and Sciences No. 5.

Shuman, Bryan, Paige Newby, Yong Song Huang, and Thompson Webb III
2004 Evidence for the Close Climatic Control of New England Vegetation History. *Ecology* 85(5): 1297-1310.
Sonnenburg, Elizabeth, Ashley K. Lemke, and John M. O'Shea
2015 *Caribou Hunting in the Upper Great Lakes: Archaeological, Ethnographic, and Paleoenvironmental Perspectives*. Museum of Anthropology, University of Michigan, Memoir 57.
Spiess, Arthur E., Ellen Cowie, and Robert Bartone
2012 Geographic Clusters of Fluted Point Sites in the Far Northeast. In: *Late Pleistocene Archaeology and Ecology in the Far Northeast*, edited by Claude Chapdelaine, pp. 95-112. Texas A&M University Press, College Station.
Storck, Peter L.
1984 Glacial Lake Algonquin and Early Paleoindian Settlement Patterns and South-Central Ontario. *Archaeology of Eastern North America* 12:286-298.
Storck, Peter L., and Arthur E. Spiess
1994 The Significance of New Faunal Identifications Attributed to an Early Paleoindian (Gainey Complex) Occupation at the Udora Site, Ontario, Canada. *American Antiquity* 59(1):121-142.
Timmins, Peter A.
1994 Alder Creek: A Paleoindian Crowfield Phase Manifestation in the Region of Waterloo, Ontario. *Midcontinental Journal of Archaeology* 19 (2): 170-197.
Tomenchuk, John, and Peter L. Storck
1997 Two Newly Recognized Paleoindian Tool Types: Single-and Double-Scribe Compass Gravers and Coring Gravers. *American Antiquity* 62 (3): 508-522.
Ver Straeten, Charles A., and Carlton E. Brett
2006 Pragian to Eifelian strata (middle lower to lower middle Devonian), northern Appalachian basin-stratigraphic nomenclatural changes. *Northeastern Geology & Environmental Sciences* 28 (1): 80-95.

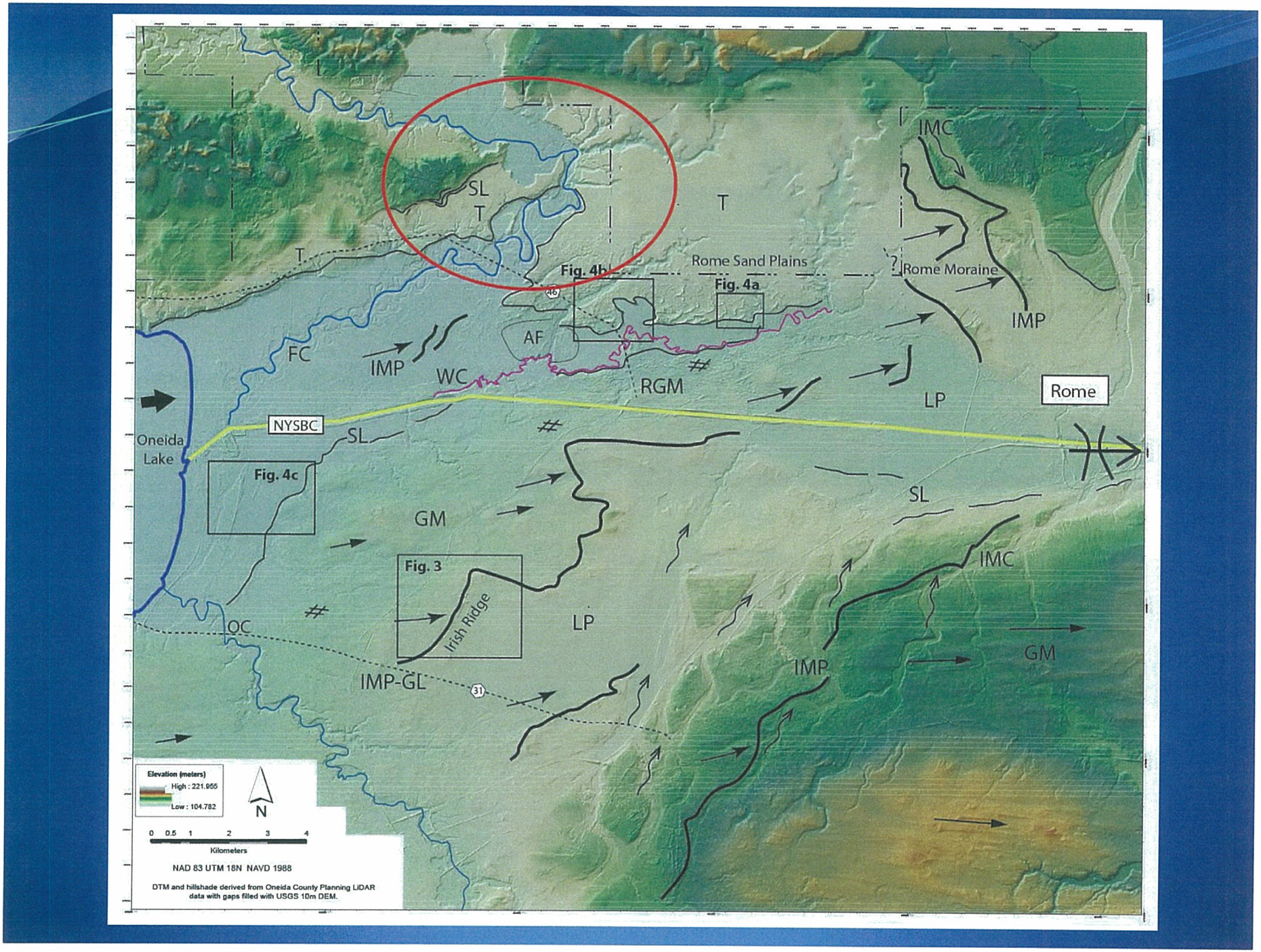
SL
T
T
T
IMC
Rome Sand Plains
Fig. 4b
Fig. 4a
Rome Moraine
IMP
AF
FC
IMP
WC
RGM
LP
Rome
NYSBC
Oneida
Lake
SL
Fig. 4c
GM
SL
IMC
Fig. 3
Irish Ridge
LP
OC
IMP
GM
IMP-GL
31
Elevation (meters)
High : 221.955
Low : 104.782
N
0 0.5 1 2 3 4
Kilometers
NAD 83 UTM 18N NAVD 1988
DTM and hillshade derived from Oneida County Planning LiDAR
data with gaps filled with USGS 10m DEM.

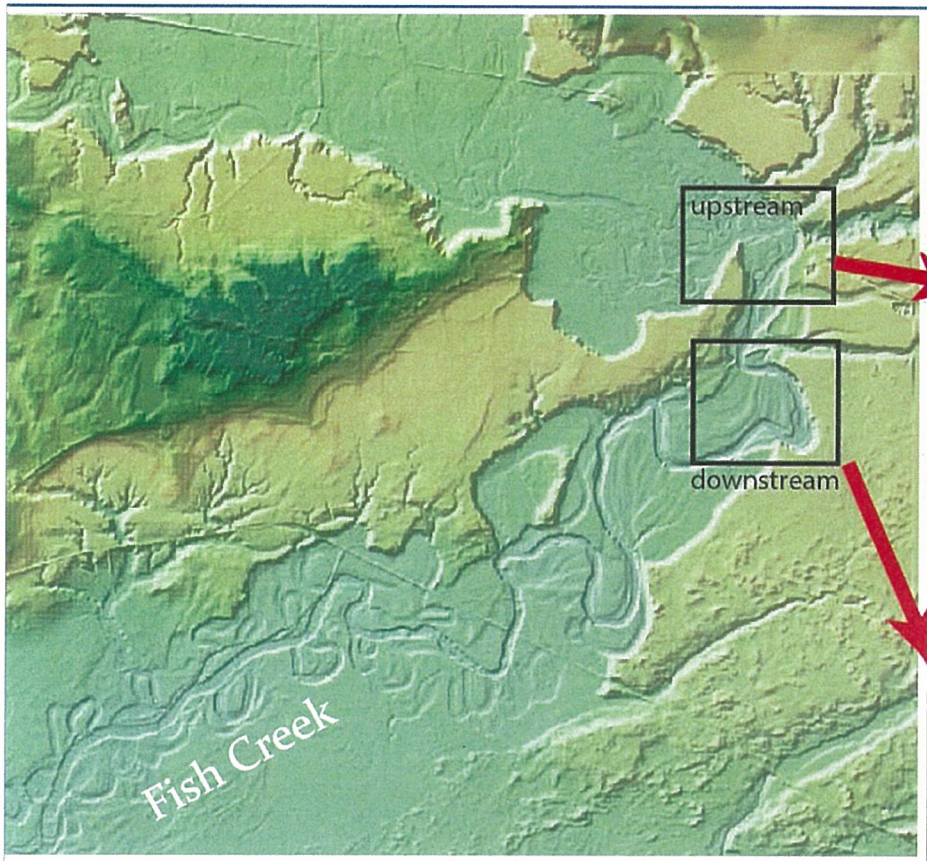
upstream
downstream
Fish Creek


Google earth

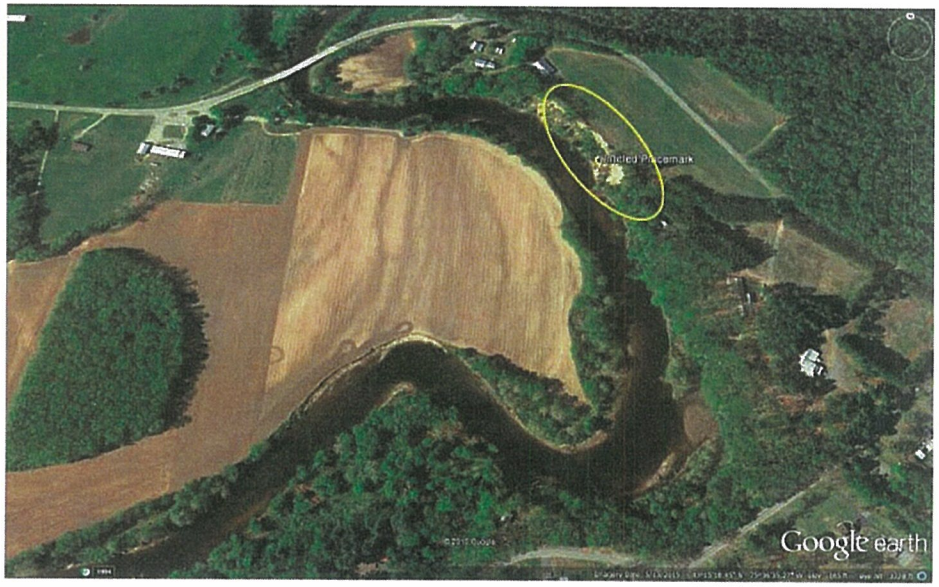
Google earth

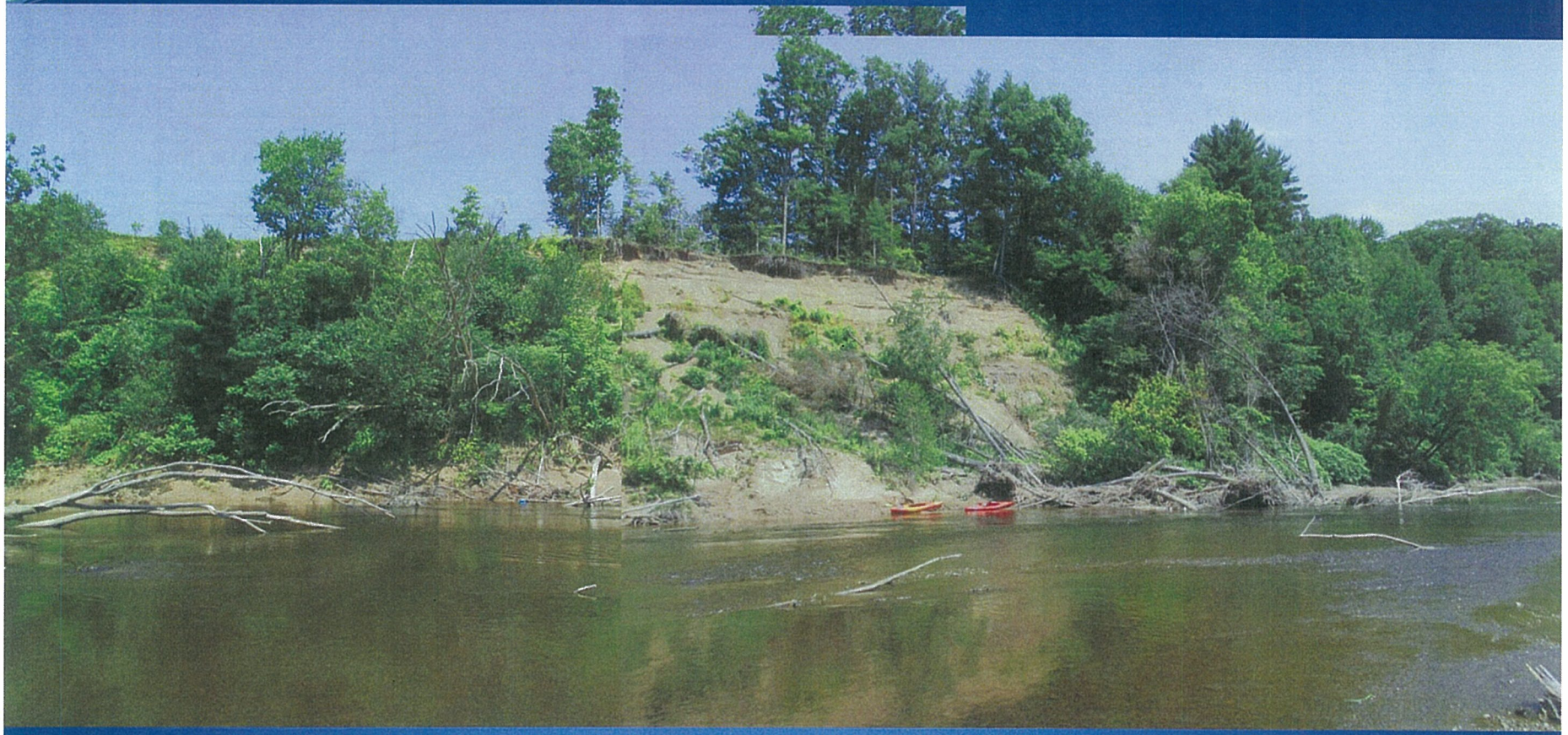

Downstream Section, Fish Creek

Fish Creek Downstream Section

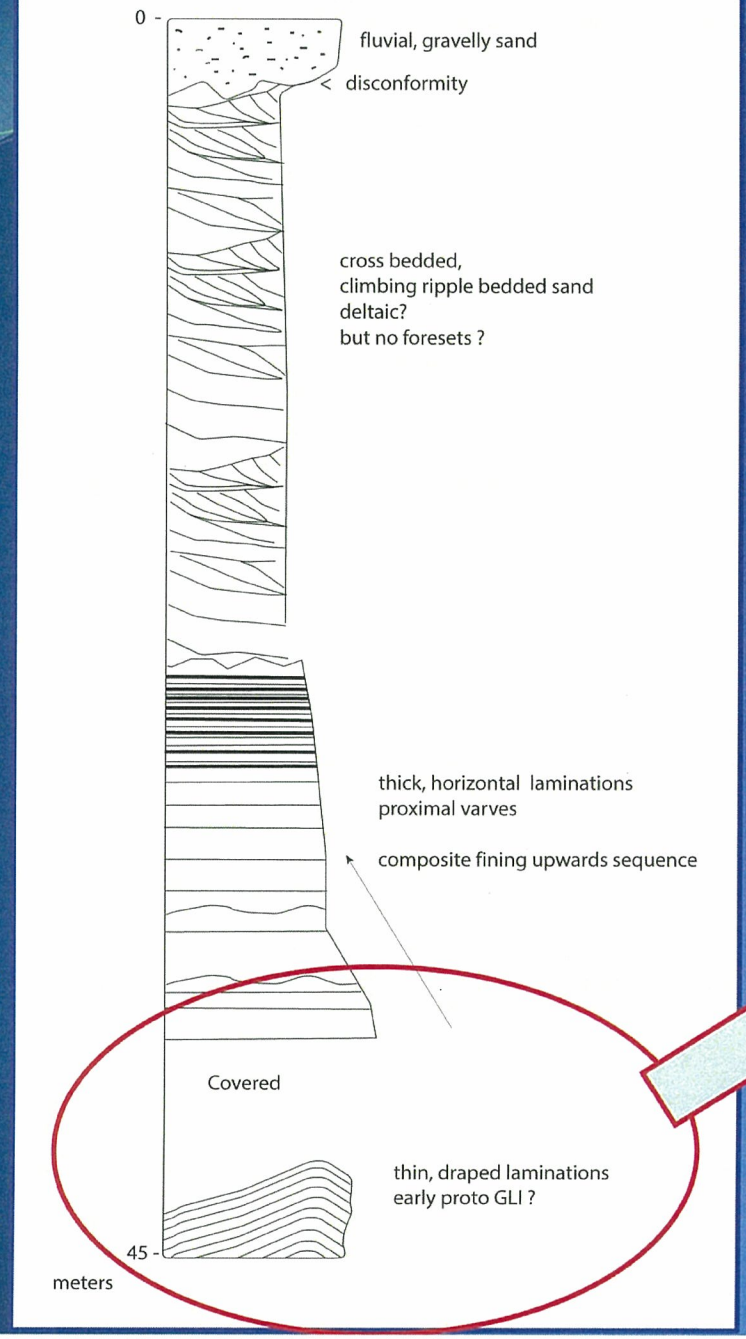

Fish Creek Downstream Section

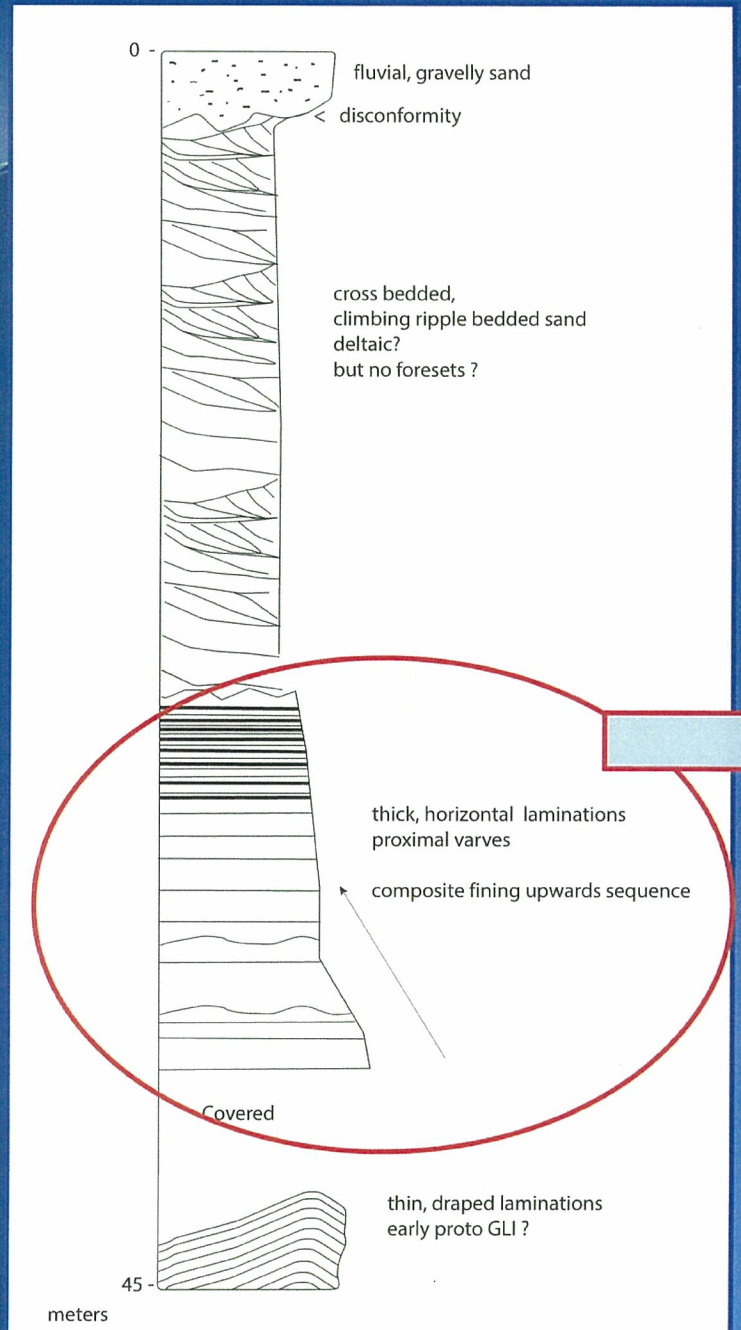

Fish Creek Downstream Section

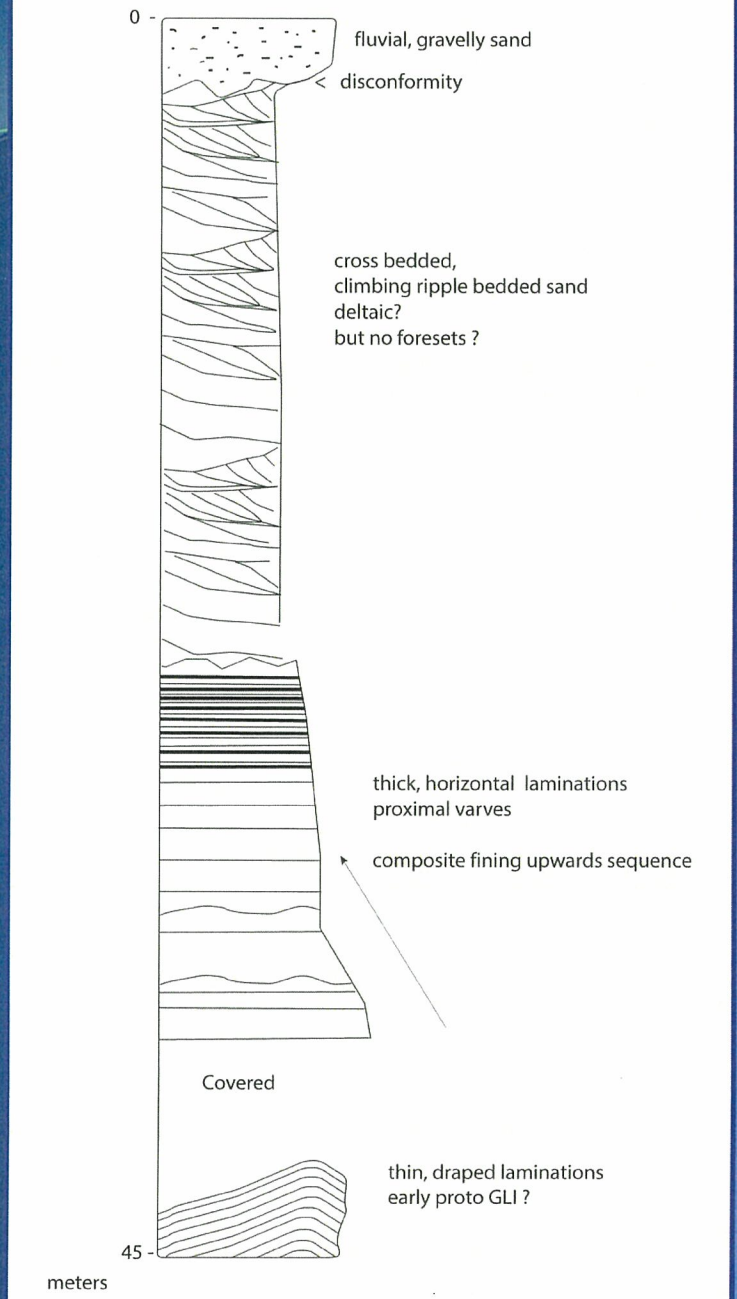

Fish Creek Downstream Section

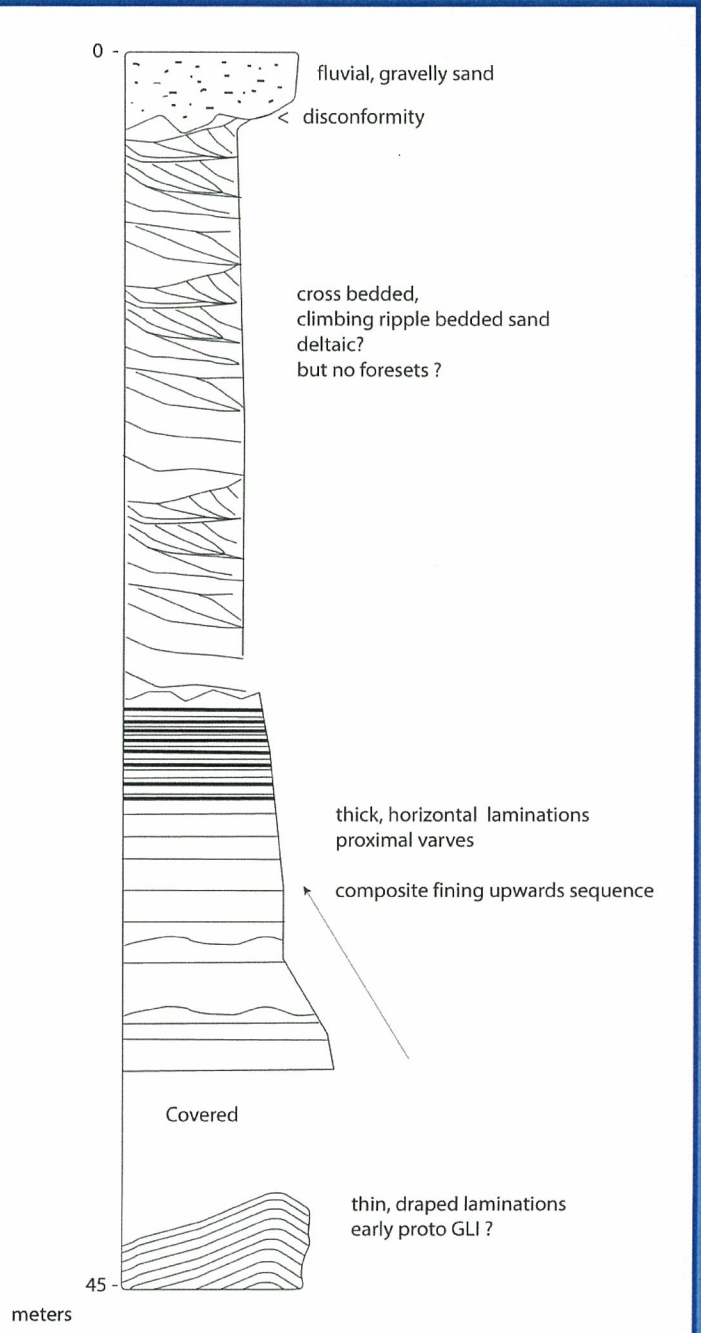

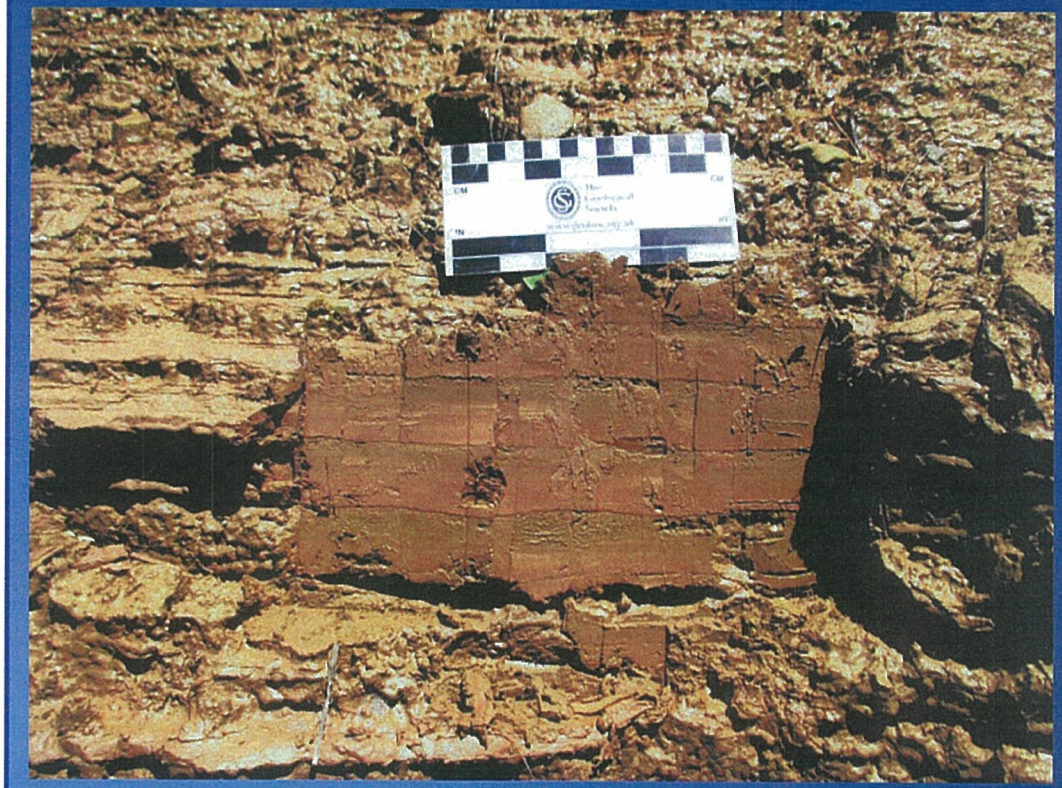

Upstream Section, Fish Creek

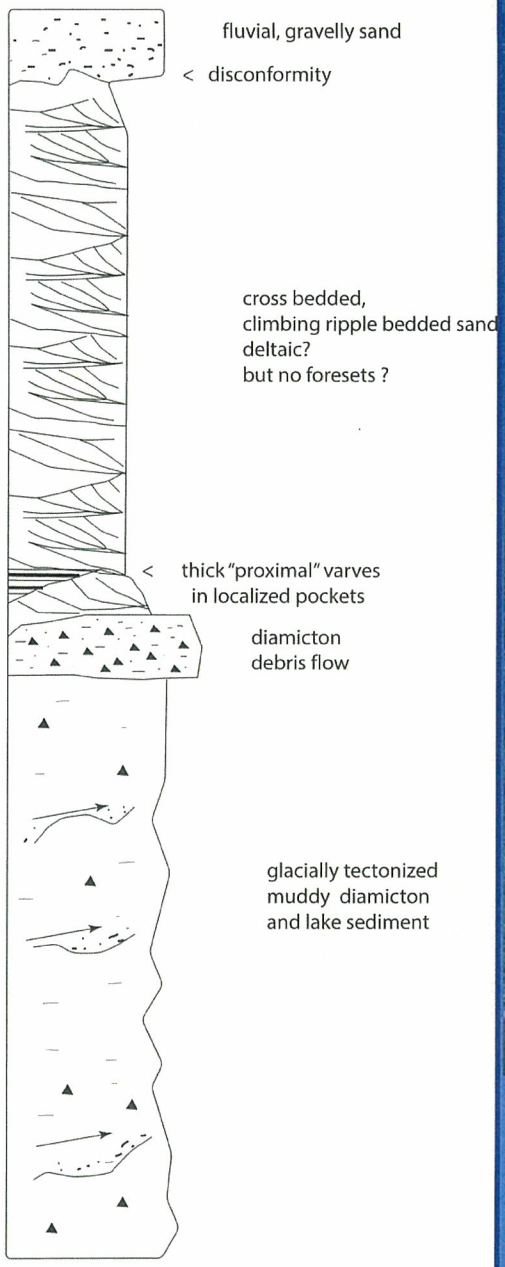
fluvial, gravelly sand
< disconformity
cross bedded,
climbing ripple bedded sand
deltaic?
but no foresets ?
< thick "proximal" varves
in localized pockets
diamicton
debris flow
glacially tectonized
muddy diamicton
and lake sediment

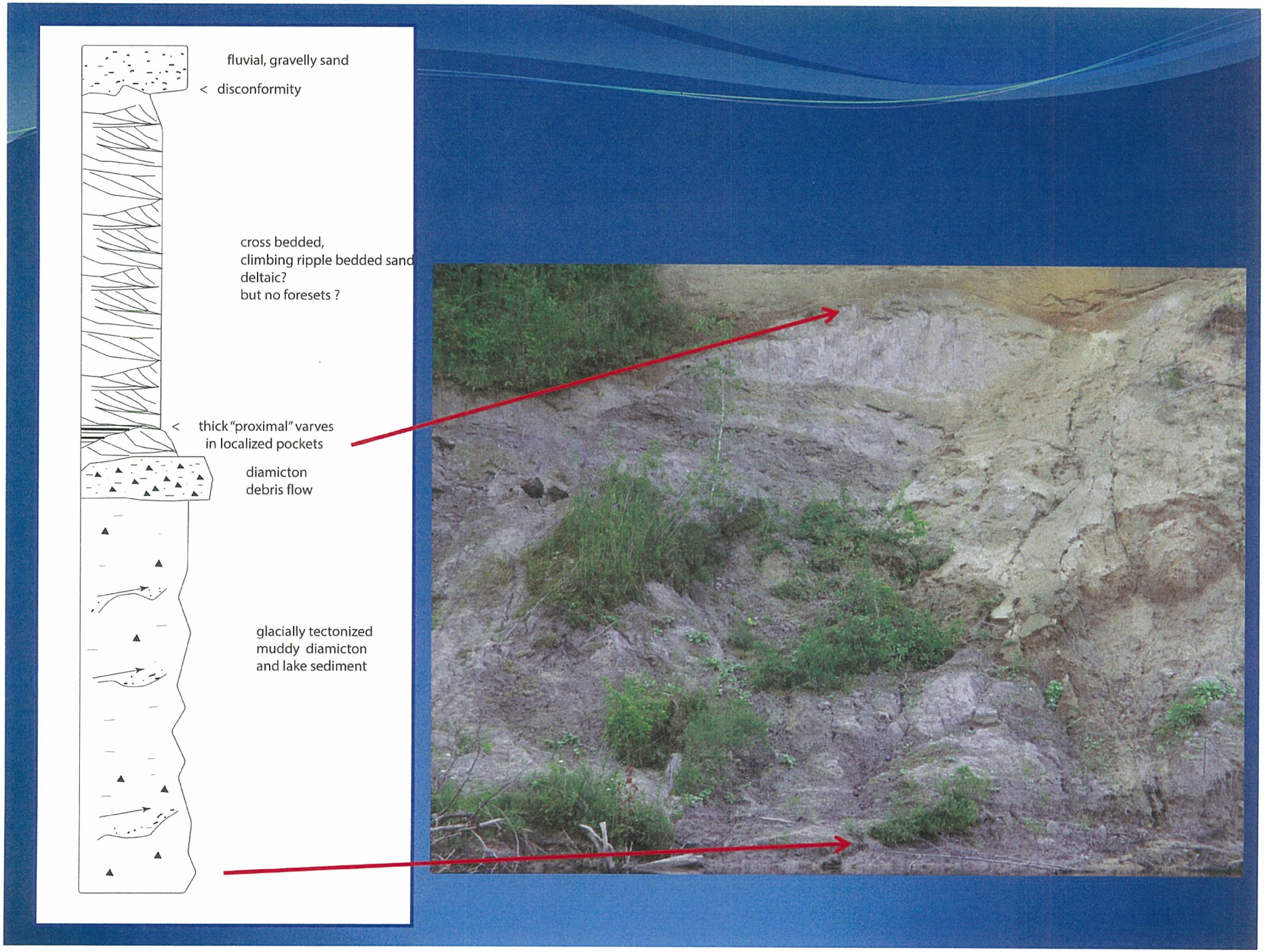
fluvial, gravelly sand
< disconformity
cross bedded,
climbing ripple bedded sand
deltaic?
but no foresets ?
< thick "proximal" varves
in localized pockets
diamicton
debris flow
glacially tectonized
muddy diamicton
and lake sediment

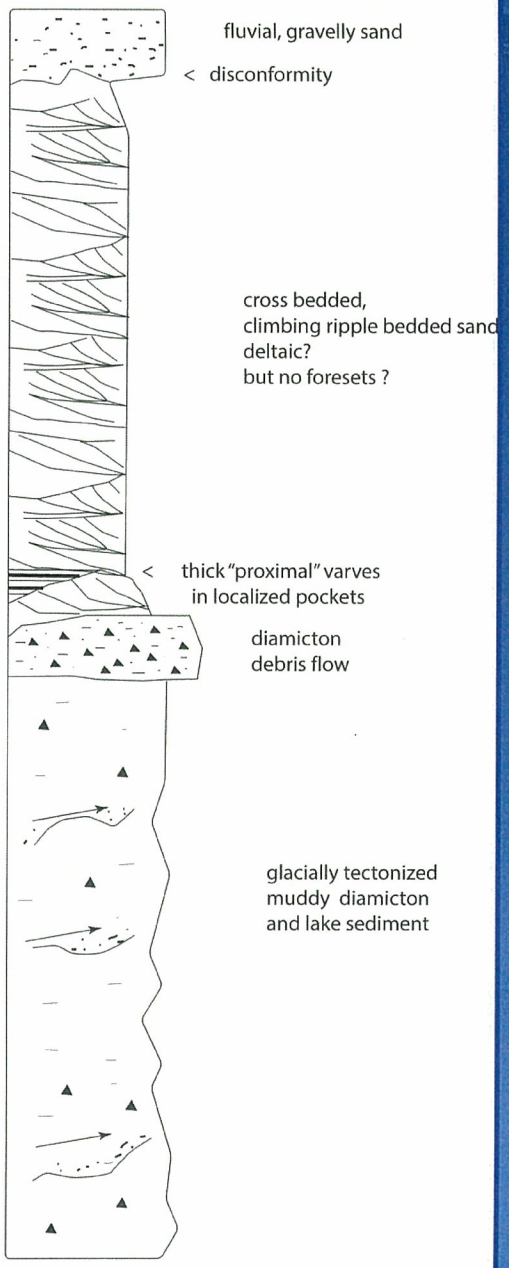
fluvial, gravelly sand
< disconformity
cross bedded,
climbing ripple bedded sand
deltaic?
but no foresets ?
< thick "proximal" varves
in localized pockets
diamicton
debris flow
glacially tectonized
muddy diamicton
and lake sediment

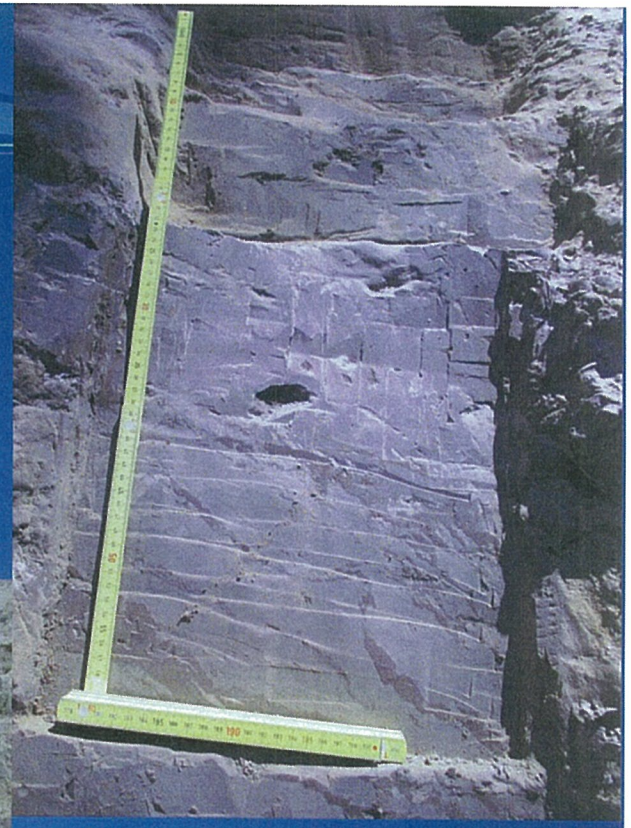

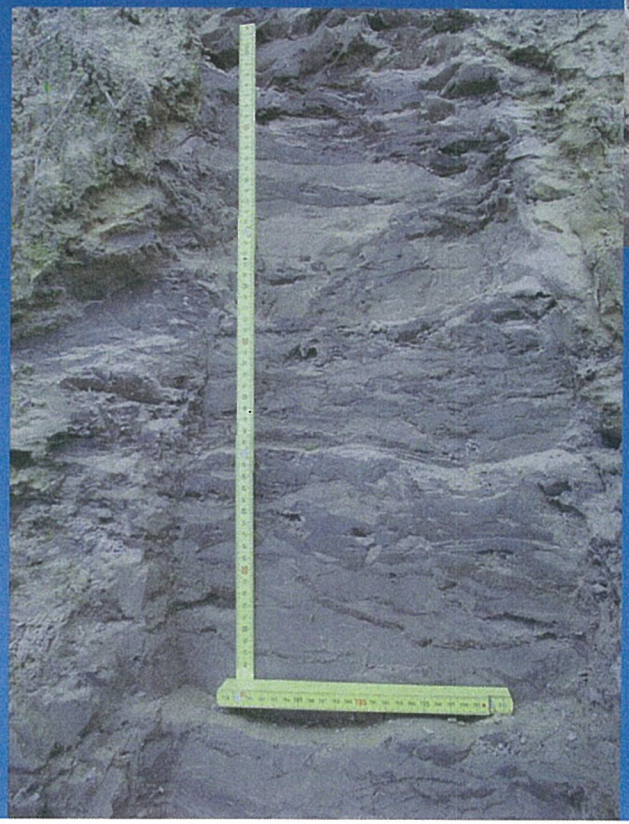

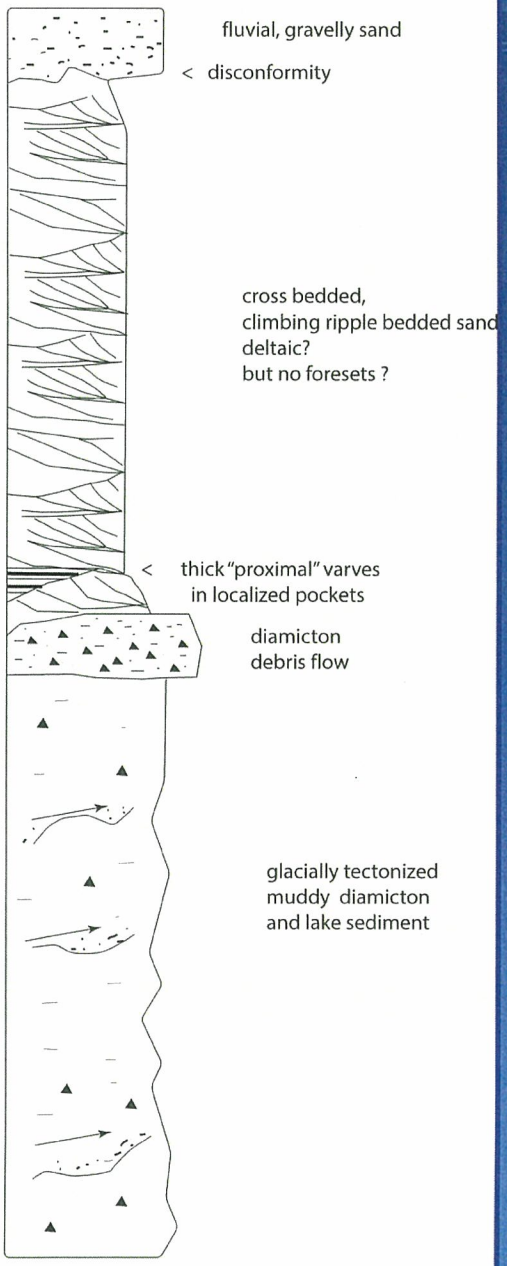
fluvial, gravelly sand
< disconformity
cross bedded,
climbing ripple bedded sand
deltaic?
but no foresets ?
< thick "proximal" varves
in localized pockets
diamicton
debris flow
glacially tectonized
muddy diamicton
and lake sediment

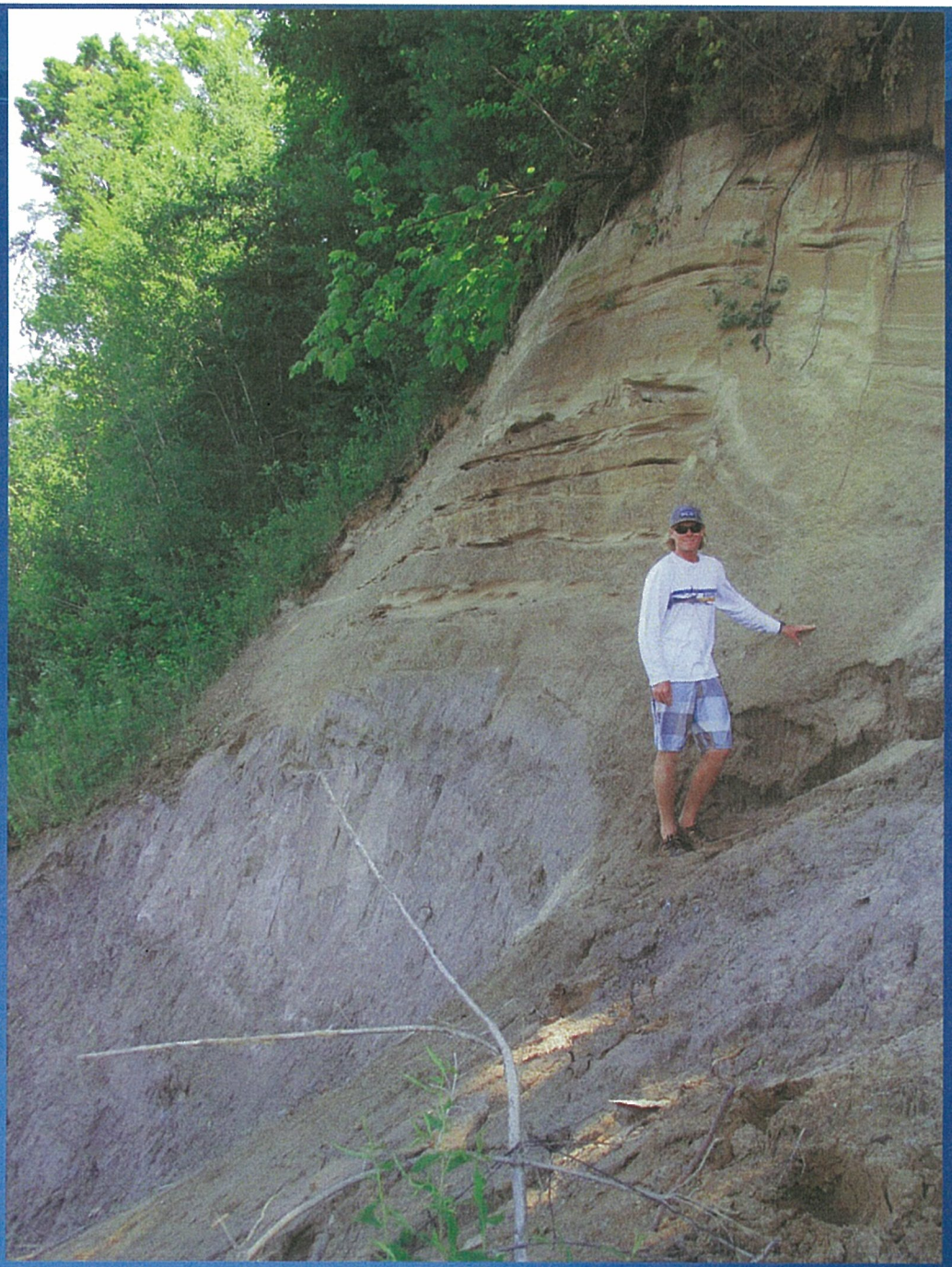

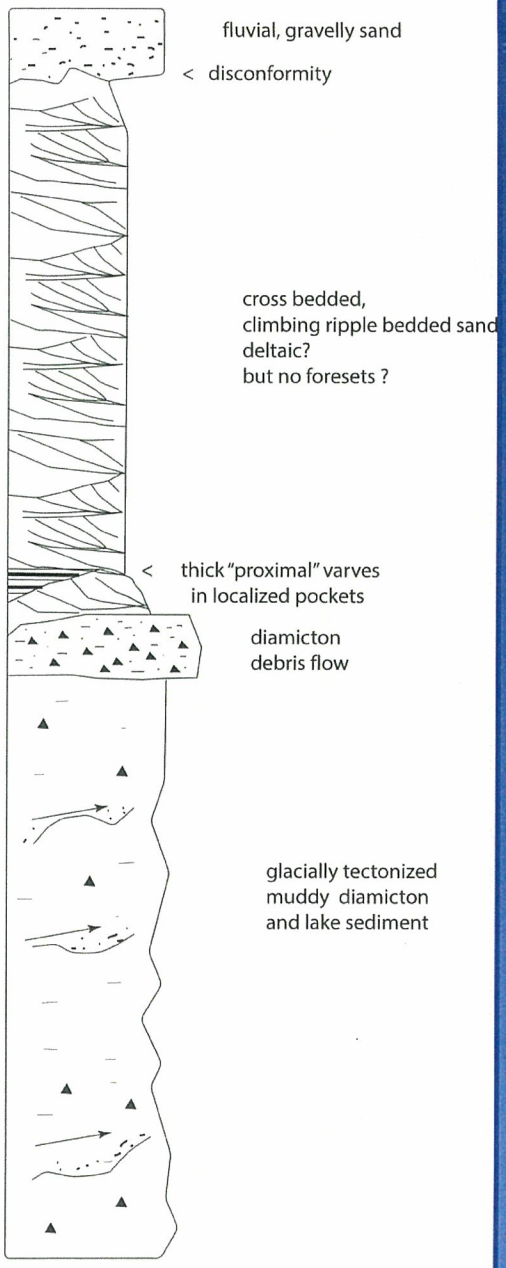
fluvial, gravelly sand
< disconformity
cross bedded,
climbing ripple bedded sand
deltaic?
but no foresets ?
< thick "proximal" varves
in localized pockets
diamicton
debris flow
glacially tectonized
muddy diamicton
and lake sediment

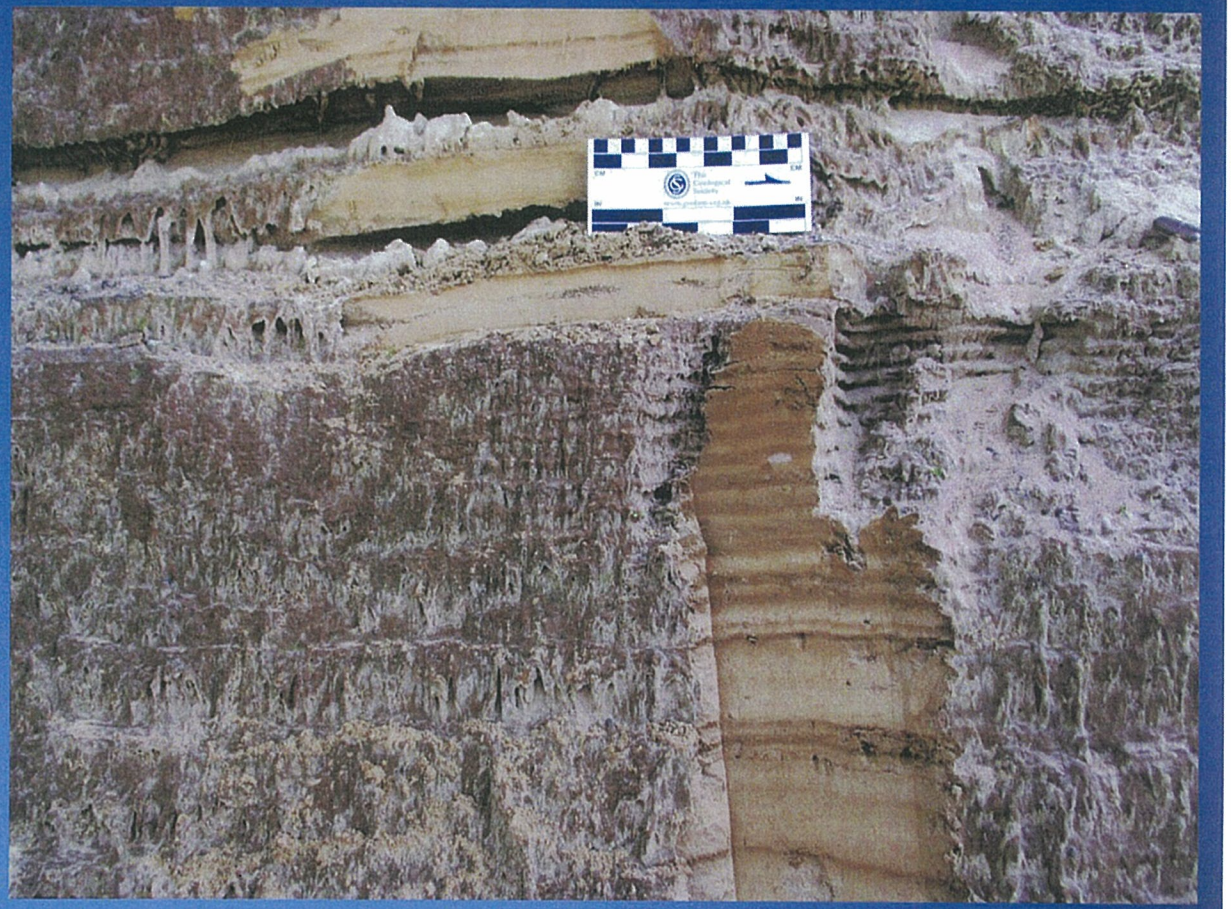

Saturday, afternoon, June 4th

Summary of Oneida Lake Acoustic Stratigraphy

Line 6 and 8 are provided in un-interpreted and interpreted fashion (Fig. 1) in order to illustrate and describe a stratigraphic model for the seismic reflection data obtained from the eastern half of Oneida Lake. Vertical scale is provided in milliseconds with maximum recording to 54 ms or about 100 m, assuming an average sediment velocity of 1800 m/sec.

Methods: Several acoustic surveys of Oneida Lake were undertaken between 2009 and 2014. Results of dual frequency 200/83 kHz echo sounding surveys are presented in various Senior Theses from Hamilton College, and those results are used to constrain the bathymetric details of eastern Oneida Lake basin. In order to image the Quaternary sedimentary section underlying the lake, we acquired ~80 km of high-resolution CHIRP subbottom profiles across the full extent of the lake in 2013 and 2014, using the Hamilton College R/V Continental Drifter, and a research vessel provided by the Cornell Biological Field Station (Fig. 1). Data were acquired using an Edgetech 424 CHIRP profiling system in 4-24 kHz mode, and stored in SEG-Y format. Positioning was achieved using a WAAS-enabled autonomous GNSS (GPS) system. Data were conditioned and displayed using PROMAX seismic processing software. Although the line spacing of the profiles is 2-4 km, the extraordinary fidelity of the images provides important insights into the late-Quaternary record of the Oneida and Glacial Lake Iroquois system. The dominant frequency of the match-filtered seismic traces is ~8 kHz, yielding decimeter-scale vertical resolution.

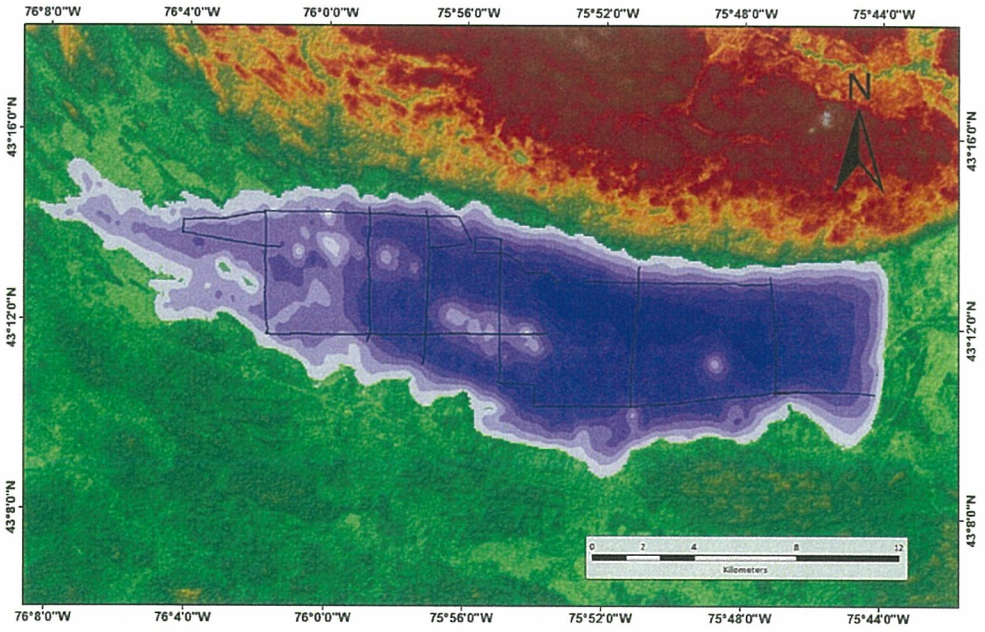

Figure 1. Oneida Lake bathymentry and catchment deitial elevation model, showing the locations of the CHIRP seismic profiels acquired in 2013 and 2014. The terrain surrounding the lake has a maximum elevation of 180 m above mean sea level, and the lake elevation is 112 m amsl. The maximum depth of the lake is ~16m.

Description

By utilizing standard seismic stratigraphic methods we divide the basin fill into three distinct seismic sequences. These are described as follows:

1) Sequence 1 is characterized by acoustically transparent to weakly defined ponded reflectors that on-lap onto the underlying surface. Where its thickness exceeds about 12 msec the acoustic signal is attenuated by interstitial gas which also masks any underlying reflectors in older sequences. Maximum thickness of Sequence 1 is undetermined due to this gas effect but extrapolation of slopes of underlying boundary suggests it may exceed 50 m (or 24 msec) in the deepest axis of the Oneida Basin. This sequence is also not continuously present across the basin and has been removed or highly condensed in areas above ~13 msec.
2) Sequence 2 is characterized by weakly stratified draped reflectors which are truncated along the upper sequence boundary and appear conformable with high amplitude reflectors of the underlying Sequence 3. The reflection character within Sequence 2 becomes increasingly weaker from the base to the top of the sequence.
3) Sequence 3 is characterized by great variability in reflection character but generally is defined by a set of high amplitude reflectors which drape an underlying surface. In places the strong set of parallel reflectors is broken by acoustically transparent units that infill topographic depressions (taking on a ponded character) and/or "incision channels" that truncate reflectors beneath them in sharp sometimes vertical walls. Along the flanks of high standing topography or basin margins deformation of the parallel reflectors causes increased relief to be developed in the upper portions of Sequence 3, and this topography is carried upward in the draped reflectors of Sequence 2. Also in places there appear to be internal surfaces of on-lap within the sets of parallel reflectors in particular above transparent "infills". In places parallel reflectors in Sequence 3 are exposed at the lake floor by erosional truncation.
4) The base of Sequence 3 appears only in places where acoustic energy has not attenuated, such as where the surface breaches the lake floor (localized "drumlin" crests). The acoustic limit appears as a high amplitude, discontinuous reflector of high relief. Where continuity is provided this reflector defines a hard surface marked by pronounced ridges and swales superimposed upon larger, higher relief features (drumlins).

Because of the high reflectivity of some layers, multiples become overprinted upon the base of Sequence 3 this is particularly evident where the basal high amplitude reflector bleeds through the multiplies. In other places it is difficult to resolve the base of Sequence 3 because of the multiple effect.

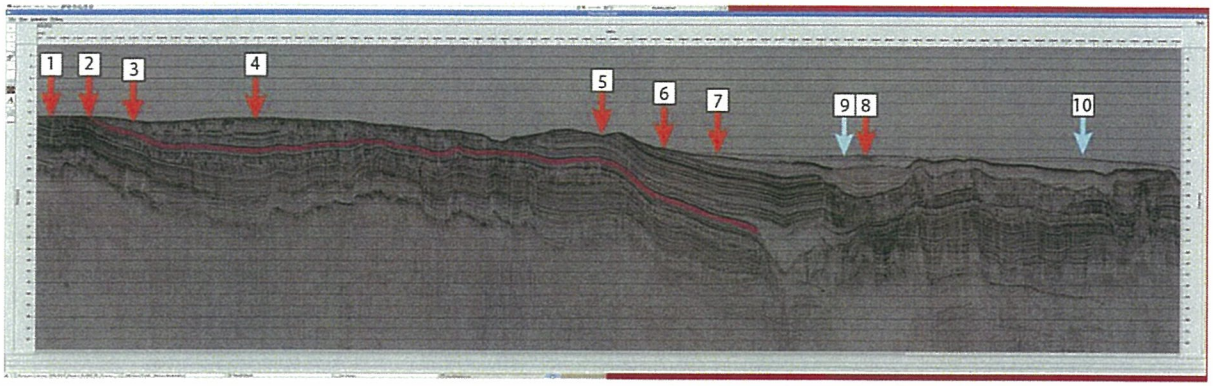
1
2
3
4
5
6
7
9
8
10

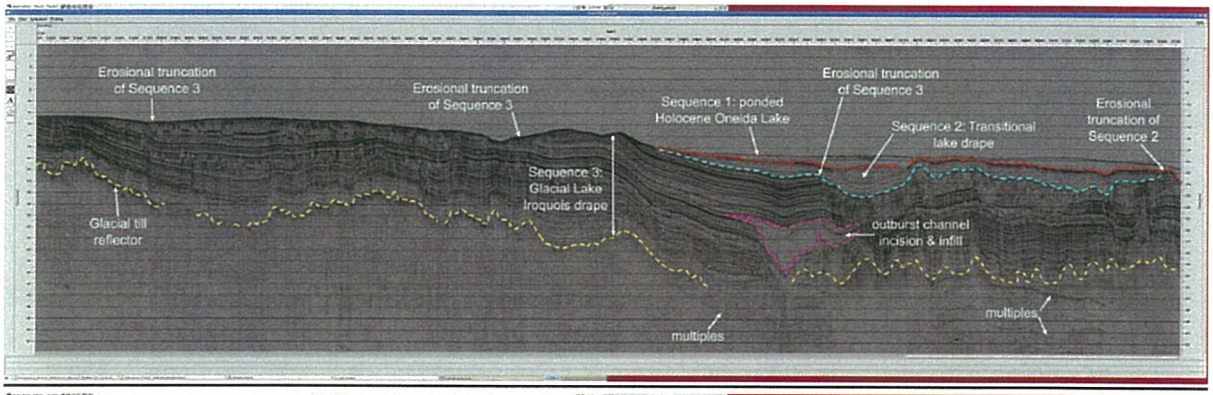
Erosional truncation of Sequence 3
Erosional truncation of Sequence 3
Sequence 1: ponded Holocene Oneida Lake
Erosional truncation of Sequence 3
Sequence 2: Transitional lake drape
Erosional truncation of Sequence 2
Sequence 3: Glacial Lake Iroquois drape
Glacial till reflector
outburst channel incision & infill
multiples
multiples

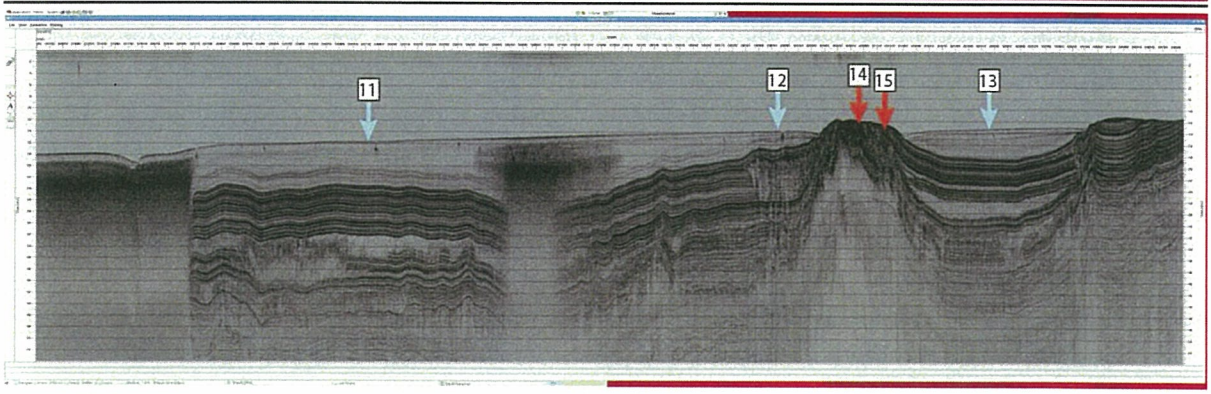
11
12
14
15
13

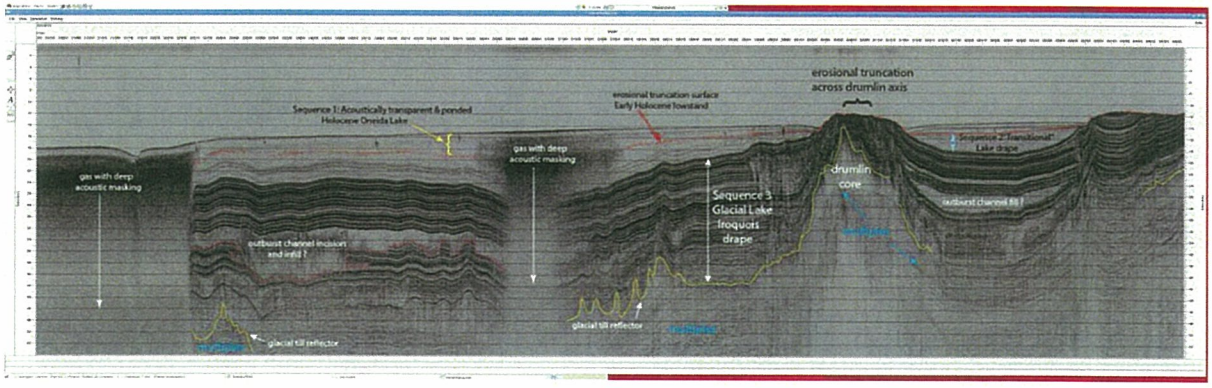
erosional truncation across drumlin axis
Sequence 1: Acoustically transparent & ponded Holocene Oneida Lake
erosional truncation surface Early Holocene lowstand
gas with deep acoustic masking
gas with deep acoustic masking
drumlin core
Sequence 3 Glacial Lake Iroquois drape
outburst channel incision and infill ?
outburst channel fill ?
glacial till reflector
glacial till reflector

Interpretation

We utilize the general knowledge of landscape development in the Oneida Lake basin, Ontario Lowland to provide a preliminary hypothesis for the genetic character of each of the sequences we describe above. This interpretation follows the sequences in reverse order, from bottom to top.

1) We interpret the basal reflector as the top of the glacial diamicton or till. Its relief reflects small scale flutes that run west to east superimposed upon the larger scale features such as drumlins that also run west to east. The compact nature of a glacial till would provide sufficient acoustic contrast with overlying stratified sediment, even when acoustic energy is low, to provide a reflector-- as is apparent near the base of the stratigraphy. Where the surface of the till rises (as on the crest of a drumlin) the reflector is more easily imaged and continuous.
2) Sequence 3 has to reflect alternating deposition from a dispersed source as settling from sediment plumes due to its ubiquitous draping character. Also, alternating textural character of the layers must be called for as the sequence is highly reflective with sets of strong parallel reflectors that are continuous. We interpret Sequence 3 as reflective of glacial lacustrine sedimentation in proximity to an ice margin and melt water source. Because the reflectors of Sequence 3 extend beyond the limits of Oneida Lake proper (as erosional truncation is apparent along the present lake margin) this system must have been related to Glacial Lake Iroquois. We interpret the acoustic laminations as reflective of varve like sedimentation where changes in the sand, silt, or clay content of varved sets produce reflectors at the scale of decimeters. Interruptions in the parallel reflectors by acoustically transparent strata may reflect outburst or jokulhaup events which infill preexisting topography by density gravity flows or cut and incise into the underlying varved layers and rapidly backfill the incisions as velocity wanes (similar to channels described by Fulthrope and Austin from offshore New Jersey; 2004). In this analogy square margin channels are typical, as we observe.
3) Conformable with Sequence 3 is the draped but poorly reflective strata of Sequence 2. The preservation of draped morphology but loss of reflectivity likely represents a loss of direct melt water feeders into the lake system from the ice margin with a dominance of fine clay laminations in the varve sets. This may therefore reflect the more distal portions of Glacial Lake Iroquois when the ice margin stepped back into the Ontario Basin proper.
4) Erosional truncation of the draped reflectors is quite apparent and this truncation surface extends across Sequence 3 and the glacial surface as well when these units rise in topography, as along the drumlin crest and lake margin. This erosion clearly marks the most easily recognized base level drop within the acoustic section (although others may be present within Sequence 3). That it terminates the most distal of the Glacial Lake Iroquois beds suggest that it may reflect changes in Lake Level coincident with the final

drainage of the system out through the St Lawrence outlet. Alternatively, it may be that the end phase of Sequence 2 also records the transition from Glacial Lake Iroquois to an early phase of Oneida Lake, as the strata become transparent near the top of Sequence 2. In this case the truncation surface could reflect the Early Holocene phase of lake drawdown recorded in all the Great Lakes at around 9-8 ka (Lewis and Anderson, 2012). This would be consistent with our observations of disconformities in beach ridge accretion in the eastern end of the basin some 1 mile east of the modern Oneida Lake shoreline (Domack et al., 2012, NYSGA field trip guide).

5) The base of Sequence 1 is characterized by ponded geometry into the underlying relief and clear on-lap of a single mid strata reflector onto the underlying truncation surface. Hence, this sequence must represent the rise in base level as modern Oneida Lake grew following a period of partial (or full ?) emergence. The gaseous character of the Sequence 1 reflects the modern organic rich nature of the muds accumulating in the basin of Oneida Lake today (Ng, 2009).

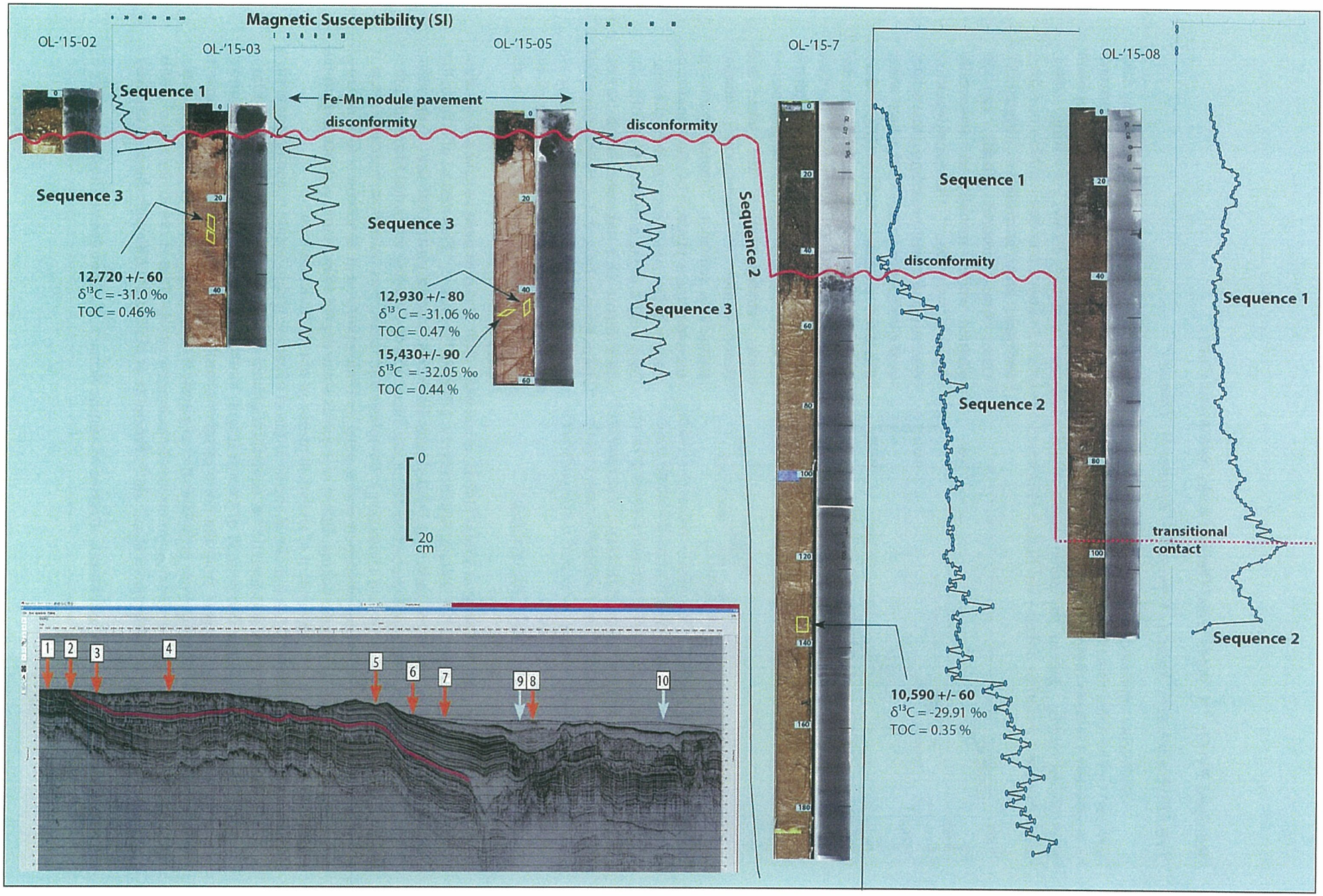
Magnetic Susceptibility (SI)
OL-'15-02
OL-'15-03
OL-'15-05
OL-'15-7
OL-'15-08
Sequence 1
Fe-Mn nodule pavement
disconformity
disconformity
Sequence 3
Sequence 3
Sequence 3
Sequence 2
Sequence 1
disconformity
Sequence 2
Sequence 1
transitional
contact
Sequence 2
12,720 +/- 60
δ13C = -31.0 ‰
TOC = 0.46%
12,930 +/- 80
δ13 C = -31.06 ‰
TOC = 0.47 %
15,430+/- 90
δ13C = -32.05 ‰
TOC = 0.44 %
10,590 +/- 60
δ13C = -29.91 ‰
TOC = 0.35 %
0
20
cm
1
2
3
4
5
6
7
9
8
10

Ramped PyrOx ^{14}C Ages from Oneida Lake Sediment Cores

Brad E. Rosenheim[1], Ryan A. Venturelli[1], Eugene W. Domack[1,2]

Sediments deposited in Glacial Lake Iroquois (GLI, now in Oneida Lake and surrounding lake terraces) can be dated using the radiocarbon (^{14}C) time scale, but dating is not necessarily straightforward. A fundamental issue is deciding what to date – carbonate mineral fossils, organic matter, terrestrial plant macrofossils (seeds). Indeed, the current North American Varve Chronology (NAVC, see Ridge, 2004, and subsequent materials online - see Figure 1) is based on some 53 radiocarbon dates, all but one from terrestrial plant macrofossils (Figure 1). Dates from carbonate fossils can be plagued with a spatially and temporally variable "hard water" effect (analogous to a reservoir age in marine settings) that relates to the difference in age of the lake water dissolved inorganic carbon (DIC), from which carbonate minerals would form, and the atmospheric CO_2. Generally, the lake DIC would be older than the atmospheric CO_2 due to inputs of surrounding carbonate rocks, stratification of the lake, and decomposition of organic-rich detrital terrigenous sediment. Organic matter in the sediment is plagued by the ubiquity of carbon in the environment and the presence of pre-aged organic carbon. Our efforts to date varved GLI sediments taken by core from Oneida Lake did not yield terrestrial macrofossils or carbonate fossils, thus we relied on the organic matter within the sediment to tie these sediments to the NAVC.

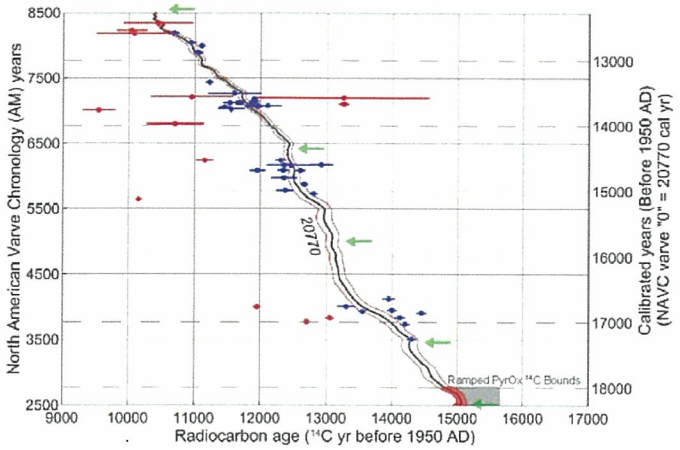

Figure 1: *Radiocarbon (^{14}C) dates from the North American Varve Chronology (NAVC) contain 14 imprecise or outlying ages (red). The NAVC currently depends on the other 50 dates (blue), however gaps still exist. The read and black shaded area near 15,000 calendar years before present represents the position of our initial Ramped PyrOx ^{14}C ages on this curve. Source:* http://eos.tufts.edu/varves/NAVC/navccalib.asp .

Since the pioneering work of Libby (1955), it has been clear that care must be taken in deciding what material is appropriate for ^{14}C dating. Speculatively, Libby (1955) wrote, "This means, of course, that the chemical form in which the carbon is bonded may have real bearing on the validity of the result obtained." In the nascent days of radiocarbon dating, the focus was on avoiding unwanted forms of carbon that could contaminate an otherwise accurate age. Samples could measure as older than their actual age if there was associated relict, pre-aged carbon, and as younger if incorporation of atmospheric CO_2 occurred after the radiocarbon clock began ticking. Either case yields some degree of inaccuracy, depending on the level of contamination and independent of analytical precision of the ^{14}C determination.

Recently, methods to date individual chemical forms of carbon within sediment and other matrices have come online (e.g. compound-specific ^{14}C analysis (Eglinton et al., 1996; Ingalls et al., 2004; Martin et al., 2013)). Using specific compounds of known origin, biomarkers, to develop chronologies allows separation of a meaningful signal from the noise of other contributing sources of carbon to sediments. Constraining the noise resulting from post-depositional physical mixing and chemical diagenesis is also important when selecting good core sites for radiocarbon chronology (Harris et al., 1996; Licht et al., 1998; Mollenhauer et al., 2003; Mollenhauer et al., 2005; Rabouille et al., 2002). Although the ages can make

Affiliations: [1]University of South Florida, College of Marine Science, [2]Colgate University Department of Geology

stratigraphic sense and fit in a regional framework, the uncertainties are large (500-1000 ^{14}y) due to the large sample size necessary for extracting enough datable material (e.g. Yokoyama et al., 2016). For instance, the biomarker approach would not necessarily be the best approach to compare ages between laminae.

Another method of separation of pre-aged carbon from carbon fixed at the time of deposition is thermochemical separation. Thermochemical separation relates the thermochemical reactivity of organic matter to the age spectrum of the organic components within a sample and reflects the sum of all organic material in the sample (Rosenheim et al., 2013b; Williams et al., 2014) over different temperature intervals. Early coupling of thermochemical decomposition techniques with ^{14}C (McGeehin et al., 2004; McGeehin et al., 2001; Wang et al., 2003) focused on soils and lake sediments, and used pre-defined temperature intervals as operational definitions of different chemical forms of carbon. More recent use of this coupling to refine Antarctic sediment chronology has relied on a smooth temperature ramp and no predefined temperature intervals in order to focus on separating the organic matter most likely related to deposition of the sediment (Rosenheim et al., 2008). This method, now being referred to as Ramped PyrOx ^{14}C, was originally conceived for improving sediment chronology where organic matter is the only choice for dating (Rosenheim et al., 2008; Rosenheim et al., 2013b; Subt et al., 2016), but has been more widely used to study age spectra (Gaglioti et al., 2014; Pendergraft et al., 2013; Pendergraft and Rosenheim, 2014; Rosenheim and Galy, 2012; Rosenheim et al., 2013a; Schreiner et al., 2014; Williams et al., 2015). The most recent chronologic applications of Ramped PyrOx ^{14}C have yielded improvements in chronology of Antarctic sediment and identical chronologies to those provided by foraminifera (Subt et al., 2016), as well as observations about the changing character of organic material downcore.

Core 3						
Sample ID	Depth (cm)	Age (^{14}C y)	Age Error (^{14}C y)	δ^{13}C (‰)	TOC (%)	Temperature (°C)
DB-1268-1	24-27 cm	12,720	60	-31	0.46	402
DB-1266-1	28-31 cm	*	*	*	0.42	403
DB-1266-2	28-31 cm	*	*	*		460
DB-1266-3	28-31 cm	24,860	220	-31.13		519
DB-1266-4	28-31 cm	23,380	220	-30.95		585
DB-1266-5	28-31 cm	21,640	210	-25.55		888
Core 5						
Sample ID	Depth (cm)	Age (^{14}C y)	Age Error (^{14}C y)	δ^{13}C (‰)	TOC (%)	Temperature (°C)
DB-1267-1	41.5-46 cm	12,930	80	-31.06	0.47	406
DB-1263-1	44-46 cm	15,430	90	-32.05	0.44	391
Core 7						
Sample ID	Depth (cm)	Age (^{14}C y)	Age Error (^{14}C y)	δ^{13}C (‰)	TOC (%)	Temperature (°C)
DB-1269-1	135-137 cm	10,590	60	-29.91	0.35	393

Table 1: *Preliminary Ramped PyrOx ^{14}C data, all ages reported with blank correction (Fernandez et al., 2015). Sample designation includes DB-run number-split. Cells marked with an asterisk (*) did not graphitize properly and provided erroneous AMS dates.*

Our preliminary Ramped PyrOx data from Oneida Lake (Table 1) show ages from the lowest temperature intervals (associated with the most diagenetically unstable, freshest organic carbon) persistently around 12,800 ^{14}C y (+/- 100), based on ages from summer varves in two different cores (Table 1). Calibration of this age using IntCal13 results in an age between 14,920 and 15,653 calendar years before present, with a median age of 15,265 calendar years before present, or near 2,600 AM years on the NAVC or older (see Figure 1). It is important to stress that these dates are preliminary and we will have to re-prepare a crucial sample that did not graphitize properly for AMS analysis (Table 1). The preliminary suggestion is that these dates cores will at least fill an important gap in the NAVC and potential extend the time series back in time. Ultimately, this will provide a better

understanding of the organic carbon systematics in the GLI setting, hence constraining our dating efforts using Ramped PyrOx ^{14}C. It is obvious from Table 1 that these sediments contain a significant amount of pre-aged carbon in subsequent temperature intervals that have ages approaching the Last Glacial Maximum. It is important to note that higher temperature intervals are more likely to have a mixture of sources of organic carbon, so ages from these higher temperature intervals reflect material potentially of infinite radiocarbon age mixed with material younger than the LGM.

References Cited

Eglinton, T.I., Aluwihare, L.I., Bauer, J.E., Druffel, E.R.M., McNichol, A.P., 1996. Gas chromatographic isolation of individual compounds from complex matrices for radiocarbon dating. Analytical Chemistry 68, 904-912.

Fernandez, A., Lapen, T.J., Andreasen, R., Swart, P.K., White, C.D., Rosenheim, B.E., 2015. Ventilation timescales of the N. Atlantic Subtropical Cell revealed by coral radiocarbon from the Cape Verde Islands. Paleoceanography 30, 938-948.

Gaglioti, B.V., Mann, D.H., Jones, B.M., Pohlman, J.W., Kunz, M.L., Wooller, M.J., 2014. Radiocarbon age-offsets in an arctic lake reveal the long-term response of permafrost carbon to climate change. Journal of Geophysical Research: Biogeosciences 119, 2014JG002688.

Harris, P.T., O'Brien, P.E., Sedwick, P., Truswell, E.M., 1996. Late Quaternary history of sedimentation on the Mac. Robertson shelf, East Antarctica: problems with ^{14}C-dating of the marine sediment cores. Papers and Proceedings of the Royal Society of Tasmania 130, 47-53.

Ingalls, A.E., Anderson, R.F., Pearson, A., 2004. Radiocarbon dating of diatom-bound organic compounds. Marine Chemistry 92, 91-105.

Libby, W.F., 1955. Radiocarbon Dating, 2nd Edition ed. The University of Chicago Press, Chicago, IL, U.S.A.

Licht, K.J., Cunningham, W.L., Andrews, J.T., Domack, E.W., Jennings, A.E., 1998. Establishing chronologies from acid-insoluble organic ^{14}C dates on Antarctic (Ross Sea) and Arctic (North Atlantic) marine sediments. Polar Research 17, 203-216.

Martin, E.E., Ingalls, A.E., Richey, J.E., Keil, R.G., Santos, G.M., Truxal, L.T., Alin, S.R., Druffel, E.R.M., 2013. Age of riverine carbon suggests rapid export of terrestrial primary production in tropics. Geophysical Research Letters 40, 5687-5691.

McGeehin, J., Burr, G.S., Hodgins, G., Bennett, S.J., Robbins, J.A., Morehead, N., Markewich, H., 2004. Stepped-combustion ^{14}C dating of bomb carbon in lake sediment. Radiocarbon 46, 893-900.

McGeehin, J., Burr, G.S., Jull, A.J.T., Reines, D., Gosse, J., Davis, P.T., Muhs, D., Southon, J., 2001. Stepped-combustion ^{14}C dating of sediment: a comparison with established techniques. Radiocarbon 43, 255-261.

Mollenhauer, G., Eglinton, G., Ohkouchi, N., Schneider, R.R., Müller, P.J., Grootes, P.M., Rullkötter, J., 2003. Asynchronous alkenone and foraminifera records from the Benguela Upwelling System. Geochimica et Cosmochimica Acta 67, 2157-2171.

Mollenhauer, G., Kienast, M., Lamy, F., Meggers, H., Schneider, R.R., Hayes, J.M., Eglinton, T.I., 2005. An evaluation of ^{14}C age relationships between co-occurring foraminifera, alkenones, and total organic carbon in continental margin sediments. Paleoceanography 20, doi:10.1029/2004PA001103.

Pendergraft, M.A., Dincer, Z., Sericano, J.L., Wade, T.L., Kolasinski, J., Rosenheim, B.E., 2013. Linking ramped pyrolysis isotope data to oil content through PAH analysis. Environmental Research Letters 8.

Pendergraft, M.A., Rosenheim, B.E., 2014. Varying relative degradation rates of oil in different forms and environments revealed by ramped pyrolysis. Environmental Science & Technology 48, 10966-10974.

Rabouille, C., Tisnérat, N., Blamart, D., 2002. Δ14C of the organic matter in sediments from the Antarctic Polar Front: origin and dynamics of sedimentary organic carbon. Deep Sea Research Part II: Topical Studies in Oceanography 49, 1953-1961.

Ridge, J.C., 2004. The Quaternary glaciation of western New England with correlations to surrounding areas, in: Ehlers, J., Gibbard, P.L. (Eds.), Quaternary Glaciations - Extent and Chronology, Part II: North America. Elsevier, Amsterdam, pp. 163-193.

Rosenheim, B.E., Day, M.B., Domack, E.W., Schrum, H., Benthien, A., Hayes, J.M., 2008. Antarctic sediment chronology by programmed-temperature pyrolysis; methodology and data treatment. Geochemistry, Geophysics, Geosystems 9, Q04005.

Rosenheim, B.E., Galy, V., 2012. Direct measurement of riverine particulate organic carbon age structure. Geophysical Research Letters 39.

Rosenheim, B.E., Roe, K.M., Roberts, B.J., Kolker, A.S., Allison, M.A., Johannesson, K.H., 2013a. River discharge influences on particulate organic carbon age structure in the Mississippi/Atchafalaya River System. Global Biogeochemical Cycles 27, 154-166.

Rosenheim, B.E., Santoro, J.A., Gunter, M., Domack, E.W., 2013b. Improving Antarctic sediment ^{14}C dating using ramped pyrolysis: An example from the Hugo Island trough. Radiocarbon 55, 115-126.

Schreiner, K.M., Bianchi, T.S., Rosenheim, B.E., 2014. Evidence for permafrost thaw and transport from an Alaskan North Slope watershed. Geophysical Research Letters 41, 3117-3126.

Subt, C., Fangman, K.A., Wellner, J.S., Rosenheim, B.E., 2016. Sediment chronology in Antarctic deglacial sediments: Reconciling organic carbon ^{14}C ages to carbonate ^{14}C ages using Ramped PyrOx. The Holocene 26, 265-273.

Wang, H., Hackley, K.C., Panno, S.V., Coleman, D.D., Liu, J.C.L., Brown, J., 2003. Pyrolysis-combustion C-14 dating of soil organic matter. Quaternary Research 60, 348-355.

Williams, E.K., Rosenheim, B.E., Allison, M., McNichol, A.P., Xu, L., 2015. Quantification of refractory organic material in Amazon mudbanks of the French Guiana Coast. Marine Geology 363, 93-101.

Williams, E.K., Rosenheim, B.E., McNichol, A.P., Masiello, C.A., 2014. Charring and non-additive chemical reactions during ramped pyrolysis: applications to the characterization of sedimentary and soil organic material. Organic Geochemistry 77, 106-114.

Yokoyama, Y., Anderson, J.B., Yamane, M., Simkins, L.M., Miyairi, Y., Yamazaki, T., Koizumi, M., Suga, H., Kusahara, K., Prothro, L., Hasumi, H., Southon, J.R., Ohkouchi, N., 2016. Widespread collapse

of the Ross Ice Shelf during the late Holocene. Proceedings of the national Academy of Sciences 113, 2354-2359.

The Younger Dryas to Early Holocene tree-ring radiocarbon, paleoecological and paleohydrological record for the Bell Creek Site, Lake Ontario Lowlands, New York State, USA

Carol Griggs, Cornell University, Ithaca, NY, cbg4@cornell.edu

Todd Grote, thecelticfs88@gmail.com

Overview

Over 100 mature spruce and tamarack logs found in sediments of the Bell Creek floodplain in the Lake Ontario lowlands, upstate New York, USA (Figure 1; 43°16.8′N, 76°21.0′W, 116 m asl), date from the mid-Younger Dryas (YD) into the Early Holocene (EH) ~12.6 to 11.1 ka cal BP (Figure 2). This was a period of extreme climatic change and transition from the cold Younger Dryas conditions into the warming temperate climate of the Early Holocene. Rarely has such a quantity of well-preserved mature logs from this period been discovered anywhere in the world, and never before in North America.

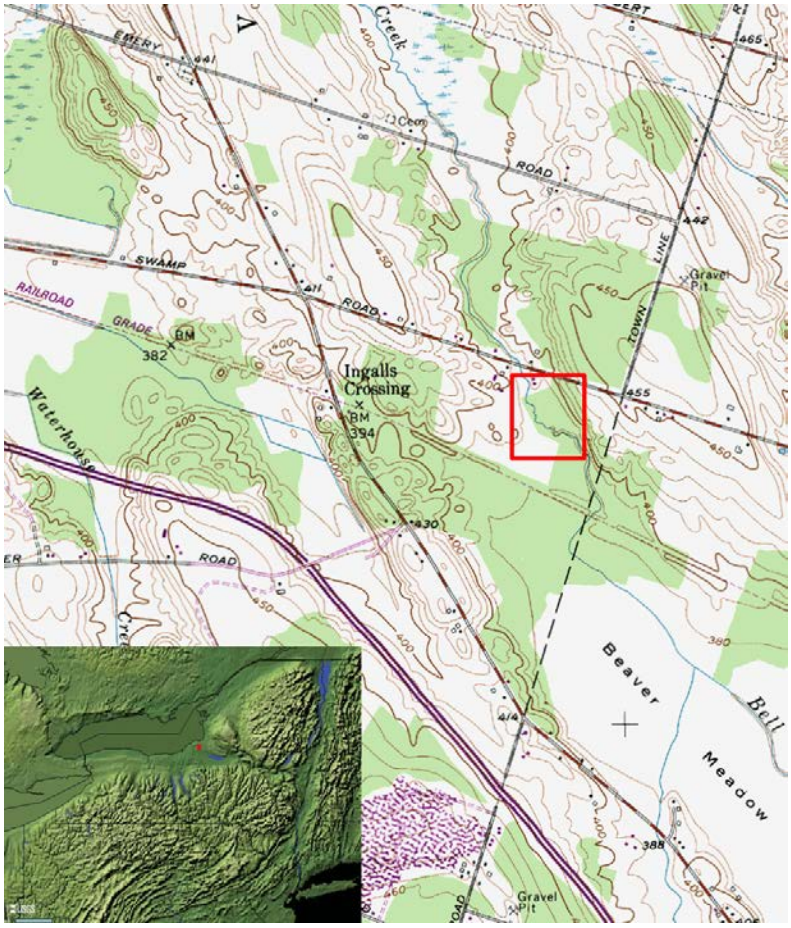

Figure 1. Topography of the Bell Creek valley, Pennellville Quadrangle (USGS O-43076-C3), in central New York State, south of Lake Ontario (see inset). The red square outlines the site. Note the wider flood plain to the south (Beaver Meadow) and the restriction to the north. The creek flows SSE today, into the Oneida River that drains into the Oswego River. The (modified) creeks to the west of Ingalls Crossing and Bell Creek drain west directly into the Oswego River. (N.B. "Swamp Road" is now Maple Avenue.)

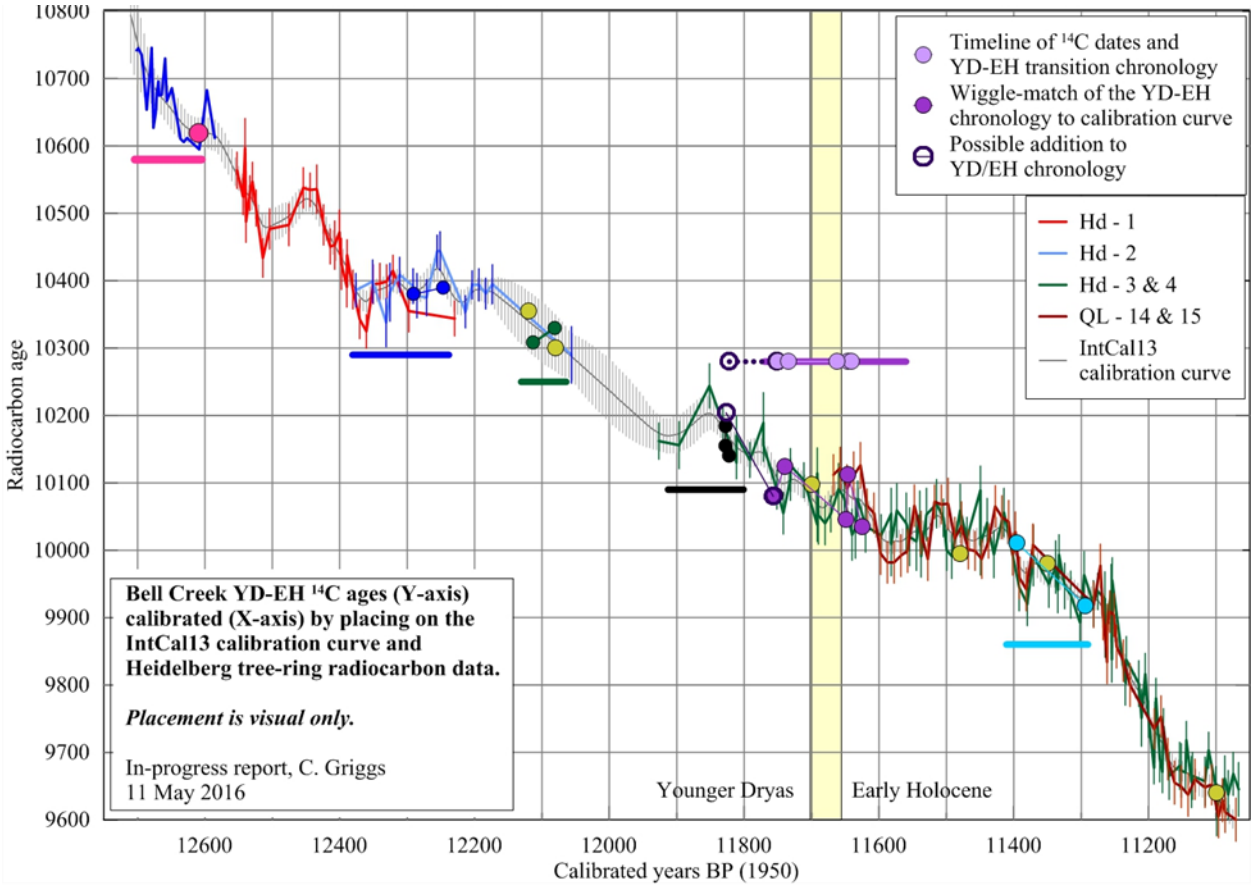

Figure 2. The ^{14}C dates (y-axis) of the Bell Creek samples (listed in Table 1) fitted on the IntCal13 calibration curve (Reimer et al. 2013b) for calibration into absolute years (x-axis). The different raw calibration data sets are the tree-ring ^{14}C data from central Europe that are used in constructing the calibration curve (Kaiser et al 2012). The purple circles and connecting lines and dashes are from the 211-year YD/EH chronology with a possible extension as shown in Figure 8. Each circle represents the ^{14}C date of one segment of rings in a log; the horizontal lines are the lengths of the sample or combined samples which include the ^{14}C-dated segment. Yellow dots are single ^{14}C dates.

Tree rings provide valuable and unique paleoclimate, radiocarbon, and environmental data because: 1) they record climatic variations on annual to multi-decadal time scales (Fritts 1976), 2) they provide an annual record of atmospheric radiocarbon content (Stuiver 1982; Kaiser et al. 2012; Reimer et al. 2013a/b), and 3) their growth characteristics and represented species reflect local and regional environmental and hydrological conditions (e.g. Toney et al 2003, Menking et al 2012, Miller and Griggs 2012). With these attributes, tree rings are the key to reconstructing high-resolution climatic variability, understanding its effects over time on the environment on a local and regional scale, and anchoring all unquestionably in time. The Bell Creek project's ultimate goal is to provide an independent atmospheric ^{14}C data set for the Younger Dryas into

Early Holocene, a period for which it is currently very limited, and will produce the first ever ^{14}C data set from eastern North America. In doing so, a detailed proxy record of paleoenvironmental conditions for the Lake Ontario region over the same time period will also be obtained.

Table 1. Below are the radiocarbon dates of 25 segments from 22 samples, grouped by the sediments in which they were deposited (not depth), and then in the chronological order of their ^{14}C ages. The calibrated dates are very approximate only (Figure 2). The five samples between the dotted lines are those in the 211-year YD-EH transition chronology, and their calibrated dates are determined by the wiggle-matching of the ^{14}C ages on the calibration curve (see text) The samples analyzed at the Heidelberg Radiocarbon Laboratory (Hd-) and the USGS lab (WW-) are from the exploratory collection; those analyzed at the Keck AMS Laboratory (UCIAMS-) are from the survey collection plus two additional exploratory samples.

Sedi-ments	**Sample**	**^{14}C Age**	**^{14}C Error**	**Approx cal BP**	**^{14}C Lab and Analysis Number**	**Sample location on site**
	OBF-227	9640	25	11150	UCIAMS-162636	T39
O	OBF-64, outer	9918	37	11280	Hd-28655	betw T17/35
R	OBF-66, outer	9921	37	11300	Hd-28654	near T35
G	OBF-135	9980	25	11400	UCIAMS-161894	T16
A	OBF-68	9995	30	11405	WW-8906	near T14
N	OBF-212	9995	25	11580	UCIAMS-162634	T32
I	OBF-64, inner	10011	44	11600	Hd-30270	betw T17/35
C	OBF-215	10035	25	11625*	UCIAMS-162635	T35
S	OBF-65, outer	10046	33	11649*	Hd-30268	betw T17/35
&	OBF-69	10125	38	11635*	Hd-28656	near T14
	OBF-79	10112	40	11730*	Hd-30278	near T14
M	OBF-65, inner	10082	38	11680*	Hd-28653	betw T17/35
U	OBF-66 middle	10080	25	11580	UCIAMS-163493	Near T35
C	OBF-66, inner	10204	34	11830	Hd-30271	near T35
K	OBF-48	10098	36	11710	Hd-30269	near T17
	OBF-63	10152	34	11800	Hd-30253	betw T17/35
Inter-face	OBF-120	10140	25	11785	UCIAMS-161893	T13
	OBF-122	10185	25	12080	UCIAMS-162632	T13
	OBF-116	10300	25	12030	UCIAMS-162631	T11
GRAVEL	OBF-67	10308	32	12050	Hd-30251	near T35
&	OBF-155	10330	20	12100	UCIAMS-163484	T23
SAND	OBF-209	10355	25	12120	UCIAMS-162633	T30
&	OBF-238	10380	25	12230	UCIAMS-162637	T45
SILT	OBF-50	10390	25	12240	UCIAMS-163492	near T24
	OBF-150	10620	25	12610	UCIAMS-161895	T22

The Younger Dryas is recognized as a significant cold period on a global scale at the end of the late Wisconsin glacial stade and Pleistocene epoch (e.g. Alley 2007, Muscheler et al. 2008, Broecker et al. 2010, and many, many others). At its onset around 12.9 ka cal BP, the Lake Ontario lowlands had just emerged from the lakebed of glacial Lake Iroquois and successor proglacial lakes, and the landscape progressively transformed from lake bed to lake shore to terrestrial as waterways drained the lowlands with the lowering of the water levels in the Lake Ontario basin to the two Early Lake Ontario (ELO) elevations (Figure 3, Anderson and Lewis 2012). On the lowlands, Bell Creek was within the outlet of the proglacial lakes into the Mohawk River Valley before the onset of the YD. As the lowlands became terrestrial, the drainage of the Bell Creek Valley was to the north into ELO, then reversed to its current streamflow direction to the south with isostatic adjustment and possibly valley fill (Figure 4). A boreal forest had developed on the lowlands no later than ~12.6 ka cal BP.

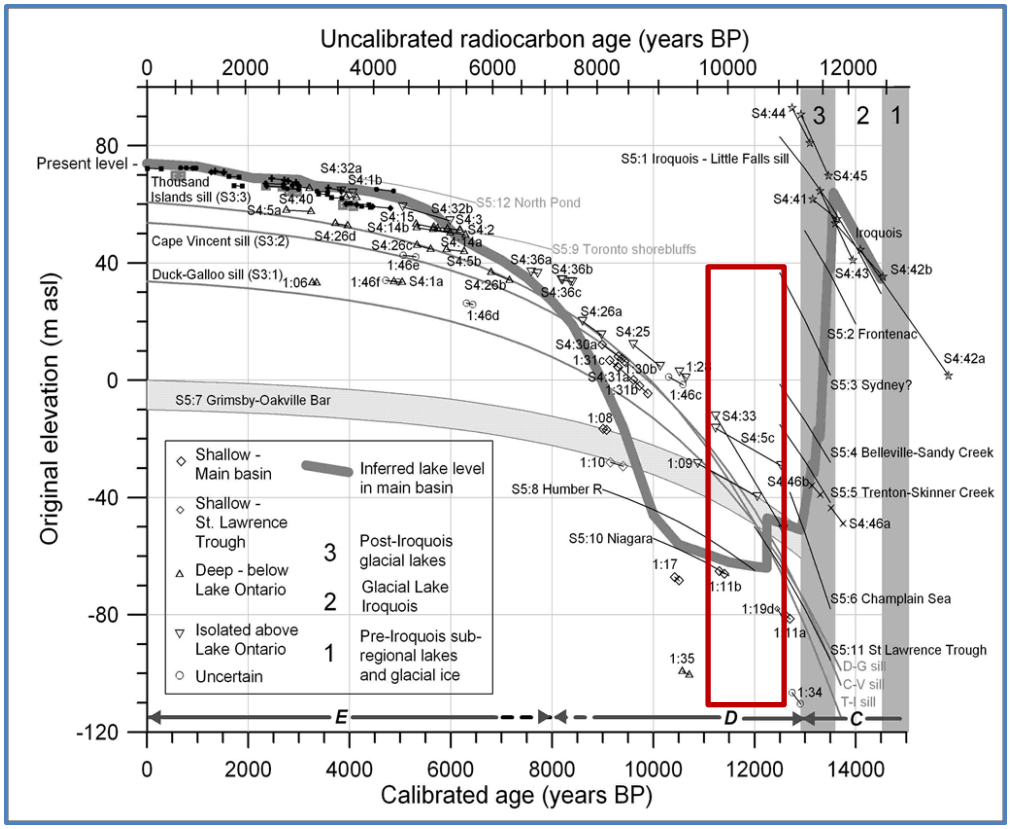

Figure 3. The elevation of the water surface of Lake Ontario (relative to present sea level) as a function in time. The time period that the YD/EH logs at the Bell Creek site accumulated is within the red box, ca 12.6-11.2 cal BP, starting when the lake was confluent with the Champlain Sea and continuing into the period when Early Lake Ontario was an evaporative basin. Also shown by light lines and a grey band are the elevation of spill points that controlled flow into and out of the lake. The spill points changed with erosion and glacial emergence. Figure from Anderson and Lewis (2012) and used with their permission.

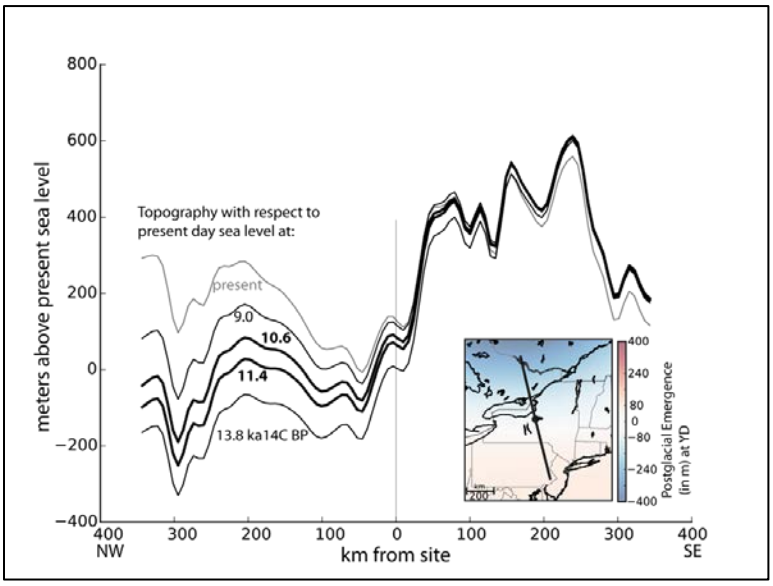

Figure 4. A model of isostatic adjustment at the Bell Creek site (at 0 km on x axis) on a NNW-SSE transect from the Ottawa River to near the Delaware River (see inset). The site sits on the E-W "ridge" in the lowlands. Evidence of change in streamflow direction is found in the sediments at the site. Note that while this illustration is a good indicator of the change in ASL away from the "0" on the x axis, the center hinge of the adjustment likely shifted over time (Samuel Kachuck)

Material and Methods:

The Bell Creek site and initial, exploratory, and survey collections

The discovery of the log-bearing YD-EH deposit was entirely due to the landowners' observations and curiosity of Bell Creek and the current channel. Changes in stream meanders over time had exposed and re-buried logs towards the base of the channel, especially after heavy precipitation and snowmelt. A new exposure along the outer bank during a particularly dry spring accentuated the three major sediment layers in the creek banks (Figure 5) which initiated the phone call from Ralph Bowering to the Cornell Tree Ring Laboratory at Cornell University, Ithaca, NY. The initial visit resulted in a collection of samples from 6 substantial logs that extended out from the banks along the outer meander. ^{14}C dates of samples from the top and bottom logs indicated deposition from EH to Middle Holocene (9.0 – 7.5 ka cal BP), but the older of the two was only in the bank at water level during the visit, suggesting that much older logs might be present in the creek bed below. A subsequent exploratory 2-day collection from a small segment of the channel (circled in Figure 6) resulted in samples from 32 logs plus additional samples of branches and roots from the base of the organic-muck sediments and the silty and sandy gravel below the muck, including those lying in the bottom of the channel. ^{14}C dates of 9 samples range from ~12.1 – 10.6 ka cal BP (10.3 – 9.4 ka ^{14}C BP; Figure 2), establishing the presence of a significant YD/EH deposit at Bell Creek.

Figure 5. The Bell Creek current channel. Top: The two upper strata, floodplain and paleowetland muck, in the bank of an outer meander on the initial visit (M1 in Figure 6). Bottom: The strata identified farther down the channel during the exploratory collection (M3). The sand lens is the most distinct here; it becomes mixed in with both the muck and gravelly silt deposits in the majority of the trenches (see text). In the top photo there is an example of a log lying in the creek today, probably similar to when at least the EH logs were deposited. The YD logs may have been deposited in a more active stream.

This collection and subsequent tree-ring analysis indicated that both spruce and tamarack were the dominant species during that period, species that are common in a boreal riparian environment and floodplain. Their ring counts range from 26 to 140, and many of the longer tree-ring sequences had matching growth patterns. In particular, seven sequences crossdated and produced a 183-year chronology covering the late YD and transition into EH, and many other

small groups of samples crossdated, producing tentative sequences from 2 to 4 samples of over 100 years in length.

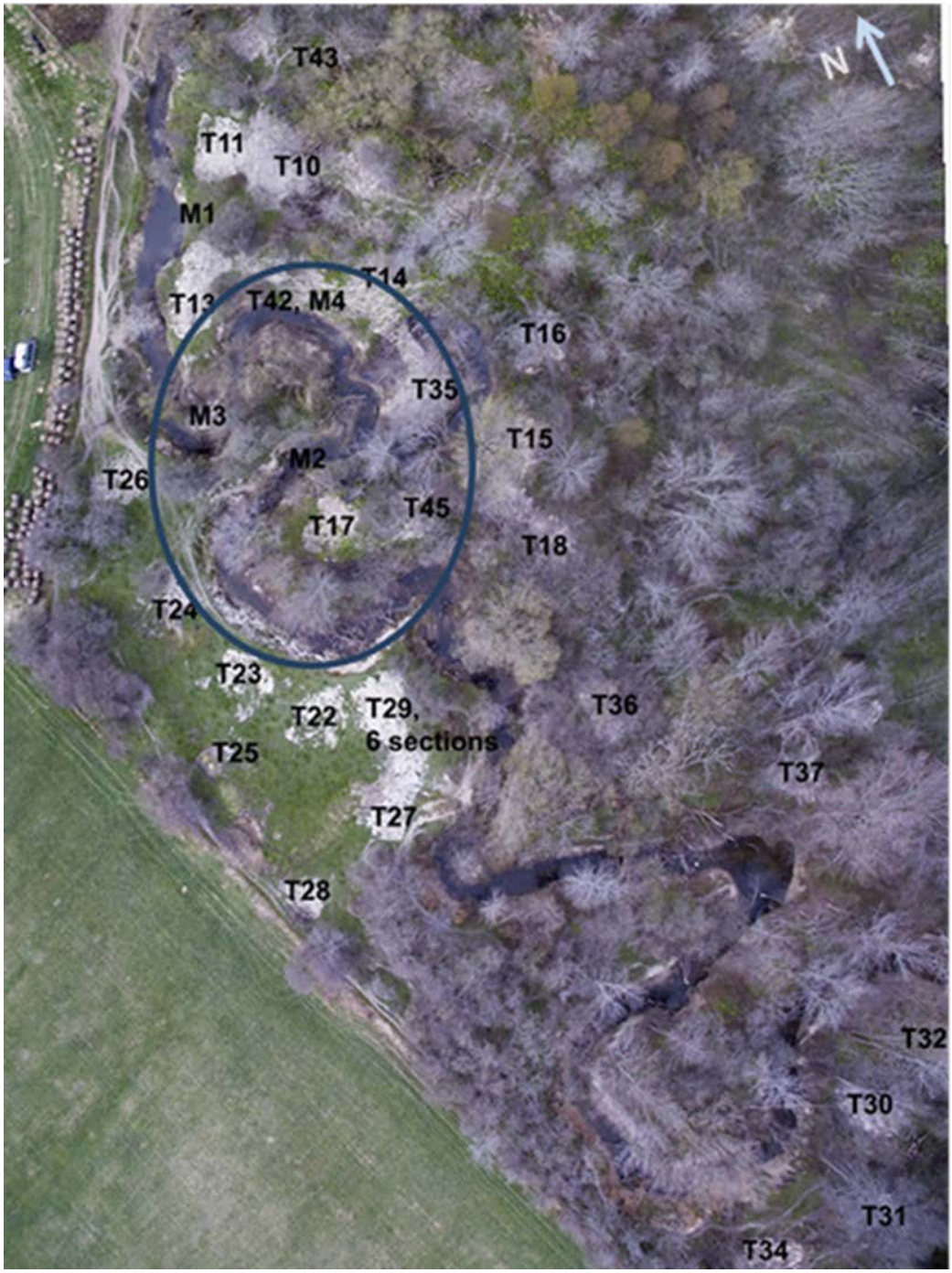

Figure 6. The locations of excavated trenches and meanders on the Bell Creek floodplain. The blue circle surrounds the channel where the exploratory YD/EH samples were collected. Most of the trenches shown here contained logs deposited in the YD-EH, with the exception of T17 and those farthest from the meanders. The oldest logs were found in T22, T23, T45, T30, and T11. For scale, the white rectangle in upper left corner is a van, about 2 x 3m in size, which was the approximate size of the excavated trenches (William Hecht, photographer).

The number of samples collected in two days and their abundance in such a small area indicated that it was very likely that many more logs were present in the Bell Creek floodplain. However, since the log-bearing sediments in the meanders were at the base of the ~2m-high banks and in the streambed, serious excavation was necessary to find and sample the number of mature logs needed for dendrochronological analysis, especially for constructing a tree-ring chronology that could cover all years of deposition. The Committee of Research and Exploration of the National Geographic Society and the Eppley Foundation funded a two-week survey and subsequent analysis to find the extent of the YD/EH deposition on the floodplain, collect samples, and analyze the collection.

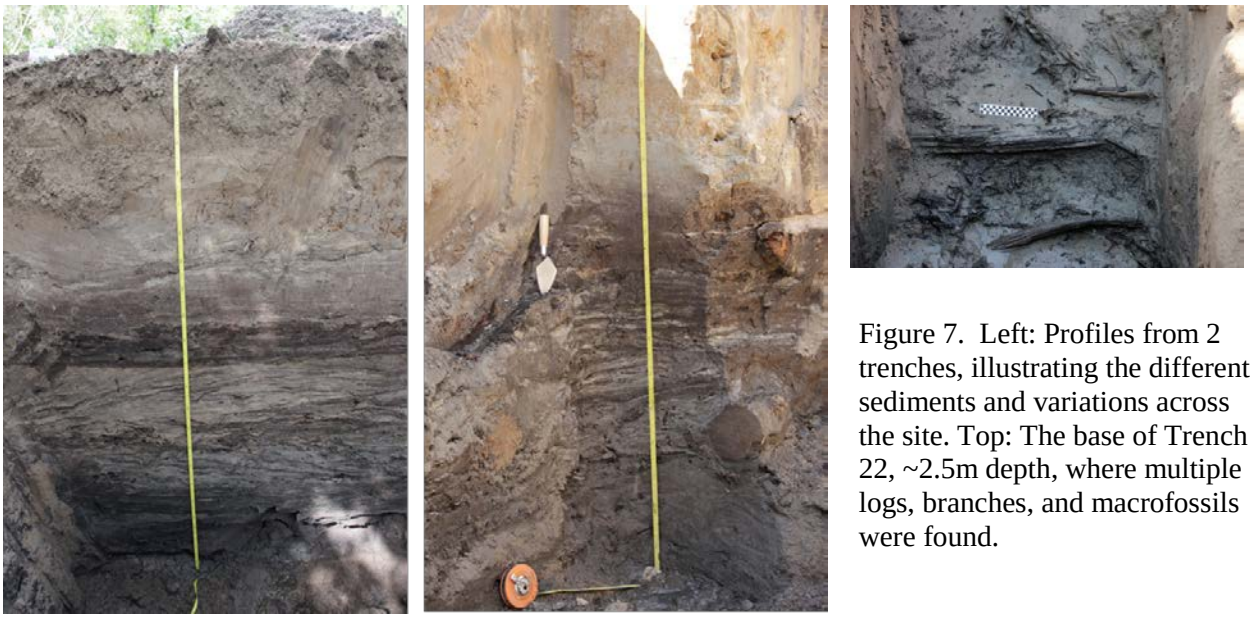

Figure 7. Left: Profiles from 2 trenches, illustrating the different sediments and variations across the site. Top: The base of Trench 22, ~2.5m depth, where multiple logs, branches, and macrofossils were found.

In August 2015, the survey of about 2 hectares of the floodplain was undertaken. 45 trenches were excavated (Figure 6), one with several extensions, with average size of ~2 x 3m, and between 2.5 and 3.5 meters deep. Extensive stratigraphic and sedimentologic analyses were conducted by Todd Grote and Brita Lorentzen, a detailed photographic record with extensive field notes were compiled by William Mastandrea and Cynthia Kocik, respectively, and aerial photos were taken with a drone camera by William Hecht. We collected a total of over 120 wood samples, with over 80 from mature logs and ~40 from branches and roots in the muck and gravel sediments (Figure 7). We also collected samples for pollen and macrofossil analysis from the profiles of two trenches, and from several mats of *in situ* organic debris.

Samples of thirteen logs were radiocarbon-dated, placing the beginning of known log deposition at approximately 12.6 ka cal BP, extending the earliest date (12.1 ka) of the exploratory collection back by 500 years (Table 1, Figure 2).

Laboratory Methods

In the laboratory, the sediments surrounding the wood samples were first inspected for their components. The samples were then washed and species identified and confirmed from small sections of their transverse, radial and tangential surfaces (Panshin and de Zeeuw 1970). The samples were kept moist and stored in a refrigerator. For tree-ring measurement, several radii on the transverse surface(s) were prepped with razor blades. Rings were counted, ring-widths measured if over 60 rings, and those of less than 60 rings measured only when context was particularly important. Ring-width sequences of over 80 years were used in tree-ring analysis by comparing the tree-ring growth patterns between samples using standard tree ring methods (Cook and Kairiukstis 1990) with their on-site location, context, and the ^{14}C dates as guides. Sequences of two or more samples with matching patterns, supported by both visual and statistical tests, were then crossdated and combined into multi-sample chronologies. Tree-ring sequences less than 80 years in length were used only to confirm crossdates and add to sample depth in a chronology.

As of 31 May 2016, the tree-ring and pollen analyses of the survey samples, especially the younger samples, are still in progress by Griggs and Dorothy Peteet, respectively.

Results and Discussion

The surficial geology of the study site consists of glaciolacustrine silt and clay, with occasional sandy facies, deposited in proglacial lakes formed during Late Wisconsin deglaciation of the Ontario Lobe of the Laurentide Ice Sheet (Cadwell 1991). Rarely are the late Wisconsin glaciogenic deposits exposed within the study area because of the overlying veneer of Holocene alluvium, with weakly to moderately well-developed alluvial soils. Hydric soils associated with poorly drained floodplain segments and organic wetland deposits, common on geomorphically young, formerly glaciated landscapes, also occur in the vicinity. Sediment deposition across the site is typical of alluvial fill along a meandering stream in a wide valley. Below the modern relatively flat surface of the floodplain, a very hummocky terrain is indicated by the very

different sedimentary units and undulating boundaries exposed in trenches and stream banks (Figures 5, 7).

Overall, below ~1m of the soil horizons and alluvial overbank deposits (Middle and Late Holocene), the stratigraphy is 0.2 to 1+ m of organic muck and silt interspersed with mats of forest debris and lenses of loam and/or fine sands. Immediately below the muck, silty and sandy gravel dominate the matrix with occasional organic lenses and mats (Figure 5). The YD/EH log-bearing sediments include the gravel-sand-silts up into the base of the muck strata. From north to south, and east to west, the muck generally thickens, but that again is extremely variable, depending on factors such as trench location relative to active meanders, location of paleochannel fills and direction of stream flow. Well over half of the YD/EH samples came from logs at the base of the muck deposit.

The gravel-sand-silt strata below the muck were not as easily excavated, thus fewer log samples were collected. In many trenches, from 10-50cm below the muck /gravel interface, the walls collapsed and water seeped in depending on depth of interface and grain size of the lower strata sediments. In general, logs exposed by the backhoe were quickly re-buried, and collection became restricted to sections of logs extracted by the backhoe. The probability of abundance of logs at that level was indicated by their presence (even when not collected), the lenses of forest mats with high macrofossil content within that deposit, and that the trenches containing the older material are located across the site rather than in one restricted area (Table 1, Figure 6). Better methods for finding and extracting the samples from those strata are the goal of a 2016 survey, using GPR and perhaps a geoprobe for a more complete picture of the extent of that deposit.

Dendrochronology

Of the 48 tree-ring samples measured by May 2016, with 32 from the exploratory collection and 16 from the survey, spruce and tamarack are equally represented in the collection, though not temporally, with lifespans ranging from 30 to 140 years (Table 2). Twenty-one have more than 80 rings, and the ~60 samples still-to-be measured should add between 20 and 30 more samples to the >80 ring group. White spruce cones are abundant, tamarack cones are present but in smaller numbers, and cones of black spruce, balsam fir, or pine species have yet to be found.

Table 2. The mature log samples with indicated ring counts.

Ring Count	Number of samples
>120	4
101 to120	5
91 to 100	7
81 to 90	5
61 to 80	13
<60	14
Totals:	
>80	21
All	**48**

The 183-yr chronology from the exploratory collection is made up of seven of the 21 samples and all have more than 80 rings. The logs found in the muck sediments in 2015 added 5 more samples and 28 years to the 183-year exploratory chronology, building a 211-year tree-ring chronology from 12 samples (Figure 8). There is a high probability that one or two other measured samples will extend its length to at least 260 years (dotted line, Figure 8), but the overlaps between the chronology and the individual samples are too short or too few samples for a valid crossdate. The remaining samples yet-to-be analyzed may confirm or reject the additions but in either case will most likely extend the chronology farther in both older and younger directions.

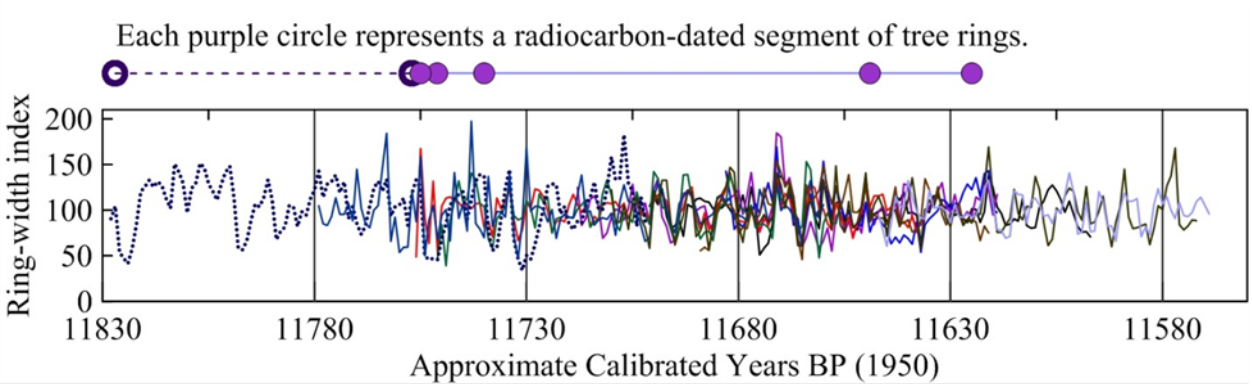

Figure 8. The crossdated tree-ring measurements from 12 samples (211 years) plus one other sample (dotted lines) that may crossdate but needs more samples with the same growth patterns to confirm its placement. The top timeline shows the ^{14}C dated segments in this chronology; see Figure 2 for their placement on the ^{14}C calibration curve.

Five segments of 5 to 22 rings from 4 samples in the chronology were radiocarbon-dated (Table 1). The ring counts between the segments in the tree-ring sequence are used to place the dates of the five segments relative to each other (Figures 2, 8). The relative placement of the 5 radiocarbon dates places the chronology in calibrated time with much less error than the calibration of a single ^{14}C date by matching the variations in their radiocarbon dates over the 211-year period (Figure 2). The calibrated dates indicate that the chronology covers from approximately 11,570 to 11,780 cal BP, which includes the transition from the Younger Dryas into the Early Holocene periods (Figure 2).

The success in building this chronology is the most important result of this project so far. The most important aspects are the high quality of the matching tree-ring patterns between trees (Figure 8), its sample count, sample lengths, and most of all, its representation of the YD/EH period. Due to these qualities, its constituents can be used to provide an independent ^{14}C data set for at least 200 years in 40 consecutive 5-ring segments (Reimer et al. 2013a). The independent data set of the 40 tree-ring ^{14}C ages can then be "wiggle-matched" with the established central European record (Figure 2; Friedrich et al 2004, Kaiser et al 2012, Reimer et al. 2013a, b) to verify (or not) the validity of the current ^{14}C calibration curve for the YD/EH. For this period, there are some differences between the current raw ^{14}C radiocarbon data sets (Figure 2), but the relationship of the constituent ^{14}C data sets in the IntCal13 calibration curve is considered secure (Kromer, Southon, personal communication 2014-2016). This Bell Creek data will unquestionably augment the current tree-ring-based high-resolution atmospheric ^{14}C record for the Younger Dryas period, and the success of the YD/EH transition chronology confirms that the abundance and quality of logs needed for a significant ^{14}C data set are available from the trees found at the site. The ~60 unmeasured samples will most likely add to that chronology and build one or more additional chronologies from the earlier periods where the ^{14}C data is sorely needed (Figure 2).

What the logs tell about growing conditions:

In general, the YD/EH logs were complete logs, with the outer ring (just below bark) intact around most of the circumference. If not complete, the logs were found in two or three pieces, split vertically, and near to each other. Ring-widths are average for the represented species, typical of moderate conditions with few showing the stress common to trees growing on the boundary of their species' range or in an environment with significant growth-limiting characteristics, such as a bog.

The oldest log was found at the base of Trench 22 in sandy silt with a large mat of forest debris, consisting of many cones, twigs, needles, and other organic material, implying an established boreal forest at that time. The log is spruce, diameter of 22cm with 99 rings, and its outer rings date to ~12.6 ka cal BP (Figure 2), and only white spruce cones were present in the collected sediments. The two next oldest logs were tamarack, one with 112 rings and a diameter of 29cm (Figure 9) and the other with 91 rings and a 15cm diameter. Their ^{14}C ages calibrate to

anywhere from ~12.4 to 12.15 ka cal BP due to the plateau in the calibration curve (Figure 2). Neither of the logs contains any substantial amount of the reaction wood found in trees where downhill creep is common such as on a streambank. Rather, their cell structure and growth indicate a more stable environment. All three logs have preservation of mainly branch collars and short nubs of the branches, equal in length around the trunk, indicating that they were transported a very short distance or had lain in an active stream channel before burial. The presence of the mat lenses also indicates little transport.

Figure 9. The second oldest log, OBF-238, a tamarack found at the base of Trench 45, dating to ca. 12.3ka cal BP.

The logs found just below the muck deposit, in the gravelly-silt sediments of slightly larger grain size and a higher percentage of gravel, were mainly tamarack with fewer ring counts and significant amounts of reaction wood, but the same nubby branches indicating only short transport. Tamarack is a pioneer species and the analysis as of May 2016 suggest that its dominance and the short life spans of the logs from that period indicate more frequent and intense flooding, or possibly fire, that altered the plant growth at the site, prohibiting forest establishment. The presence of beaver and the effect of a dammed stream on the flora cannot be ruled out, but no gnawed branches or any other distinctive remains were uncovered in the trenches, and spruce and tamarack are not preferred species for beaver

In the muck deposit, spruce and tamarack are both present in approximately equal amounts, with less reaction wood than in the gravelly deposit, but more than in the lower sediments. Most of the logs had longer life spans (~ 65-140 years), plus intact branches of longer and differing lengths than those below, in the gravel and sand deposits (Figure 10), suggesting they had not been transported at all, just fell into the channel and gradually buried, an environment very similar to the floodplain today.

Figure 10. Sample OBF-120 from muck - gravel interface with branches extending out, indicating little weathering or transport once fallen.

The immediate environment inferred from log species and characteristics, and the differing strata of the YD/EH deposition can be put in time by the ^{14}C of logs in the different strata (Table 1). The oldest samples and strata indicate a relatively stable forest regime from at least 12.6 to around 12.2 ka cal BP period (10.6-10.38 ka ^{14}C BP). More turbulent conditions are suggested from ~12.2 to ~11.9 ka cal BP from the short-lived tamarack trees, and finally a quieter period from late YD into the Early Holocene, ~11.9 to 11.6 ka cal BP. This interpretation is tentative at this time (May 2016), but results of the ongoing analyses have not significantly altered the supporting evidence of that interpretation. Further ^{14}C dates of the tree-rings will place those periods and changes more securely in time.

Conclusions

The tree-rings from Bell Creek can now provide an independent high-resolution atmospheric radiocarbon data set for the late Younger Dryas into Early Holocene. This data from North America will be a counterpart to the central European ^{14}C series across the North Atlantic Ocean and perhaps resolve issues with the radiocarbon calibration of dates in the YD – EH, including the timing of the end of the Younger Dryas, the differences between the ^{14}C content of the northern and southern hemispheres (e.g. Hogg et al 2013), between tree-ring and other lower-precision archives used in calibration of atmospheric ^{14}C (e.g. speleothems, sediments; Southon et al. 2012, Ramsey et al. 2012), and between atmospheric and oceanic ^{14}C content over that period in particular (Stuiver et al 1998, Hughen et al 2000, 2006, Muscheler et al. 2008).

Going into the future, the ultimate goal of the Bell Creek project is building a sound tree-ring chronology covering the 1200, maybe 1400 years (12.4 to 11.2, maybe 12.6 to 11.2 ka cal BP), or significant portions thereof. Then we can obtain the high-resolution ^{14}C record that will

provide a new perspective on the variation of atmospheric ^{14}C content over that period, which is still in dispute (Figure 2).

There are several suggestions of possible environmental conditions and changes in the region coming out of the tree ring and pollen analysis, but at present they are only tentative except for one: the tamarack story. There is no doubt that the presence of so much tamarack wood and cones will aid in clarifying the relationship of the abundance of tamarack trees to the limited preservation of tamarack pollen on a local scale. It is well known that tamarack pollen underrepresents the species presence within a study region, and the abundance of tamarack logs and other macrofossils compared to its pollen at this site is a great opportunity to better understand that ratio.

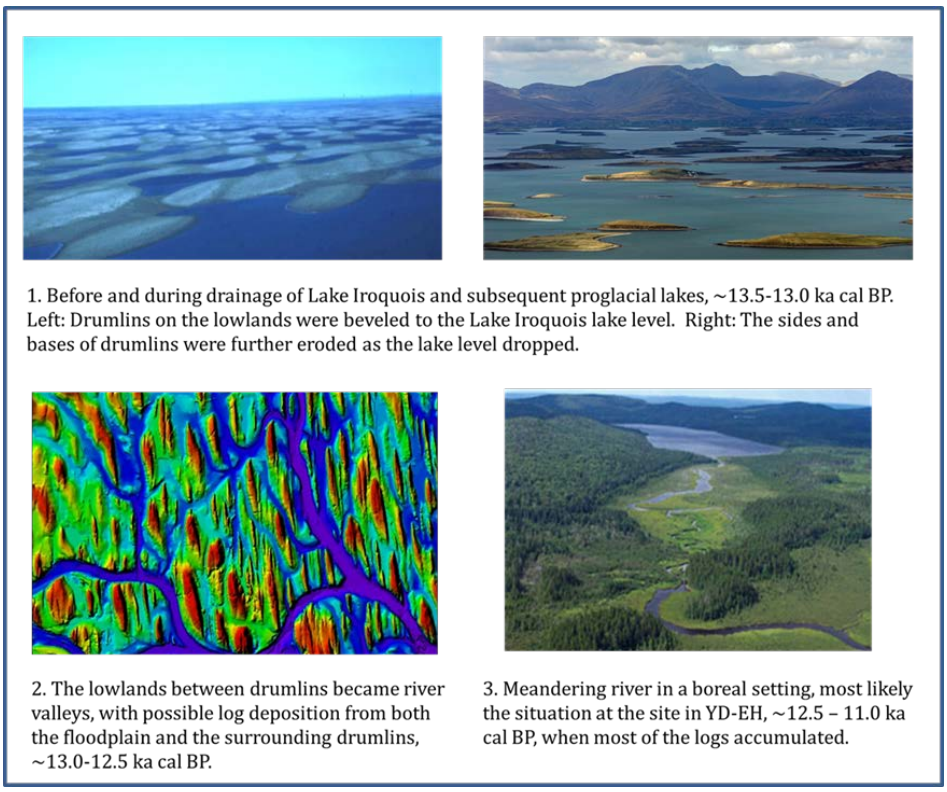

1. Before and during drainage of Lake Iroquois and subsequent proglacial lakes, ~13.5-13.0 ka cal BP. Left: Drumlins on the lowlands were beveled to the Lake Iroquois lake level. Right: The sides and bases of drumlins were further eroded as the lake level dropped.

2. The lowlands between drumlins became river valleys, with possible log deposition from both the floodplain and the surrounding drumlins, ~13.0-12.5 ka cal BP.

3. Meandering river in a boreal setting, most likely the situation at the site in YD-EH, ~12.5 – 11.0 ka cal BP, when most of the logs accumulated.

Figure 11. A possible scenario of the evolution from the lowering of Lake Iroquois and subsequent lakes, rivers, and creeks over the YD and into the Holocene.

On the local, but possibly not-so-local, scale, the immediate geography of the Bell Creek Valley includes a restriction in the width of the floodplain directly north of the site (Figure 1), The valley was part of the drainage system of Lake Iroquois into the Mohawk River Valley, and probably along a shoreline for at least a short while as Lake Iroquois and successive lake levels lowered by the start of the YD (Figures 3 and 11; Anderson and Lewis 2012). For the Bell Creek

Valley, the isostatic depression, presence of the restriction, and the preservation and quantity of logs south of the restriction suggests that streamflow was to the north from the start of the YD and during the YD/EH deposition. Future collection, tree-ring analysis and stable isotope tests of the YD/EH logs, and possibly above their strata, is likely to clarify the paleohydrologic record, and possibly connect the change in streamflow with isostatic adjustment.

On a much larger regional scale, the site is 250 km south of the Ottawa River in Ontario, Canada. At the end of the late glacial period, the margin of the retreating Laurentian Ice Sheet was north of that river, and meltwater flow went through Georgian Bay and ancestral Ottawa River into the Champlain Sea (Anderson and Lewis 2012, Hladyniuk and Longstaffe 2016). There were no significant orographic barriers between the ice sheet and the Lake Ontario basin, and Bell Creek is on the easternmost point of the Great Lakes system, at altitudes far below the Alleghany plateau to the south (**Figure 4**) and the Adirondacks to the east. From the site, the mouth of the St. Lawrence Valley is to the northeast and the west shore of the Champlain Sea was only around 100 km away from the site at the start of deposition. There is no modern analog to compare or test these conditions, no ice sheet the size of the Laurentide which was retreating with its margin on a continental land surface the size of eastern North America. The effects of the ice sheet on atmospheric circulation and temperature is postulated as glacial anticyclonic circulation but within a limited distance from the ice sheet (Krist and Schaetzl 2001). However, the Great Lakes basin would have been a natural catchment for cold air at ground level, particularly the Lake Ontario and Erie basins with their E-W orientation, and the presence of meltwater flowing just south of the ice sheet would have preserved lower temperatures of the meltwater (rather than through the eastern Great Lakes), which may have affected ground-level temperatures on land and water temperatures of the Champlain Sea at least at the point of drainage (Hladyniuk and Longstaffe 2016). The proxy data from the tree-ring analyses of the site do not indicate any particularly cold periods or abrupt changes at the end of the YD such as to the south and east (e.g. Peteet et al. 1993, Menking et al. 2012) but the persistence of the boreal conditions west of the site (e.g. Twiss Marl Pond, Yu 2000; Jacobson et al. 1987, Yansa 2006) may have been caused by these processes, possibly causing cold winter temperatures restricting the migration of the more temperate species to the lowlands. With the tree rings, this project has the potential for providing high-resolution proxy data for a better assessment of this interplay and the overall atmospheric dynamics in this unique region during a period of extreme climate change.

Addendum for those intrigued by / interested in isostatic adjustment: Below is a New York State map (Rickard and Fisher 1970) of the bedrock under the area of the 2016 FOP Field Tour. The interface between ~ mid-Silurian and the undifferentiated lower Silurian/ upper Ordovician bedrock is directly south of the Bell Creek Site. Of possible importance to the site is the isostasy of the region and its impact on the location of the "divide" (dotted line) and the direction of stream flow, currently to the south for Bell Creek and to the north for the streams above the divide.

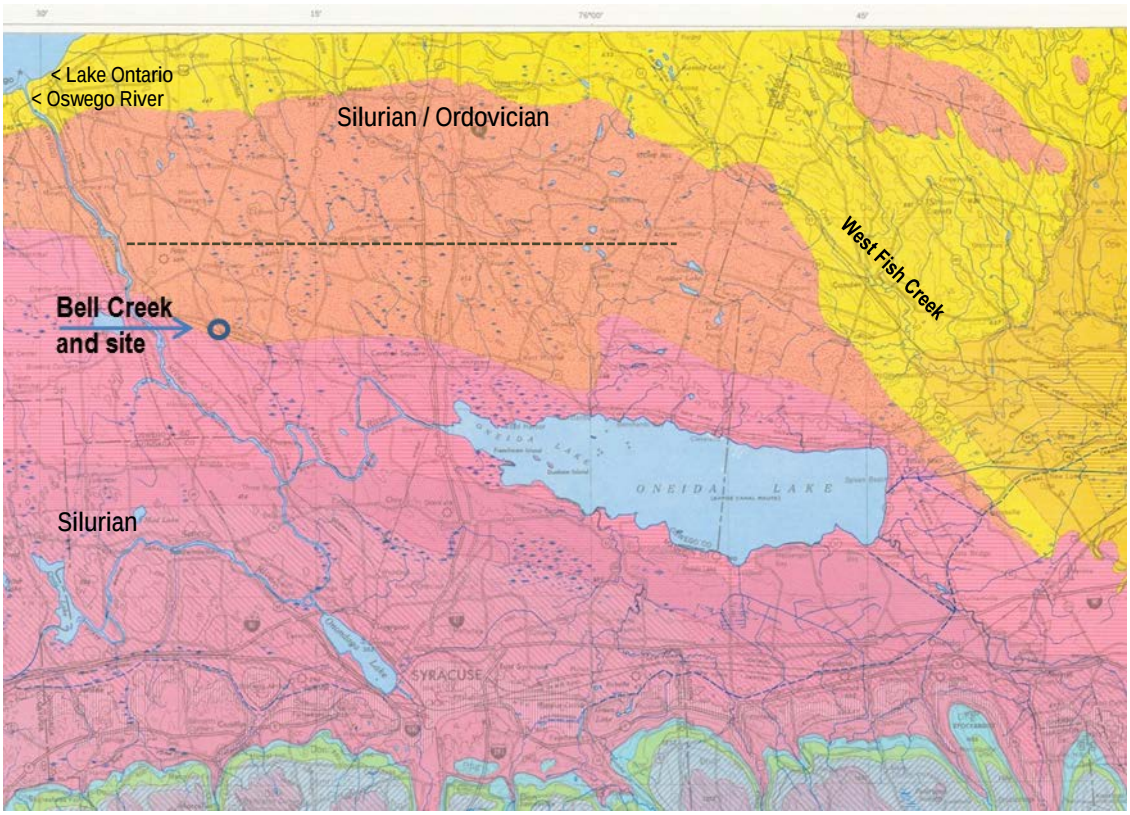

References:

Alley, RB. 2007. Wally was right: predictive ability of the North Atlantic "conveyor belt" hypothesis for abrupt climate change. Annual Review of Earth and Planetary Sciences 35:241-272; doi:10.1146/annurev.earth.35.081006.131524

Anderson, TW and CFM Lewis. 2012. A new water-level history for Lake Ontario basin: Evidence for a climate-driven early Holocene lowstand. Journal of Paleolimnology 47 (3): 513-530; ISSN 0921-2728, 03/2012.

Arseneault, D and S Payette. 1997. Reconstruction of millennial forest dynamics from tree remains in a subarctic tree line peatland. Ecology: 78 (6):1873-1883.

Broecker, WS, GH Denton, RL Edward, H Cheng, RB Alley, AE Putnam. 2010. Putting the Younger Dryas cold event into context. Quaternary Science Reviews 29:1078-1081.

Cadwell, D.H., 1991. Surficial Geologic Map of New York, 1:250,000 scale. New York State Museum GIS coverage. Available URL: "http://www.nysm.nysed.gov/gis/" [Accessed July 2008].

Cook, ER and LA Kairiukstis, Eds. 1990. *Methods of Dendrochronology*. Kluwer Academic Press, Dordrecht, 394 pp.

Friedrich, M, S Remmele, B Kromer, J Hofmann, M Spurk, KF Kaiser, C Orcel, M Küppers. 2004. The 12,460-year Hohenheim oak and pine tree-ring chronology from Central Europe – a unique annual record for radiocarbon calibration and paleoenvironment reconstructions. Radiocarbon 46(3):1111–22.

Fritts, HC. 1976. Tree Rings and Climate. London: Academic Press. 567pp.

Hladyniuk, R, FJ Longstaffe. 2016. Oxygen-isotope variations in post-glacial Lake Ontario. Quaternary Science Reviews 134: 39-50.

Hogg, A, C Turney, J Palmer, E Cook, B Buckley. 2013. Is there any evidence for regional atmospheric ^{14}C offsets in the Southern Hemisphere? Radiocarbon 55(4): 2029–2034.

Hughen, KA, JR Southon, SJ Lehman, JT Overpeck. 2000. Synchronous radiocarbon and climate shifts during the last deglaciation. Science 290: 1951–1954.

Hughen, K, J Southon, S Lehman, C Bertrand, J Turnbull. 2006. Marine-derived ^{14}C calibration and activity record for the past 50,000 years updated from the Cariaco Basin. Quaternary Science Reviews 25: 3216–3227.

Jacobson, Jr, GL, W Thompson III, EC Grimm. 1987. Patterns and rates of vegetation change during the deglaciation of eastern North America. In: North America and Adjacent Oceans During the Last Deglaciation, (WF Ruddiman and HE Wright Jr, eds). Boulder, CO, The Geological Society of America, Inc., pp 277-288, and Plate 2.

Kaiser, KF, M Friedrich, C Miramont, B Kromer, M Sgier, M Schaub, I Boeren, S Remmele, S Talamo, F Guibal, O Sivan. 2012. Challenging process to make the Lateglacial tree-ring chronologies from Europe absolute - an inventory. Quaternary Science Reviews 36:78-90.

Krist Jr., F., Schaetzl, R.J., 2001. Paleowind (11,000 BP) directions derived from lake spits in Northern Michigan. Geomorphology 38, 1-18.

Menking, KM, DM Peteet, RY Anderson. 2012. Late-glacial and Holocene vegetation and climate variability, including major droughts, in the Sky Lakes region of southeastern New York State. Palaeogeography, Palaeoclimatology, Palaeoecology 353-355:45-59, doi:10.1016/j.palaeo.2012.06.033.

Miller, NG. 1973. Late-glacial and postglacial vegetation change in southwestern New York State. N.Y. State Museum Bulletin 420.

Miller, NG and CB Griggs. 2012. Tree macrofossils of Younger Dryas age from Cohoes, New York State, U.S.A. Canadian Journal of Earth Sciences, 2012, 49(5): 671-680, 10.1139/e2012-010.

Muscheler, R, B Kromer, S Bjorck, A Svensson, M Friedrich, KF Kaiser, J Southon. 2008. Tree rings and ice cores reveal ^{14}C calibration uncertainties during the Younger Dryas. Nature Geoscience 1: 263 – 267, doi:10.1038/ngeo128.

Panshin, AJ and P de Zeeuw. 1970. Textbook of Wood Technology, 3rd ed. McGraw-Hill, New York. 705pp.

Peteet, DM, JS Vogel, DE Nelson, JR Southon, RJ Nickmann, LE Heusser. 1990. Younger Dryas climatic reversal in northeastern USA? AMS ages for an old problem. *Quaternary Research*, *33*(2), 219-230.

Peteet, DM, RE Daniels, LE Heusser, JS Vogel, JR Southon, DE Nelson. 1993. Late-glacial pollen, macrofossils and fish remains in northeastern U.S.A.—The Younger Dryas oscillation. Quaternary Science Reviews, 12: 597–612.

Ramsey, CB, RA Staff, CL Bryant, F Brock, H Kitagawa, J van der Plicht, G Schlolaut, MH Marshall, A Brauer, HF Lamb, RL Payne, PE Tarasov, T Haraguchi, K Gotanda, H Yonenobu, Y Yokoyama, R Tada, T Nakagawa. 2012 A Complete Terrestrial Radiocarbon Record for 11.2 to 52.8 kyr B.P. Science 338(6105): 370-374.

Reimer, PJ, E Bard, A Bayliss, JW Beck, PG Blackwell, C Bronk Ramsey,DM Brown, CE Buck, RL Edwards, M Friedrich, PM Grootes, TP Guilderson, H Haflidason, I Hajdas, C Hatté, TJ Heaton, AG Hogg, KA Hughen, KF Kaiser, B Kromer, SW Manning, RW Reimer, DA Richards, EM Scott, JR Southon, CSM Turney, J van der Plicht. 2013a. Selection and treatment of data for radiocarbon calibration: an update to the international calibration (IntCal) criteria.Radiocarbon 55 (4): 1869–1887.

Reimer, PJ, E Bard, A Bayliss, JW Beck, PG Blackwell, C Bronk Ramsey, CE Buck, HCheng, RL Edwards, M Friedrich, PM Grootes, TP Guilderson, H Haflidason, I Hajdas, C Hatté, TJ Heaton, DL Hoffmann, AG Hogg, KA Hughen, KF Kaiser, B Kromer, SW Manning, M Niu, RW Reimer, DA Richards, EM Scott, JR Southon, RA Staff, CSM Turney, J van der Plicht. 2013b. Intcal13 and Marine13 radiocarbon age calibration curves 0–50,000 years cal BP. Radiocarbon 55 (4): 1869–1887.

Rickard, LV, DW Fisher, compilers. 1970. Geologic Map of New York; Finger Lakes Bedrock Sheet. New York State Museum and Science Series Map and Chart no. 15. Available URL: http://www.nysm.nysed.gov/research-collections/geology/gis. Accessed May 2016.

Southon J, AL Noronha, H Cheng, RL Edwards, Y Wang. 2012. A high-resolution record of atmospheric ^{14}C based on Hulu Cave speleothem H82. Quaternary Science Reviews 33:32–41.

Stuiver, M, PJ Reimer, TF Braziunas. 1998. High-precision radiocarbon age calibration for terrestrial and marine samples. Radiocarbon 40(3): 1127-51.

Yansa, CH. 2006. The timing and nature of Late Quaternary vegetation changes in the northern Great Pains, USA and Canada: a re-assessment of the spruce phase. Quaternary Science Reviews 25:263-281.

Yu, Z. 2000. Ecosystem response to Lateglacial and early Holocene climate oscillations in the Great Lakes region of North America. Quaternary Science Reviews 19:1723-1747.